Accepted Manuscript

Title: High-nuclearity cobalt coordination clusters: Synthetic, topological and magnetic aspects

Authors: George E. Kostakis, Spyros P. Perlepes, Vladislav A. Blatov, Davide M. Proserpio, Annie K. Powell

Please cite this article as: G.E. Kostakis, S.P. Perlepes, V.A. Blatov, D.M. Proserpio, A.K. Powell, High-nuclearity cobalt coordination clusters: Synthetic, topological and magnetic aspects, *Coordination Chemistry Reviews* (2010), doi:10.1016/j.ccr.2012.02.002

Research highlights

- We analyzed aspects of the synthetic, reactivity, structural and magnetic chemistry of Co CCs
- We classified all the polynuclear Cobalt coordination clusters found in CCDC (CCDC 5.32 Nov. 2010) higher than 4.
- All the known Co coordination clusters can be searched by cluster topological symbol and nuclearity, compound name, dimensionality and Refcode.

Edited Feb 6

High-nuclearity cobalt coordination clusters: Synthetic, topological and magnetic aspects

George E. Kostakis[a*], Spyros P. Perlepes[b*], Vladislav A. Blatov,[c] Davide M. Proserpio,[d] Annie K. Powell[a*]

[a] *Institute of Nanotechnology, Karlsruhe Institute of Technology, Hermann-von-Helmholtz Platz 1, 76344 Eggenstein-Leopoldshafen, Germany*

[b] *Department of Chemistry, University of Patras, 265 04 Patras, Greece*

[c] *Samara State University, Ac. Pavlov St. 1, Samara 443011, Russia*

[d] *Università degli Studi di Milano, Dipartimento di Chimica Strutturale e Stereochimica Inorganica (DCSSI), Via G. Venezian 21, 20133 Milano, Italy*

E-mails: george.kostakis@kit.edu, perlepes@patreas.upatras.gr, annie.powell@kit.edu . Fax: +49 721 608 8142; Tel: +49 721 608 2135.

Keywords: Cobalt, Coordination clusters, Magnetic properties, Topology

Contents

1

Edited Feb 6

ABSTRACT

Polynuclear coordination clusters of 3d metals continue to attract the intense interest of scientists from the synthetic inorganic chemistry, bioinorganic chemistry and molecular magnetism communities. In this review we have focused on describing aspects of synthesis, structures and magnetic properties of Co coordination clusters with nuclearities higher than 4. Adopting our recently developed topological

2

Edited Feb 6

approach for the description of coordination clusters, we have classified the structural motifs of Co complexes which range in nuclearity from 5 to 36. Emphasis is given to the magnetic properties of Co coordination clusters. Some of them display slow magnetic relaxation at very low temperatures, mainly due to their large magnetic anisotropies. The possibility of magnetic anisotropies one and two orders of magnitude larger than seen so far for single-molecule magnets of other 3d-metal ions, promises a brilliant future in the research of polynuclear Co complexes.

1. Scope, organization and general information

This review presents a focused overview of the chemistry of homometallic polynuclear Co complexes (clusters [1]) with nuclearities higher than 4. We have searched the literature up to October 2010 (CCDC 5.32 Nov. 2010). It aims to be almost comprehensive in terms of a discussion of every discrete known Co_x complex ($x \geq 5$) and provide the reader with some idea of the range of chemistry that has been carried out (and indeed remains still to do) in this area. We survey some of the synthetic approaches that have been employed in the synthesis of Co clusters. Since the structures of the complexes have been extensively discussed in the cited references, our aim is to concentrate on their topologies using a new and convenient approach that we have recently introduced [2 − 5]. Assigning a topological nomenclature to the existing motifs should help chemists and physicists in identifying and classifying clusters in terms of structural and physical properties by recognising the connectivity modes in 0D systems. From the viewpoint of properties, an eye will be on the magnetism of the clusters. Co^{II} clusters are key players in the interdisciplinary field of Molecular Magnetism [6].

The article contains six sections, including this one. The next section is introductory; the reader can find general information on the class of metal complexes known as clusters or better as "coordination clusters (CCs)" [3]. In section 3 we shall give the central idea of our new approach [2 − 5] to describing the topology of polynuclear complexes. Section 4 deals with the basic characteristics of the coordination chemistry of Co with focus on the electronic structures of its complexes and the magnetic properties of

3

Edited Feb 6

Co^{II}. This information is essential to discuss the chemistry and magnetism of the Co complexes that are described in section 5 which is the "main menu" of this review. Organometallic complexes have been excluded from our survey. Sections 2 – 4 thus provide a "hors d'oeuvre" for section 5. Section 6 provides initial conclusions and perspectives for future research. Sections 4 and 5 are divided into parts for clarity.

A review article on high nuclearity Co complexes has never appeared. An excellent tutorial review by Murrie published in 2010 covers recent progress in the area of polynuclear Co^{II}-based single-molecule magnets (SMMs) and it includes the Co_5, Co_6, Co_7, Co_8 and Co_{12} systems that display slow magnetization relaxation at low temperature [7]. Overlap of topics will be kept to a minimum herein. A survey of the crystal structures of Co_4 cubanes containing the $\{Co_4(\mu_3\text{-}OR)_4\}$ core was reported by Williams and co-workers four years ago [8]. In an interesting critical review, Kurmoo has examined the diversity of magnetic exchange interactions between nearest-neighbour Co^{II} centres in magnetic metal-organic frameworks (MOFs), some of which contain oligomeric (Co_3, Co_4, Co_5, Co_6 and Co_7) repeating units [9].

We shall use the term CC [3] throughout this review. CCs consist of oligo- or polynuclear molecules in which the metal ions are linked by elements from the p-block, such as oxygen bridges (e.g. provided by oxides, alkoxides, carboxylates and so on). These compounds are different from the metal-metal bonded complexes [10], termed simply "clusters" by many groups. In the former case, any exchange between the metal ions results from the nature of the bridging ligand. In the latter case, the metal-metal bonding dictates the electronic structure. In general, metal – metal bonded clusters can be thought of as "closed shell" or 18-electron systems and are described in terms of the 18 electron rule and MO theory, whereas CCs are composed of "open shell" ions and are satisfactorily described using ligand field approaches [3].

The method currently used to describe the binding of polydentate ligands to multiple metal centres involves a mixture of Greek letters and sub- and superscripts; this η/μ notation is sometimes confusing. An alternative is "Harris notation" [11]. This describes the binding mode as $X.Y_1Y_2Y_3 \ldots Y_n$, where X is the overall number of metal ions attached to the different donor atoms. The order of Y groups follows the Cahn-Ingold-Prelog priority rules; hence (for most of the ligands included in this review) O comes before

4

Edited Feb 6

N. In the case of complicated chelating/bridging ligands, to distinguish between several alternatives, a subscripted number is included to show to which metal centre the donor atom is attached.

2. A broad introduction to coordination clusters

Only in the last 25 years or so has the synthesis and study of CCs of paramagnetic metals in *moderate oxidation states* begun to attract the attention [2 – 4, 12 – 15] given to CCs of metals in high or low oxidation states. The highest-nuclearity, low–valent species structurally characterized is $[Ag_{490}S_{188}(StC_5H_{11})_{144}]$, where the Ag^I/S^{2-} core can be described as a narrow-waisted cylinder of dimensions 2.8-3.1 nm [16]. The highest-nuclearity, high-valent species known is the anion $[H_xMo^{IV}_{256}Mo^V_{112}O_{1032}(SO_4)_{48}(H_2O)_{240}]^{48-}$, having approximately the size of haemoglobin [17]. Moderate oxidation state, transition-metal CCs are in general an order of magnitude smaller than the complexes just mentioned. However, this picture has been changing after the syntheses of the protein-sized chiral anionic cages $[Na_{24}Fe^{III}_{168}(L\text{-tart})_{96}O_{48}(HCO_2)_{144}]^{96-}$ and $[Na_{24}Fe^{III}_{168}(D\text{-tart})_{96}O_{48}(HCO_2)_{144}]^{96-}$ [18], where tart is the tartrate (-4) ligand, the four-cell, nesting doll-like heterometallic cation $[Ni^{II}_{54}Gd^{III}_{54}(OH)_{144}(CO_3)_6(ida)_{48}(H_2O)_{25}]^{18+}$ [19], where ida is the iminodiacetate(-2) group, and the molecule $[Mn_{84}O_{72}(OMe)_{24}(OH)_6(O_2CMe)_{78}(MeOH)_{12}(H_2O)_{42}]$ [20], which has a 4 nm-diameter torus structure representing the long-sought-after meeting of the bottom-up and top-down approaches to nanomagnetism.

The simplest general formula of CCs of 3d metals in moderate oxidation states is $[M_x(\mu\text{-}L)_yL'_z]^n$, where μ-L is a bridging organic or inorganic ligand, L' is a terminate ligand, x is an integer number larger than 2, y and z are integer numbers and n can be zero (molecule), positive (cationic CC) or a negative (anionic CC) integer number. In many cases there are two or more bridging ligands, often a combination of organic and inorganic ones, and more than one type of terminal (monodentate or chelating) ligands including solvate molecules. This class of compounds is found in the literature with several names such as oligomeric, polynuclear, high-nuclearity or polymetallic complexes, cages, clusters and CCs; as mentioned above we prefer the latter term.

5

Edited Feb 6

The chemistry of the CCs of paramagnetic 3d-, 4f- and 3d/4f-metals is today an area of modern science whose interfaces with many disciplines have provided invaluable opportunities for crossing the boundary both inside and between the fields of chemistry, physics, biology and materials. The current intense interest by many groups around the world in this chemistry is due to the combination of the aesthetically pleasing structures that many such molecular species possess and their relevance to a variety of fields such as Bioninorganic Chemistry and Molecular Magnetism.

In the field of Bioinorganic Chemistry there is a continuous search for various nuclearity oxide-bridged complexes to model M_x sites in biomolecules, including understanding the assembly of the multinuclear Fe^{III}/O^{2-} core of the iron-storage protein ferritin [21,22] and elucidating the structure, spectroscopic properties and mechanistic aspects of the $\{CaMn_4O_5\}$ core of the H_2O oxidizing complex within the photosynthetic apparatus of green plants and cyanobacteria [23 − 27]. The latter opened up a new era in Mn chemistry and led to the realisation that manganese can be stabilized in the formal oxidation state III by certain ligands, even in the presences of II and IV states.

In the field of Molecular Magnetism, 3d, 3d/4f and 4f-metal CCs often display interesting and sometimes exciting magnetic properties, including high ground-state spin values (currently up to $S=83/2$ [28]) and single molecule magnetism. It has been 18 years since the discovery that the discrete CC $[Mn^{III}_8Mn^{IV}_4O_{12}(O_2CMe)_{16}(H_2O)_4]$ (Mn_{12}) could possess an energy barrier to the reorientation of its molecular spin that was large enough to observe magnetic hysteresis below a blocking temperature (T_B) [29,30]. Such SMMs [31-37] can have magnetization relaxation times that are more than 10^8 times slower than normal paramagnets. This area thus represents a molecular, "bottom-up" approach to nanoscale magnets, complementary to the standard "top-down" approach to nanoparticles of traditional magnetic materials (e.g. Fe, Fe_3O_4, CrO_2) which are atom based with d-(or f-) orbital-based spin sites and with extended network bonding on the three dimensions. For a molecule to function as a SMM, it must possess a large ground state spin (S) and a large uniaxial anisotropy of an Ising type which can be a result of a favourable zero-field splitting parameter, D, or in the case of lanthanide (Ln) ions an overall anisotropy parameter, rather than intermolecular interactions and long-range ordering as required in other 3D

6

Edited Feb 6

molecule-based magnets [38]. This combination of *intra*molecular properties leads sometimes to a significant barrier, *U*, to relaxation (reorientation, reversal) of the magnetisation vector, whose maximum value is given by $S^2|D|$ or $(S^2 -1/4)|D|$ for integer and half-integer *S* values, respectively, although a relatively recent reappraisal of this suggests that the relationship is always linearly dependent on the total spin *S* [39]. For these reasons, CCs containing the high spin octahedrally coordinated $3d^4$ Mn^{III} ion, with its relatively large ground spin state and uniaxial anisotropy, have received increasing attention since SMM behaviour was first reported in 1993. Since then high-nuclearity and/or high spin Mn complexes have been the main source for new SMMs [31 – 37]. However this family of SMMs has been extended to various other metals including V^{III}, Fe^{II}, Fe^{III}, Co^{II}, Ni^{II}, homometallic Ln^{III} CCs and combinations of 3d with 4d, 5d and 4f paramagnetic metal ions [31 – 37]. Experimentally, a SMM shows superparamagnet-like properties, exhibiting both frequency-dependent out-of-phase ac magnetic susceptibility signals and hysteresis in a plot of magnetization (*M*) vs. applied direct-current (dc) magnetic field [35]. The record values of the effective energy barrier to magnetization reversal (U_{eff}) and T_B for a 3d-metal-based SMM are 86.4 K and ~4.5 K, respectively, for the compound $[Mn^{III}_6O_2(Etsao)_6\{O_2CPh(Me)_2\}_2(EtOH)_6]$ with *S* = 12 and *D* = -0.43 cm^{-1}, where $Etsao^{2-}$ is the dianion of 2-hydroxyphenylpropanone oxime [40].

The molecular nature of SMMs has some obvious advantages, e.g. synthesis by solution methods, crystallinity, uniform size distribution, easy variation of peripheral ligands, solubility in organic solvents, sub-nanoscale dimensions, etc. From the potential applications viewpoint, SMMs offer the possibility of creating switchable, molecular-scale devices that store information using the orientation of their molecular spin [41,42]. Due to their quantum coherent properties, SMMs offer the possibility of applications in quantum computing [43-45]. Recent studies have shown that SMMs can be successfully transferred to surfaces with retention of their magnetic properties [46] and potentially exploited as spintronic devices [47]. However, for the moment applications are in the realm of fantasy due to the extremely low temperatures or fast timescale required for observation of slow magnetization relaxation [31].

7

Edited Feb 6

High-spin CCs with a small magnetic anisotropy attract the intense interest of scientists working in the area of magnetic refrigerants (coolants) [48]. Magnetic refrigeration is based on the magnetocaloric effect (MCE), which was first discovered in 1881 by Warbourg [49]. MCE is the thermal effect of magnetic materials subjected to magnetic field variation. When a magnetic field is applied to magnetic materials, their magnetic moments become ordered, which reduces the total entropy of the material. In the reverse process-adiabatic demagnetization [50] the entropy of the material increases and this has to be balanced by a change in the free energy of the surroundings. As a result, the system cools down. This energy-efficient and environmentally friendly technique is promising for refrigeration in the ultra-low-temperature region, providing, e.g., a valid alternative to the use of helium-3 which is becoming rare and expensive [51]. Studies have demonstrated that the MCE of selected CCs can be much larger than in the best intermetallic and Ln alloys, and magnetic nanoparticles, conventionally studied and employed for low-temperature cooling applications [48]. Recent work to prepare such molecular magnetic refrigerants include $\{Fe_x\}$ (x=14, 17), $\{Mn_y\}$ (y=10, 14, 17, 19, 32) $\{Mn_4Ln_4\}$, $\{Co_zLn_\omega\}$ (z, ω vary), $\{Ni_6Gd_6\}$, $\{Cu_5Gd_4\}$, $\{Gd_2\}$ and $\{Gd_7\}$ complexes [52 – 61].

Due to the properties and application potentialities of CCs, there continues to be a need for an arsenal of synthetic methods to CCs. There are two broad synthetic approaches that are being pursued to make new 3d-metal CCs. The "designed assembly" approach uses rigid inorganic or organic ligands that have strong preferences for specific bonding modes and metal ions with preferred coordination geometries. The structures of such complexes are moderately predictable on the basis of the number of preorganized donor sites presented by the ligand, its limited flexibility and the coordination geometry of the metal ion. Typical examples of rigid ligands are the cyanido ion [62,63] and various tailored derivatives of 4,4'-bipyridine [64,65], while examples of metals with preferred geometries are the Pd^{II} and Pt^{II} ions.

Other synthetic inorganic chemists, including our groups, use much less well-behaved bridging organic or inorganic ligands for the synthesis of 3d- and 3d/4f-metal CCs. This route allows a "dialogue" between the preferred coordination geometry of the metal sites and the coordination mode of the ligand.

8

Edited Feb 6

Once exclusive formation of five- or six-membered chelating rings is excluded, the coordinative flexibility of any polydentate ligand increases enormously. This flexibility in turn allows stabilization of many unpredictable structures (which can lead to interesting properties), almost invariably incorporating further auxiliary bridging ligands such as hydroxy, alkoxy, oxido etc. groups. This approach has been termed "serendipitous assembly" [66] and has led to thousands of exciting CCs. Serendipitous assembly often relies on creating a mismatch between the number or type of coordination sites available on a single metal centre and the donor set supplied by the ligand. It is clear, however, that we can not simply trust to luck in preparing 3d-metal CCs; there thus has to be considerable forethought in the conditions for any general reaction scheme (ligand, metal salt, "pH", ligand : metal ratio, solvent, concentration of solution, temperature, pressure, crystallization method, reaction time, …) for any progress to be made. Along these lines, alkoxide-based ligands, oximate-based ligands and/or carboxylates have been widely employed, amongst many others, in the synthesis of CCs [67 – 72; these representative references come from our groups]. Alkoxy and oximato ligands are particularly versatile in that they possess chelating and bridging capabilities, while carboxylates are famous for exhibiting a huge variety of coordination modes. Moreover, from a magnetic point of view, alkoxide arm(s) often promote ferromagnetic exchange interactions between the metal centres that they bridge [3]. The metal sources are either simple 3d-metal "salts" or preformed low-nuclearity complexes such as $[Mn^{III}_3O(O_2CR)_6L_3]^{0/+}$ (R=Me, Ph, etc; L = H_2O, MeCN, ROH, py, etc.] and $[M^{II}_2(OH_2)(piv)_4(pivH)_4]$ (pivH=pivalic acid).

As the field develops the boundary between "designed" and "serendipitous" assembly becomes less clear [73,74]

## 3. A method for the topological description of coordination clusters

Before embarking on Co chemistry, it is helpful to remind the reader of our approach to describing the topology of CCs. The IUPAC rules for the nomenclature of coordination clusters result in names that are lengthy and hard to follow. Thus, generally, CCs are described relatively vaguely apart from the cases in which the researchers have recognised a structural description of the metal core in terms of a trapped

9

Edited Feb 6

mineral [75,76] or have found analogies with motifs found in main group chemistry [16,28]. Our inspiration was from the concept of using a topological representation for 2D and 3D coordination polymers and Metal-Organic Frameworks - MOFs [77,78]. Below we briefly describe an improved version of this approach that has been implemented into the program package TOPOS [79] and tested for the analysis of Mn CCs.[80]

In our approach we designate each metal centre of a CC as a straightforward "node". The bridging monoatomic heteroatoms then play the role of the "linker". The resulting graph (CC skeleton) consists of only metal atoms and its topology is described by a unique *NDk-m* symbol [81], where *N* is the set of coordination numbers of topologically non-equivalent nodes (the number of terms in the set defines uninodal, binodal, trinodal, … clusters; the shorter *N*, the more symmetrical is the skeleton), D is dimensionality; D=M for finite (molecular) clusters, *k* is the number of nodes in the cluster, and *m* enumerates topologically different clusters with the same *NDk* symbol. If the CC skeleton consists of several unconnected parts the *NDk-m* symbols of different parts are written together with their stoichiometric coefficients. An isolated metal atom is designated (0). Thus, every *NDk-m* symbol denotes a topological type, i.e. a set of topologically equivalent but likely conformationally different CC skeletons. Many examples of this nomenclature are considered below.

For example, Scheme 1 shows the simplified metallic core of a centrosymmetric complex belonging to the defect dicubane class of CCs, i.e. compounds that consist of two cubanes sharing a face and each missing one vertex. The cluster in Scheme 1 has symbol **2,3M4-1**, i.e. this is the first type of 4-atom cluster with two topologically non-equivalent atoms of coordination 2 and 3.

10
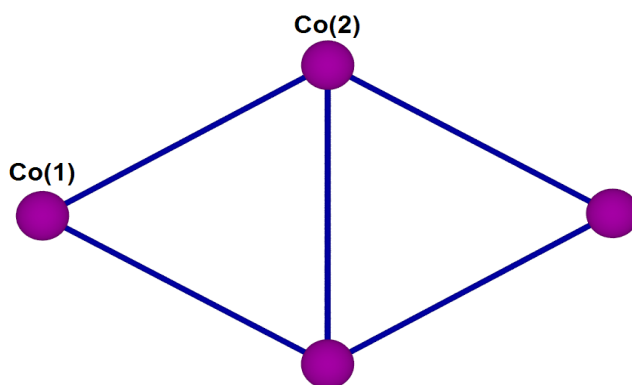
Edited Feb 6

Scheme 1. The simplified metallic core of a centrosymmetric CC with a defect dicubane structure.

This formalism allows for a computer implementation as a rigorous algorithm to be applicable to any kind of CCs. In TOPOS, the separation of a CC skeleton is a completely automated procedure that can be applied both to a single crystal structure and to any number of structures at once. All atoms that are not bridges between the metal atoms are ignored while all linkers are contracted to nodes and form the skeleton edges. TOPOS uses strict methods to compare the topology of the resulting skeleton with the reference topologies from the TTD Collection [81] and either assigns this topology to an existing topological type or designates it with a novel *NDk-m* symbol.

By applying the above-mentioned approach to high-nuclearity CCs, it becomes easier to describe the skeleton by a *NDk-m* symbol, rather than to find or devise a suitable polyhedron to describe the overall cluster core geometry. Other advantages of this method are: (i) We can gain insights into the crystal growth and crystal engineering of CCs, because it is easy to compare lower-nuclearity to higher-nuclearity complexes and understand aspects of synthetic and structural chemistry, and (ii) we can facilitate the comparison of the physical properties of compounds that have similar or slightly different cores which will assist in establishing structure-property relationships. At present, with the TOPOS program package, we are establishing a database which will classify all CCs according to our approach. A similar analysis was performed on Mn CCs [80]. With this approach, we have extracted and assigned *NDk-m* symbols to 284 Co_x complexes (x≥5) from the Cambridge Structural Database (release 5.32, Nov. 2010). The complete topological classification is given in the ESI. In section 5 we shall describe the structural motifs and topological representation of some of the Co skeletons with interesting magnetic properties.
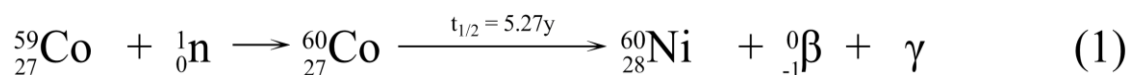
4. Coordination chemistry of cobalt : Basic features

4.1. *The element [9, 82]*

11

Edited Feb 6

The Egyptians used Co ores to give glass and pottery a blue colour 4500 years ago. In the 16th century Leonardo da Vinci rediscovered the brilliant blue pigment produced by fusing potash, silica and cobalt oxide. In 1735 the Swedish chemist Georg Brandt identified the source of the colour by isolating the crude metal, which he named "cobaltrex". Bergman in 1780 proved this to be a new element. The name is believed to derive from the German word Kobald, meaning "goblin" or "evil spirit", since the miners of northern Europe thought the spitefulness of these creatures was responsible for the metal being difficult and hazardous to extract from its ores by smelting.

More than 150 ores containing Co are known, but only cobaltite (CoAsS), smaltite ($CoAs_2$) and linnacite (Co_3S_4) are of commercial value. Major sources are in Africa and Canada, with smaller reserves in the Urals (Russia) and Australia. Isolation is essentially as a by-product of Cu. Gecamines (South Africa) is the main producer of Co. Much of the metal is used to produce high-temperature alloys (with Fe) and for the manufacture of magnetic alloys (Co is ferromagnetic and has the highest Curie temperature among the three ferromagnets of the 1st-row transition metals, being also the most anisotropic magnetically). "Alnico" is the most famous of these and is used for the manufacture of permanent magnets which are lighter, and can be up to 25 times more powerful than steel magnets. Chemical production is largely associated with the ceramic and paint industries, while some of its compounds are also used as catalysts.

Cobalt is lustrous and silvery with a black tinge, existing in two allotropic forms. There is only one naturally occurring isotope (^{59}Co), but with thermal neutrons this can be converted into radioactive ^{60}Co, Eq (1), which is used in various fields of medicine as a convenient and concentrated source of γ-rays. ^{59}Co has a nuclear spin (I=7/2) and ^{59}Co NMR spectroscopy is becoming increasingly useful for the detection of the metal both in solid and biological materials.

$$^{59}_{27}\text{Co} + ^{1}_{0}\text{n} \longrightarrow ^{60}_{27}\text{Co} \xrightarrow{t_{1/2} = 5.27y} ^{60}_{28}\text{Ni} + ^{0}_{-1}\beta + \gamma \qquad (1)$$

Co is stable in oxygen unless heated, when it is oxidized to Co_3O_4; above 900°C the product is CoO. It slowly dissolves in mineral acids, forming CoX_2 salts. Co reacts with halogens on heating, giving

12

Edited Feb 6

CoF_3 or CoX_2 (X=Cl, Br, I). It is unreactive towards H_2 and N_2, and no simple hydrides or nitrides are known.

4.2. *Cobalt complexes and their electronic structures [9, 82 – 85]*

The most common oxidation states of the metal are II and III. Few Co^{IV} and Co^{V} compounds exist, e.g. Cs_2CoF_6 and K_3CoO_4. There are also some important complexes of Co^{I}, e.g. $[CoBr(PR_3)_3]$. Low oxidation states (Co^{-I}, Co^{0}) are known in relatively few coordination complexes, where they are invariably associated with CN^-, CNR, CO, phosphine and phosphite ligands.

Co^{II} forms numerous complexes, mostly either octahedral or tetrahedral, but five-coordinate and square planar species are also known. Because of the small stability difference between octahedral and tetrahedral Co^{II} complexes (due to the small difference in ligand field stabilization energies), there are several cases in which the two types with the same ligand are known and may be in equilibrium. The colour of octahedral Co^{II} complexes (usually pink to violet, ~500 nm) is dominated by the $^4T_{1g}(F) \rightarrow$ $^4T_{1g}(P)$ transition (ν_3) with the two lower-energy transitions (to $^4T_{2g}$ and $^4A_{2g}$ levels) occurring in the near-IR and visible regions (weak) of the spectrum, respectively. Tetrahedral Co^{II} complexes (usually intense blue, ~600 nm) are dominated by the $^4A_2 \rightarrow {}^4T_1(P)$ transition (ν_3), with the lower-energy transitions to $^4T_1(F)$ and $^4T_2$ levels occurring in the near-IR and IR regions, respectively. Most octahedral Co^{II} complexes are high-spin ($t_{2g}^5 e_g^2$). A sufficiently strong ligand field ($\Delta_o > 15000$ cm^{-1}) can cause an ^2E state originating in the ^2G state of the free ion to become the ground state. The electron configuration in this case is $t_{2g}^6 e_g$, and a Jahn-Teller distortion would be expected. Consequently, octahedral low-spin complexes are rare, an example being the axially distorted $[Co(CNPh)_6]^{2+}$ ion, tending to lose ligands and form low-spin square planar of 5-coordinate species. Both high-spin (three unpaired electrons) and low-spin (one unpaired electron) configurations are found for both trigonal bipyramidal (tbp) and square pyramidal (spy) as well as intermediate stereochemistries; when the heavier donor atoms (e.g. P, As, Br, S) are present (as compared with O and N), the greater is the tendency to spin pairing.

13

Edited Feb 6

Co^{III} complexes are almost exclusively octahedral and diamagnetic. This is due to the weak ligand field necessary to cause electron pairing; exceptions are $[CoF_6]^{3-}$ and $[CoF_3(H_2O)_3]$ which are paramagnetic. A very few unusual four- and five-coordinate paramagnetic Co^{III} systems are known. The two absorption bands found in the visible spectra of regular octahedral Co^{III} complexes represent transitions from the $^1A_{1g}$ ground state to the upper states $^1T_{1g}$ (v_1) and $^1T_{2g}$ (v_2). Complexes of the $[Co^{III}A_4B_2]$ type can exist in both *cis* and *trans* configurations and certain spectral features are diagnostic of the stereochemistry; the origin of theses features lies in the splitting of the $^4T_{1g}$ state by the lower than O$_h$ symmetry, with the splitting being larger in the *trans* isomer whenever there is a substantial difference in the positions of A and B in the spectrochemical series of ligands. Octahedral Co^{III} complexes generally undergo ligand-exchange reactions slowly and have, from the early days of Werner and Jørgensen, been extensively used in understanding isomerism and the mechanisms of substitution reactions at metal centres.

The interactions of Co^{II} complexes in solution with O$_2$ can lead to reversible carriers of O$_2$ and the products have been much studied because of their potential utility and as models for natural oxygen transport systems. Cobalt complexes of corrinoid ligands are found in many organisms, including man, and are known as cobalamins; they are extremely rare examples of naturally occurring organometallic compounds containing a metal-carbon σ bond. Several cobalamins are biologically active, including vitamin B$_{12}$.

4.3. *Magnetism of Co(II) [6, 7, 9, 83, 86 – 88]*

Because of the intrinsic orbital angular momentum in the octahedral ground state of Co^{II} [$^4T_{1g}$(F)], there is consistently a considerable orbital contribution (especially above 77K), and effective magnetic moments (μ_{eff}) at room temperature are in the range 4.7-5.2 BM falling off appreciably with decreasing T, i.e. a non-Curie behaviour is observed. Co^{II} centres in real octahedral complexes do not display a strict octahedral geometry. In distorted octahedral systems, the degeneracy of the $^4T_{1g}$ state is lifted. If the

14

Edited Feb 6

distortion is tetragonal, the ground state becomes $^4A_{2g}$ and the excited level is ^4E_g. Spin-orbit coupling in these levels results in six Kramer's doublets, with an $M=\pm1/2$ ground state and an $M=\pm3/2$ first excited state (Fig. 1) The separation ($2D$) between the $M=\pm1/2$ and $M=\pm3/2$ states can be considered as a zero-field splitting (ZFS) of the quartet state. The orbital moment has been incorporated, in part, into D. Hence, the ZFS here is larger, larger than for a metal ion with a quarter ground state and no first order orbital moment, such as Cr^{III}. D values up to 100 cm^{-1} have been reported for distorted octahedral Co^{II} complexes. If the magnitude of D for Co^{II} is compared to that found in mononuclear Mn^{III} complexes (-5 to +5 cm^{-1}), the advantage of using Co^{II} to generate a large magnetic anisotropy is obvious. It is seen in Fig. 1 that the D parameter for single-ion Co^{II} in a tetragonally distorted octahedral environment will be positive, since $M=\pm1/2$ is lowest in energy. Therefore, the orientation of the axial ZFS tensor on each Co^{II} atom which is a part of a CC, with respect to the molecular easy axis, is of paramount importance in order to achieve an overall negative value (Ising type) for the compound anisotropy.
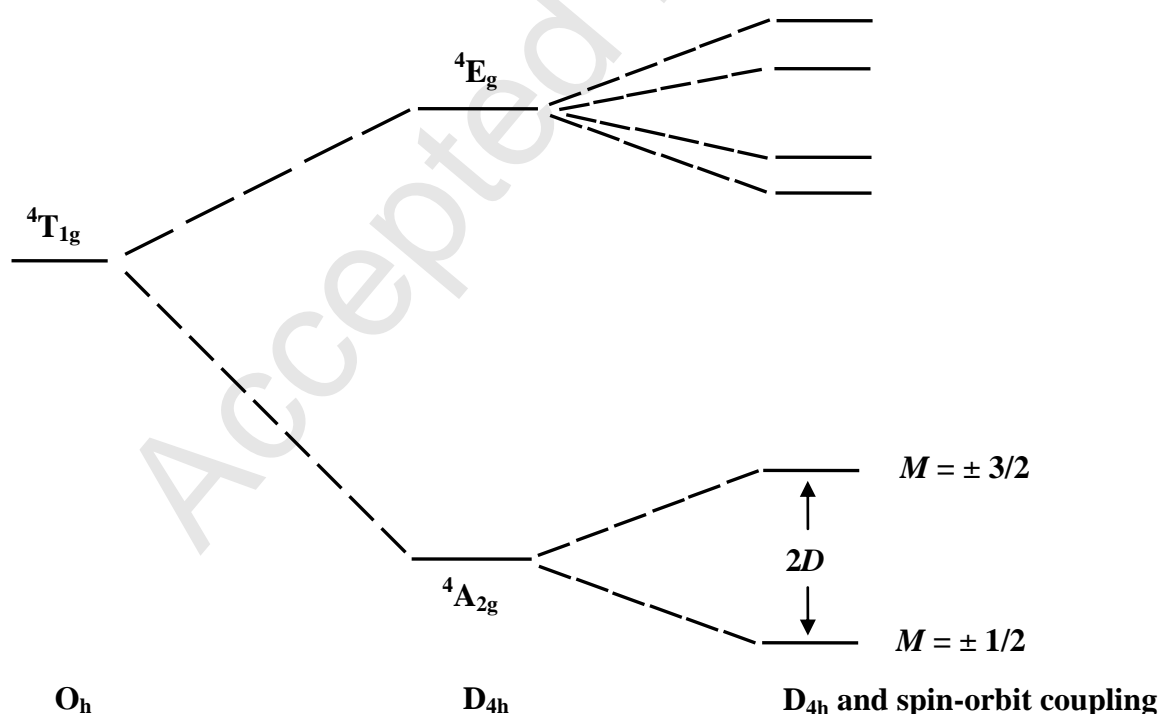
Fig. 1. The effects of a tetragonal distortion and spin-orbit coupling on the energy levels of high-spin Co^{II}. [6,7]

15

Edited Feb 6

From the theoretical point of view, the problem of the magnetic exchange in Co^{II} CCs is a hard nut to crack. Many of the works dealing with the magnetic properties of Co complexes are based on the assumption that the exchange interaction between Co^{II} ions has the Heisenberg form, $H_{ex} = -2JS_AS_B$, S_A and S_B being the real spins of the ions ($S_A = S_B = 3/2$). Although this simple form of the exchange may not always be entirely adequate for the orbitally degenerate ions, it has been successfully used in the description of numerous Co^{II} CCs. On the other hand, there is another approach that deals with the phenomenological effective Hamiltonians describing the interaction between the low-lying Kramer's doublets, the so called pseudo-spin-1/2 formalism. Extension of this effective spin model to describe small CCs at low temperatures is possible, as long as the Co^{II}-Co^{II} exchange interactions are smaller than the spin-orbit coupling (weak-exchange limit). The exchange coupling between the effective $S'=1/2$ spins is anisotropic (J_x, J_y, J_z); the Ising limit is reached when $J_x = J_y = 0$ and $J_z \neq 0$.

The weak-exchange limit presents a different situation to most SMMs based on ions with only second order spin-orbit coupling, e.g. Mn^{III}, where generally the exchange interactions are larger than the effects of the magnetic anisotropy. In this limit, equation $S^2|D|$ is not applicable to the description of the barrier for magnetization reversal, since it involves the total spin S of the complex, which is no longer a good quantum number. Thus, in Co^{II} complexes, the anisotropy and the exchange interaction can both contribute to the height of the barrier. Generally, however, the origin of the SMM behaviour in the weak-exchange limit is difficult to elucidate. The conclusion is that octahedrally coordinated Co^{II} is a promising candidate for preparing good SMMs, and there are a few reports in the literature of Co^{II}-based SMMs (vide infra). Some scientists believe that control over both the sign and magnitude of the magnetic exchange coupling and the magnetic anisotropy will permit the synthesis of Co^{II}-based SMMs with T_B values that surpass the current records.

For tetrahedral Co^{II} complexes, the ground state ($^4A_2$, $e^4t_2^3$) acquires angular momentum only indirectly through mixing with the $^4T_2$ state by a spin-orbit coupling perturbation. The observed range of μ_{eff} values is 4.4. – 4.7 BM, $g_{av} = 2.4$, S = 3/2. For non-interacting tetrahedral Co^{II}, the Weiss constant is close to zero. For high-spin trigonal bipyramidal and square pyramidal complexes, the behaviour is

16

Edited Feb 6

intermediate between those of octahedral and tetrahedral Co^{II}. Square planar Co^{II}, which is very rare in CCs, adopts the low-spin state (S=1/2). The average g value is slightly larger than the free-electron value due to a rather small orbital contribution resulting in a μ_{eff} range of 2.2-2.7 BM.

## 5.   Cobalt coordination clusters with nuclearities higher than 4

5.1. Co_5

There are various motifs present in the Co_5 CCs. The most common corresponds to two triangles, either twisted or coplanar (Fig. 2). Thus, the complexes can be numerically described with the *NDk-m* symbol **2,4M5-1**. This motif was first reported by Englert and Strahle back in 1987 in complex $[Co_3^{II}Co_2^{III}(\mu\text{-}OH)_2(\mu\text{-}NO_2)_2(acac)_8]$ (**1**) (FOHWUU) [89], although from 2003 more examples can be found in the literature which contain the Co nodes in oxidation state II [90 – 94]. Complex $[Co^{II}_5(\mu_3\text{-}OH)_2(\mu\text{-}piv)_4(\mu\text{-}L)_4(MeCN)_2]$ (**2**) (EKUYUE), where piv$^-$ is the pivalate ion and L$^-$ the anion of 3-hydroxy-6-(3,5-dimethylpyrazol-1-yl)-1,2,4,5-tetrazine, exhibits rich reactivity chemistry due to the presence of the labile MeCN groups [90]. It should be mentioned that ligand L$^-$ derived in situ from the hydrolysis of the initially used bis[3,5-(dimethylpyrazolyl)]-1,2,4,5-tetrazine (Scheme 2).
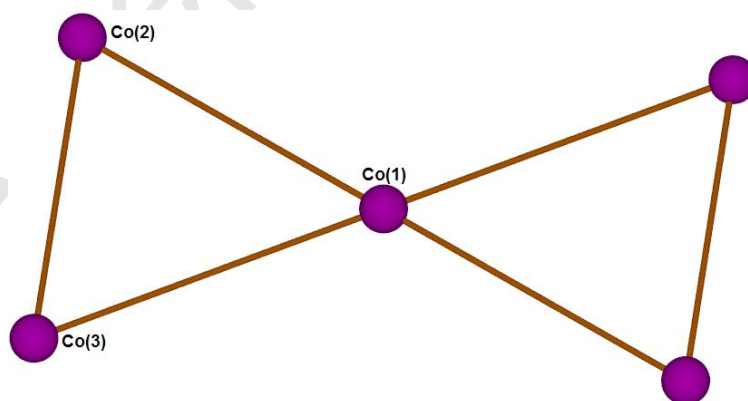
Fig. 2. The simplified core **2,4M5-1** of complexes **1** – **4** (FOHWUU, EKUYUE, FICSOA, YENKEI). Colour code: Co^{II} pink

17

Edited Feb 6
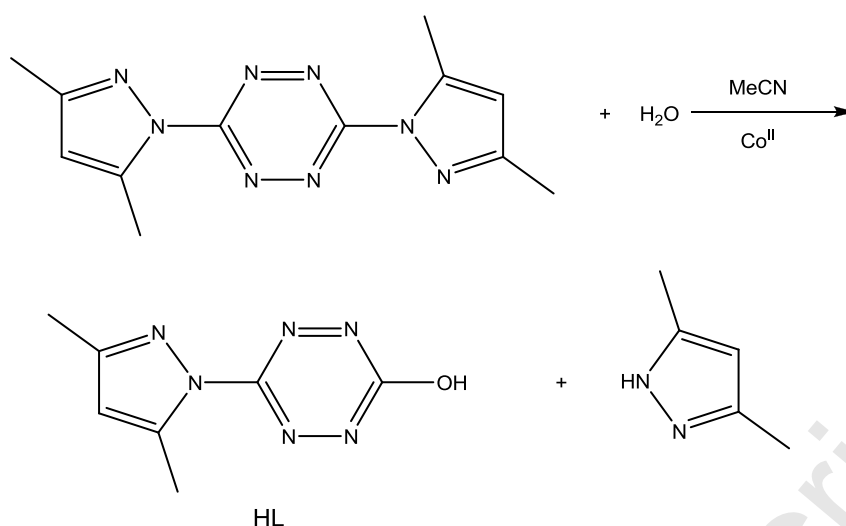
Scheme 2. The in situ formation of ligand HL (which is subsequently deprotonated) during the preparation of complex **2**.

Complex $[Co^{II}_5(phenSQ)_4(phenCat)_3(H_2O)]$ (**3**) (FICSOA), where phenSQ$^-$ is 1,10-phenanthrenesemiquinonate group and phenCat^{2-} the 1,10-phenanthrenecatecholate ligand, was prepared by the reaction of $[Co^{II}_4(phenSQ)_8]$ [95] with 4,5-dichloro-1,2-phenylenediamine in THF under a dinitrogen atmosphere; its formation is triggered by a dehydration condensation reaction between the semiquinonate and the *o*-phenylenediamine [92]. Compound **3** can be considered as a ligand-based mixed-valence CC. Complex $[Co^{II}Co^{III}_4(HL)_2(H_2L)_2]$ (**4**) (YENKEI), where H$_5$L is the interesting ligand 2-[bis(2-hydroxyethyl)amino]-2-(hydroxymethyl)propane-1,3-diol ("Bis-tris", Scheme 3) was prepared from the reaction of CoCl$_2$ 6H$_2$O, H$_5$L and NaOMe in an 1:1:4 molar ratio in MeOH under aerobic conditions in a low yield (<10%) [94]. ·
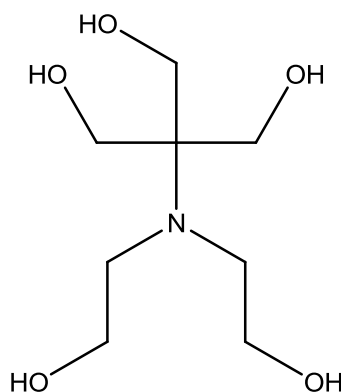
Scheme 3. The interesting ligand Bis-tris used for the preparation of the mixed-valence cluster **4**.

18

Edited Feb 6

A series of pentanuclear cobalt CCs (Fig. 3), including both neutral (Co^{II}_5) and one-electron oxidized forms (formally $Co^{II}_4Co^{III}$), were synthesized and studied by Peng's group [96 – 98]. Their formulae are [Co^{II}_5(tpda)$_4$X$_2$] (**5**) (RENYAK) and [$Co^{II}_4Co^{III}$(tpda)$_4$X$_2$](Y) (**6**) (IGEMEM), where H$_2$tpda is the pentadentate ligand *N,N'*-dipyridyl-2,6-diaminopyridine (Scheme 4), X = NCS, Cl, N$_3$, CN, CF$_3$SO$_3$ and Y = ClO$_4$, CF$_3$SO$_3$. The one-electron oxidation products were prepared from the Co^{II}_5 complexes either by reactions with Ag$^+$ salts or by bulk electrolysis. In all of these complexes, the pentacobalt chain adopts a symmetrical arrangement and is helically wrapped by four tpda^{2-} ligands. Applying our topological approach [2 – 5, 80], we observe that each terminal metal ion is bound to only one node and the rest are 2- c.n. , and thus the *NDk-m* symbol of these families is **1,2,2M5-1**. The magnetic measurements indicate that the neutral and one-electron oxidized molecules have spin states of *S* = 1/2 and 1, respectively. Theoretical calculations [98] for the Co^{II}_5 complexes have shown that the bond order between metal centres is 0.5 with σ character.
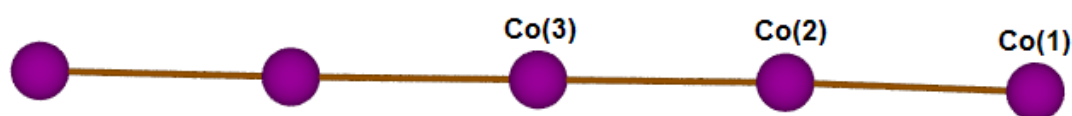
Fig. 3. The simplified core **1,2,2M5-1** of the families of Co$_5$ complexes **5** (RENYAK) and **6** (IGEMEM). Colour code: Co^{II} pink.
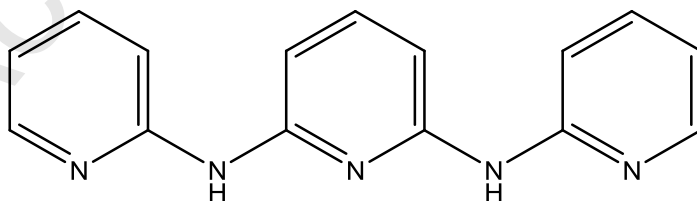
Scheme 4. The ligand *N,N'*-dipyridyl-2,6-diaminopyridine that has led to the families of Co$_5$ complexes **5** and **6**.

19

Edited Feb 6

A third structural motif in the group of Co_5 complexes is present in the mixed coordination-organometallic cluster $[Co_5(CO)(\mu\text{-}CO)(\mu_3\text{-}S)_3(pyS)_3(\mu\text{-}pyS)_4]$ (**7**) (RUQKOD), where pyS^- is pyridine-2-thiolate [99]. The formal oxidation level of the complex is $Co^ICo^{II}_4$. The five Co centres in the molecule are in raft topology, where three Co_3 triangles are aligned linearly sharing edges (Fig. 4). The *NDk-m* symbol of the decorated core of this pentanuclear CC is **2,3,4M5-1**. The absence of inorganic sulphur in the $[Co_2(CO)_8]$/NaOH/pySH/Et$_4$NCl reaction mixture in THF implies hydrodesulfurization of pySH [99]. The same motif is present in the pivalate clusters $[Co^{II}_3Co^{III}_2(\mu_3\text{-}OH)_2(\mu\text{-}OEt)(\mu_3\text{-}OEt)(piv)_8(pivH)(EtOH)_3]$ (**8**) (UMAJAT) and $[Co^{II}_3Co^{III}_2(\mu_3\text{-}OH)_2(\mu\text{-}OEt)_2(piv)_8(EtOH)_4]$ (**9**) (UMAJEX) [100]. The complexes can be described based on a tetranuclear rhomboid core, but a more natural description is as an incomplete bicapped heterocubane. Complex **8** shows four ^{1}H NMR signals in CDCl$_3$, the strongest at -24.1 and 18.1 ppm of approximately equivalent intensity, and two broader peaks at 0.62 and about 3 ppm. Surprisingly the structurally similar complex **9** (the only change being the replacement of the terminal pivH group in **8** by one terminal EtOH ligand in **9**) displays a different behaviour. From the spectroscopic study it was concluded that the paramagnetic cobalt aggregates do not conserve the symmetry observed in their solid-state structures in solution [100]. This has been attributed to the lability of the Co^{II} ion, which may involve decomposition of the core of the cluster and leading to a fluxional process involving exchange of ligands.
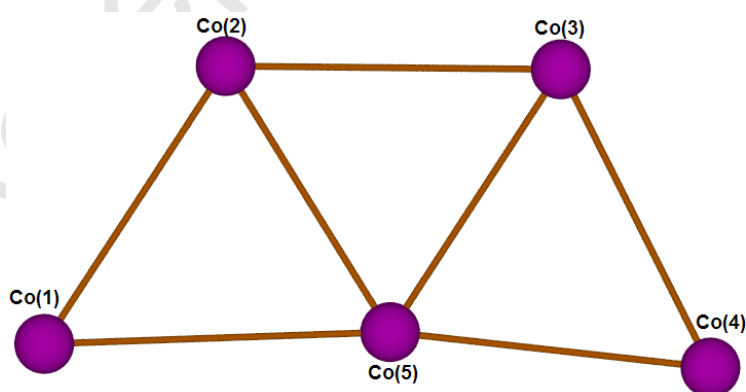
Fig. 4. The simplified core **2,3,4M5-1** of complexes **7 – 9** (RUQKOD, UMAJAT, UMAJEX). Colour code: Co pink.

20

Edited Feb 6

A fourth motif is found in complex $[Co^{II}_5(poap-H)_6](ClO_4)_4$ (**10**) (SUXPOQ) [101], where poap-H is the monoanion of the polytopic ligand shown in Scheme 5. The pentanuclear homoleptic CC involves five six-coordinate pseudo-octahedral Co^{II} centres arranged at the apexes of a trigonal bipyramid, with each apical [Co(1) and Co(4) in Fig. 5] metal ion connected to each equatorial metal ion by an alkoxide bridging atom from each of the six tetradentate ligands. Each ligand actually fills five Co^{II} coordination positions because of the bridging nature of the deprotonated oxygens. Therefore there is an exact match between the donor requirements of the five metals (30 coordination sites) and available donors provided by the ligands (30). The complex can be described with the *NDk-m* symbol **2,3M5-1**. The μ_{eff} value for **10** drops from 10.6 BM at 300 K (a value consistent with the presence of five high-spin Co^{II} centres) to 2.7 BM at 2 K, indicating significant antiferromagnetic coupling within the pentanuclear cation. The low value at 2K may indicate that the ground state for this system is $S = 1/2$. No attempt was made to fit the data to an isotropic Co^{II}_5 tbp exchange model.
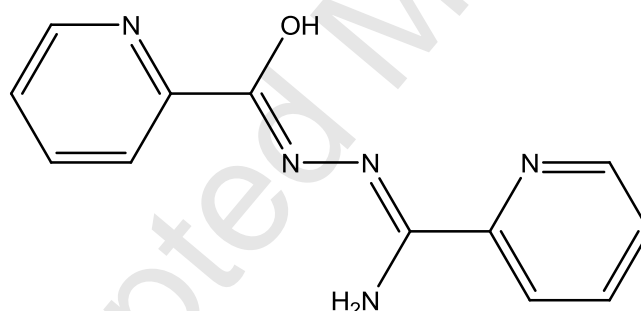
Scheme 5. The ligand poapH that is present (in its anionic form) in complex **10.**
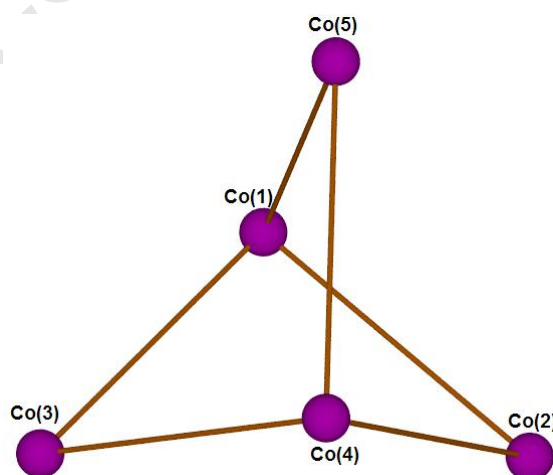
Fig. 5. The simplified core **2,3M5-1** of **10** (SUXPOQ). Colour code: Co^{II} pink.

21

Edited Feb 6

A last, but magnetically more interesting motif, is based on a square pyramidal metallic skeleton. This was first reported in 2003 in the CC $[Co^{II}_5(\mu_4\text{-OH})(\mu\text{-OMe})(\mu\text{-O}_2CMe)(L)(MeOH)_4](O_2CMe)$ (**11**) (FISLOJ) [102], where L^{6-} is the hexadeprotonated pinched conic, anion of *p-tert*-butylthiacalix[6]arene which acts as a pentanucleating ligand. In this motif each node is connected to the other four nodes (Fig. 6) and the *NDk-m* symbols is **4M5-1**.
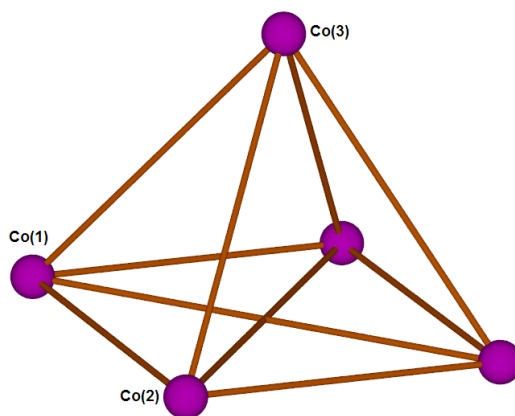

Fig. 6. The simplified core **4M5-1** that is present in complexes **11** – **14** (FISLOJ, GUMNIM, GUMNOS, GUMNEI). Colour code: Co^{II} pink.

Our group have studied the $Co^{II}/pivH/t$bdeaH$_2$ reaction system, where $t$bdeaH$_2$ is *N-tert*-butyldiethanolamine. The systematic investigation of several synthetic parameters led to products [103] $[Co^{II}_5(\mu_4\text{-N}_3)(\mu\text{-piv})_4(piv)(t\text{bdea})_2(MeCN)_2]$ (**12**) (GUMNOS), $[Co^{II}_5(\mu_4\text{-Cl})(Cl)(\mu\text{-piv})_4(t\text{bdea})_2(pivH)_2]$ (**13**) (GUMNIM) and $[Co^{II}_5(\mu_4\text{-N}_3)(Cl)(\mu\text{-piv})_4(t\text{bdea})_2(pivH)_2]$ (**14**) (GUMNEI) which all have the simplified core shown in Fig. 6. In **12** the end-on $\mu_4\text{-N}_3^-$ ligand bridges the square face of the distorted square pyramidal complex. The $\mu_4\text{-N}_3^-$ in **12** has been replaced by a $\mu_4\text{-Cl}^-$ group in **13**, while **14** can be considered to be a hybrid of structures **12** and **13**. It was found that while the chloro-bridged complex **13** does not show an out-of-phase magnetic susceptibility signal, which excludes SMM behaviour, the azido-bridged compounds **12** and **14** show out-of-phase signals as well as frequency dependence of the ac susceptibility, as expected for SMMs (Fig. 7). From the fitting of the $\chi_M T$ vs T data, we have proposed an $M_Z = \pm 5/2$ ground state. The U_{eff} value for **12** is 14 K. Compound **13** possesses an $M_Z = \pm 1/2$ ground state and hence no energy barrier. The study highlights the sensitivity of Co^{II} SMMs to the local structure.

22

Edited Feb 6

We have also established a physical model, which fits the $\chi_M T$ vs T and M vs field curves of the three compounds and reproduces the observed SMM trend. The analysis showed that small changes in the ligand shell modify the magnitude of exchange constants, and affect the J and g matrices in a non-trivial way [103].
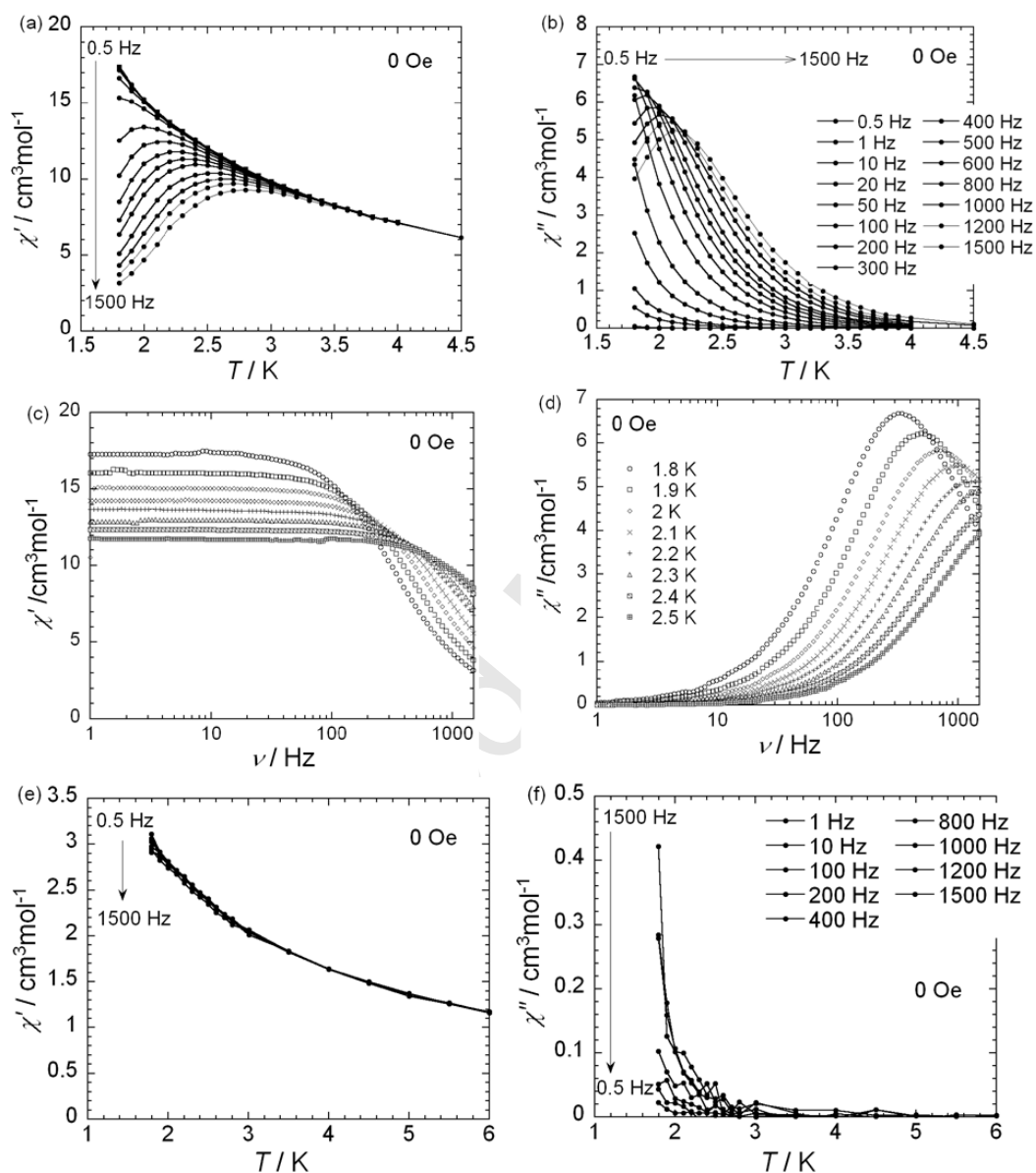

Fig. 7. Various magnetic data for complexes **12** (curves a-d) and **14** (curves e and f). Complex **14** is likely a SMM with a blocking temperature (T_B) well below 1.8 K.

5.2. Co$_6$

Edited Feb 6

The structural chemistry of the Co_6 CCs is rich. A common motif is that of Fig. 8. It was first reported [104] in compound $[Co^{II}_6(\mu_3\text{-}OH)_2(L)_{10}]$ (**15**) (AJITES), where L^- is the phenylcinnamate ligand. The molecule contains both octahedral and tetrahedral Co^{II} sites. Topologically, the decorated version of **15** can be considered as the fusion of four triangles or as a half heptanuclear disk (vide infra) with an extra node. Co(1), Co(2) and Co(3) are 4, 2 and 3-c.n., respectively, and the *NDk-m* symbol for the complex is **2,3,4M6-1**. It should be mentioned that in Mn chemistry the same motif has been observed in the $[Mn^{III}_6O_2(Etsao)_6\{O_2CPh(Me)_2\}_2(EtOH)_6]$ SMM [40] which still holds the record U_{eff} and T_B for a 3d-metal-based SMM. The some motif was subsequently found in mixed-valence Co clusters [105-109]. Q-band EPR spectra and variable-temperature magnetic susceptibility studies for $[Co^{II}_4Co^{III}_2(O_2CR)_4(hmp)_8](ClO_4)_2$ [R=Me(**16**) (JISNUV), Ph(**17**) (JISNOP); Hhmp = 2-(hydroxymethyl)pyridine] provide strong evidence that the Co^{II} centres are antiferromagnetically coupled [106]. $[Co^{II}_4Co^{III}_2(O_2CMe)_6(ampd)_4(H_2O)(MeOH)]$ (**18**) (SEQPOU) was obtained from the reaction of $Co(O_2CMe)_2$ $4H_2O$ and 2-amino-2-methyl-1,3-propanediol (ampdH$_2$) in MeOH [108]. Below 30 K, the effect of intramolecular ferromagnetic exchange interactions becomes apparent in the $\chi_M T$ vs T curve. The ferromagnetic coupling was analyzed in terms of an anisotropic exchange model, and inelastic neutron scattering data are consistent with the proposed model. No peak in the out-of-phase ac magnetic susceptibility was observed down to 1.8 K. Compound $[Co^{II}_4Co^{III}_2(piv)_4(dea)_2(Hdea)_4](ClO_4)_2$ (**19**) (PUPWON), where H$_2$dea is diethanolamine, exhibits an overall antiferromagnetic behaviour with a ground singlet spin state [109]. In 2007, the CC $[Co^{II}_4Co^{III}_2(\mu_3\text{-}OMe)_4(O_2CMe)_2(fsaea)_2(NO_3)_2(MeOH)_2]$ (**20**) (TICVAD), where H$_3$fsea is 3-[*N*-(2-hydroxyethyl)formimidoyl]-salicylaldehyde, was reported [110]. The magnetic behaviour of **20** is indicative of ferromagnetic exchange interactions between the Co^{II} atoms. The ferromagnetic behaviour can be understood by the accidental orthogonality [6] of the magnetic orbitals of Co^{II} atoms derived from the metal topology.

24

Edited Feb 6
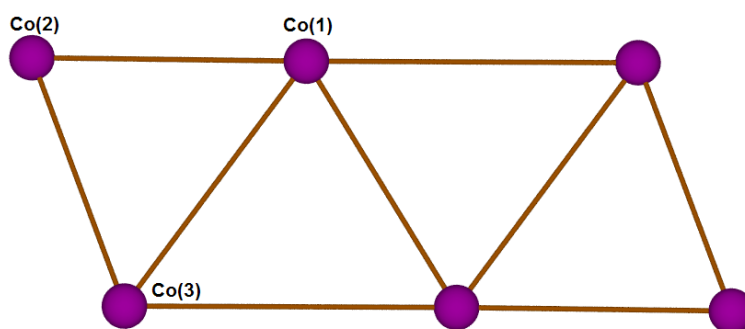
Fig. 8. The simplified core **2,3,4M6-1** that is present in **15 – 20**. Colour code: Co pink.

In 2003, the CC $[Co^{II}_3Co^{III}_3L^1_6(OH)(H_2O)_3]Cl_2$ (**21**) (AMEVOD) where H_2L^1 is *N*-(2-hydroxybenzyl)ethanolamine] with a core of quadruple face-sharing defective cubane-like units was reported. [110] Magnetic studies showed dominant antiferromagnetic interactions among the Co^{II}_3 moiety. Its topological analysis reveals a binodal cluster with the *NDk-m* symbol **2,4M6-1**.
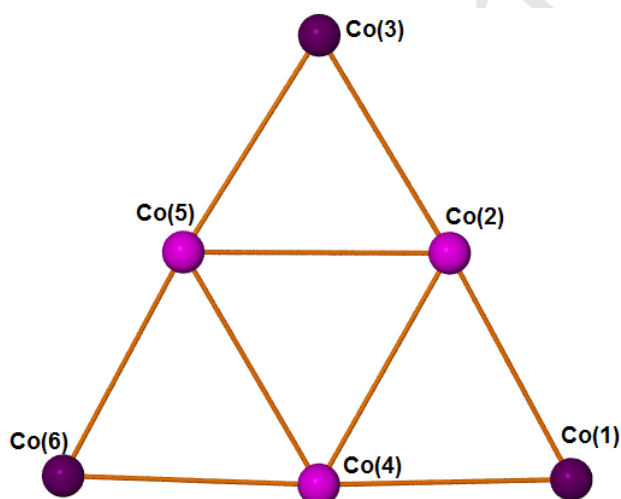
Fig. 9. The simplified core **2,4M6-1** that is present in **21**. Colour code: Co^{II} pink, Co^{III} mauve.

The "chair" motif of Fig. 10 was first observed [111] in complex $[Co^{II}_6(Ph_2PCH_2CH_2CO_2)_{12}]$ (**22**) (CAWJIT) using the hybrid ligand 3-(diphenylphosphino)propanoic acid. All nodes are 2-c.n. and the *NDk-m* symbol is **2M6-1**. The same motif is also present in $Co^{II}_2Co^{III}_4$ CCs [112]. However, this numerical presentation corresponds also to "wheel" motifs [113,114]. Complex $[Co^{II}_6(O_3P^tBu)_2(chp)_8(Hchp)_2(H_2O)_2]$ (**23**) (TIWFOV) was prepared from the reaction of $Co(NO_3)_2 \cdot 6H_2O$, 6-chloro-2-hydroxypyridine (Hchp) and *tert*-butylphosphonic acid ($^tBuPO_3H_2$) in MeCN in the presence of Et_3N [114]. The complex contains a centrosymmetric plane of six Co^{II} centers; within the

25

Edited Feb 6

asymmetric unit the three metal sites are bridged by a 3.111 phosphonate (Scheme 6). The two halves of the molecule are held together by two μ_2-oxygens from a 2.21 chp$^-$ ligand. The asymmetric unit contains three 2.21 chp$^-$ ligands, one 2.11 chp$^-$ group and one terminal 1.10 Hchp molecule (Scheme 6). Two Co^{II} atoms are six-coordinate and the other four 5-coordinate. Terminal H$_2$O molecules are found attached to the six-coordinate metal sites. The complex shows a steady decrease in $\chi_M T$ as T falls. This is largely due to single ion effects of Co^{II}. The maximum in the curve at ~8 K reflects a non diamagnetic ground state for **23**. An out-of-phase signal was not detected above 1.8 K.
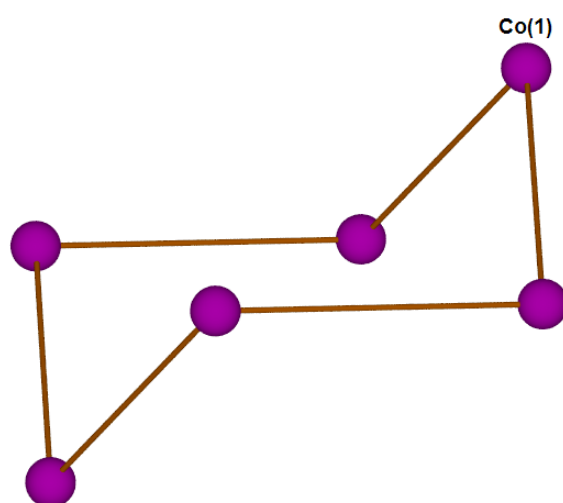
Fig. 10. The simplified core **2M6-1** that is present in **22–23** (CAWJIT, TIWFOV). Colour code: Co^{II} pink.

3.111   2.11   2.21
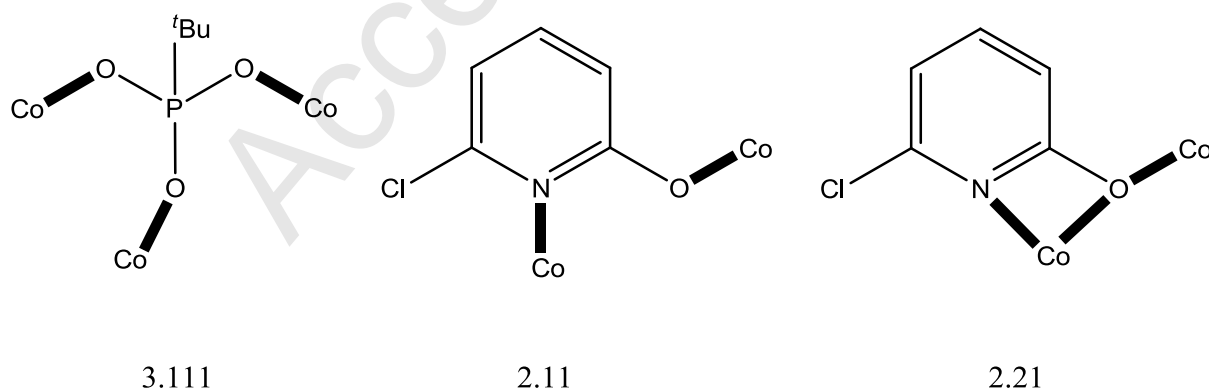
Scheme 6. The coordination modes of the bridging ligands in **23** and the Harris notation [11] that describes these modes.

26

Edited Feb 6

Another motif in Co_6 structural chemistry derives from the linking of two triangles (Fig. 11). This pattern is found in $[Co^{II}_6(\mu_3\text{-}OH)_2(O_2CPh)_{10}(PhCO_2H)_4]$ (24) (DAVYEF) [115] and other complexes [116 – 118]. The metal nodes are 2- and 3- c.n. and the *NDk-m* symbol is **2,3M6-1**.
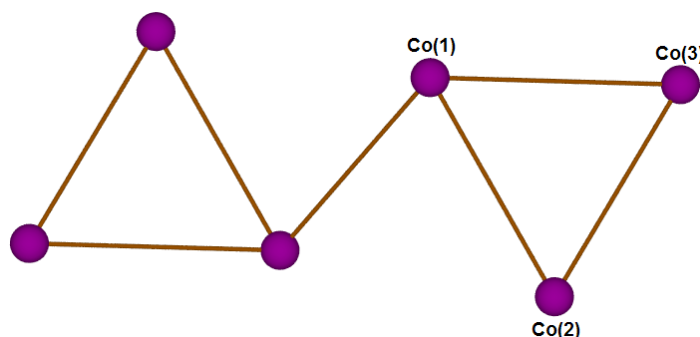
**Fig. 11**. The simplified core **2,3M6-1** that is present in **24** (DAVYEF). Colour code: Co^{II} pink.

The next two motifs are similar. Both can be described as two fused (through one edge) tetrahedra (Fig 12), although in one case there is an extra connection between the two top vertices of the tetrahedra (Fig 12, left). An alternative description of the latter is as a half wheel in which the sixth metal ion is placed out of the plane [93, 100, 107, 119]. Numerically, Co(5) and Co(6) are 3-c.n., Co(2) and Co(4) 4-c.n., and Co(1) and Co(3) are 5-c.n.; thus the *NDk-m* symbol is **3,4,5M6-1**. Typical example of CCs with this motif is $[Co^{II}_6(\mu_3\text{-}OH)(piv)_5(L)_6]$ (25) (SISKUB) [118], where HL is 6-methyl-2-hydroxypyridine. In the second case (Fig. 12, right), Co(3), Co(4), Co(5) and Co(6) are 3-c.n., while Co(1) and Co(2) are 5-c.n.; thus the binodal CC can be described as **3,5M6-1** [120]. Typical examples of this motif are the compounds $[Co^{II}_4Co^{III}_2(\mu_4\text{-}O)_2(piv)_{10}(EtOAc)_2]$ (26) (UMAJIB) and $[Co^{II}_4Co^{III}_2(\mu_4\text{-}O)_2(piv)_{10}(pivH)_4]$ (UMAJOH) (27) [100].

27
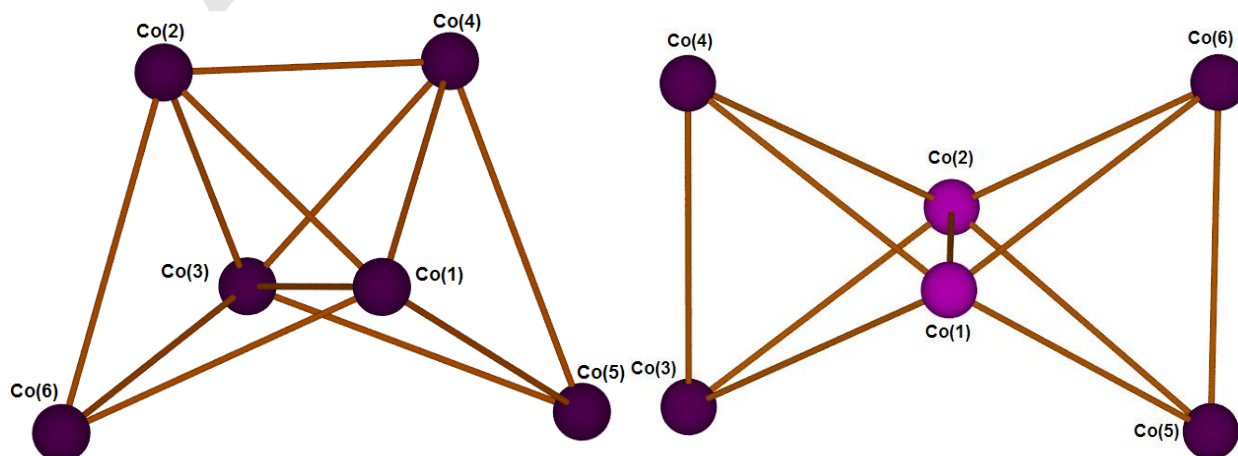
Edited Feb 6

Fig. 12. Two related simplified cores **3,4,5M6-1** found in **25** (SISKUB) (left) and **3,5M6-1** found in **26-27** (UMAJIB-UMAJOH) and related complexes. Color code: Co^{II} pink, Co^{III} mauve.
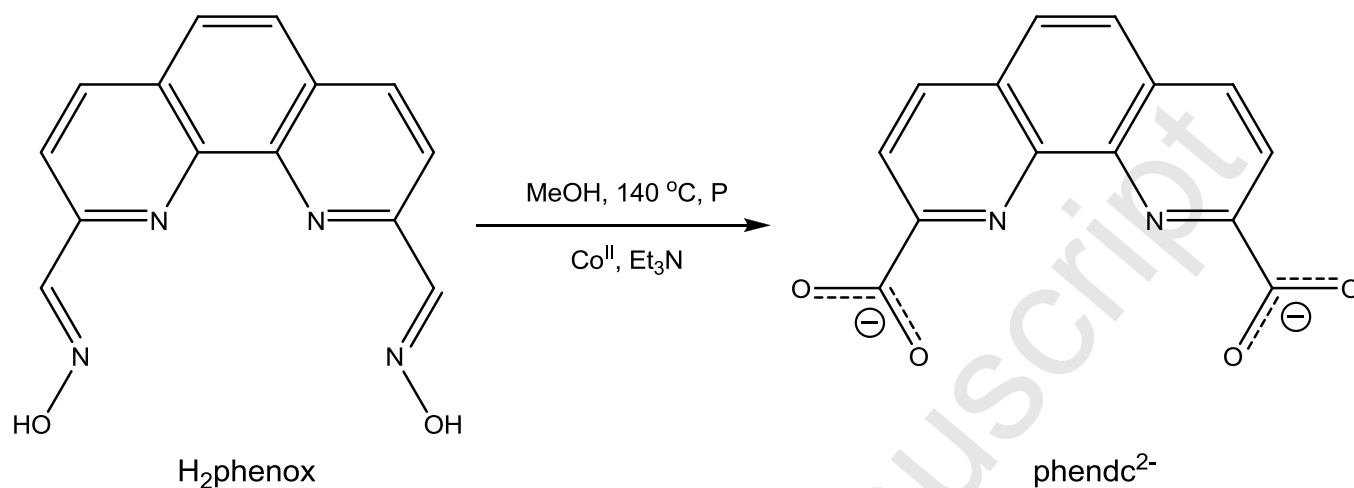

H_2phenox $\qquad$ phendc^{2-}

Scheme 7.The observed, Co^{II}-mediated transformation of H_2phenox to phendc^{2-} during the preparation of **28** and **29**. The formation of coordinated phendc^{2-} is most probably triggered by hydrolysis of H_2phenox to the corresponding dialdehyde, followed by the atmospheric oxygen oxidation of the latter to H_2phendc which is then deprotonated by the base.

Recently, Zeng, Kurmoo and co-workers reported [121] the two structurally interesting complexes (Et$_3$NH)[Co$^{II}_6$(μ_6-Cl)(phendc)$_6$] (**28**) and (Et$_3$NH)[Co$^{II}_6$(μ_6-F)(phendc)$_6$] (**29**) where H_2phendc is 1,10-phenanthroline-2,9-dicarboxylic acid. Complex **28** was accidentally obtained by the solvothermal reaction of 1,10- phenanthroline-2,9-dicarbaldehyde dioxime (H_2phenox) and CoCl$_2 \cdot 6H_2O$ in MeOH under alkaline (Et$_3$N) conditions (Scheme 7). The X-ray structure of a red crystal of **28** reveals one encapsulated chloride (Cl$^-$) ion sitting almost symmetrically in the centre of the six Co^{II} atoms that form a slightly distorted octahedron. Each Co^{II} adopts a rarely observed pentagonal bipyramidal coordination; the chromophore is Co^{II}O$_2$N$_4$Cl. The central μ_6-Cl is weakly coordinated to Co^{II} with unusually long bonds [Co $-$ Cl = 2.702 Å]. It is obvious that the chloride acts as a template around which a symmetric CC is generated. The replacement of the Cl$^-$ anion with other halides appears to be restricted to the size of the latter. When the same synthetic procedure was performed, with CoF$_2$ 6H$_2$O instead of CoCl$_2$ 6H$_2$O,

28

Edited Feb 6

compound **29** with a completely similar structure was isolated. Attempts to prepare the Br$^-$ and I$^-$ analogues of **28** and **29** were not successful. Thermal decomposition of the Et$_3$NH$^+$ counter ion of **28** leads to complex H[Co$^{II}_6$(μ_6-Cl)(phendc)$_6$] (**30**) through a single crystal-to-single crystal (SC-SC) transformation. The single-crystal X-ray structure of **30** reveals a {Co$^{II}_6$(μ_6-Cl)}$^{11+}$ core almost identical with that of **28**. The SC-SC transformation is accompanied by a contraction of 10.5% in cell volume from **28** to **30** because of shortening of the distances between neighbouring CCs.

The topological analysis of **28** - **30** (Fig. 13) results in a uninodal cluster, where each node participates in ten three-membered rings. This motif is very close to an octahedron; however additional links are provided by the halide templates. The *NDk-m* symbol of the cluster is **5M6-1**. Detailed magnetic analysis suggests spin-glass behaviour for **28** and **30** at different blocking temperatures of 5.3 and 7.8 K, respectively [121]. This behaviour is a consequence of the severe magnetic frustration due to the geometrical arrangement of the magnetic moments. The absence of this behaviour for **29** raises an interesting question regarding its origin and provides a remarkable example of fine-tuning of frustrated magnetic properties via host-guest interactions.
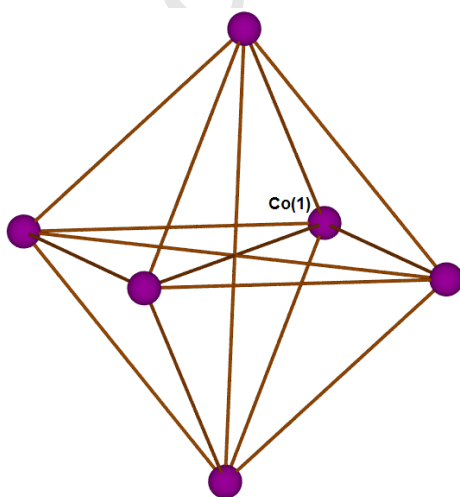

Fig. 13. The simplified core **5M6-1** that is present in **28** – **30**. Colour code: Co^{II} pink.

Using the ligand 2,7-bis(α-pyridylamino)-1,8-naphthyridine (H$_2$bpyany, Scheme 8), Lee, Peng and co-workers prepared and studied [122] the string complexes [Co$^{II}_6$(μ_6-bpyany)$_4$(NCS)$_2$](PF$_6$)$_2$ (**31**), [Co$^{II}_6$(μ_6-bpyany)$_4$(OTf)$_2$](OTf)$_2$ (**32**), and their one-electron reduced analogues [Co$_6$(μ_6-

29

Edited Feb 6

bpyany)$_4$(NCS)$_2$](PF$_6$) (**33**) and [Co$_6$(μ_6-bpyany)$_4$(OTf)$_2$](OTf) (**34**), where OTf$^-$ is the triflate anion. The ligand bpyany is a hexadentate analogue of H$_2$tdpa (Scheme 4). Compounds **33** and **34** are air-stable. Compound **33** displays rich redox chemistry. Its cyclic voltammogram exhibits four reversible redox couples at E$_{1/2}$ = -0.55, +0.38, +0.91 and +1.18 V (vs Ag/AgCl). All electrochemical reactions involve one-electron transfer, which has been confirmed by spectroelectrochemistry. Attempts to isolate and crystallize the two and three-electron oxidation products were unsuccessful. The magnetic data show that compounds **33** and **34** are in a spin state of S = 1/2, while the Co$^{II}_6$ complexes **31** and **32** in a spin state of S = 1. Extended Hückel Molecular Orbital (EHMO) calculations reveal the sum of Co-Co bond orders for **31** and **33** are 3.0 and 2.5, respectively, in agreement with their magnetic measurements.
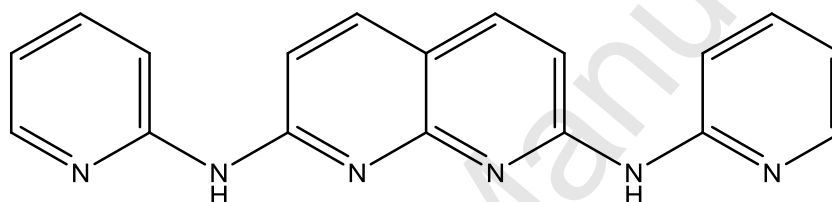
Scheme 8. The ligand 2,7-bis(*a*-pyridylamino)-1,8-naphthyridine that has led to the Co$_6$ complexes **31** – **34**.

Compounds **31** - **34** all have roughly D_4 symmetry without considering axial ligands on terminal Co sites. On the basis of structural analysis of the four CCs, the reduction of **32** and **33** occurs on the delocalized hexacobalt chain. The topological analysis of the complexes (Fig. 14) shows that Co(1) and Cl(6) are terminal nodes, while the rest metal ions are 2-c.n., thus the *NDk-m* symbol is **1,2,2M6-1**.


Fig. 14. The simplified core **1,2,2M6-1** that is present in **31** – **34** (LEJGUD, LEJHAK, LEJHEO, LEJHIS). Colour code: Co^{II} pink.

5.3. Co$_7$

30

Edited Feb 6

Two different compounds with a similar motif are present in Co^{II}_7 CCs reported by Winpenny's group [123,124]. The two compounds $[Co^{II}_7(\mu_3\text{-OH})_2(piv)_4(chp)_8(Hchp)_{0.69}(MeCN)_{0.31}]$ (**35**) (TAWJOQ) and $[Co^{II}_7(\mu_3\text{-OH})_2(O_2CPh)_4(chp)_8(MeCN)]$ (**36**) (LOSXAS) have different formulae although applying our topological approach the similarity becomes more obvious. The authors have described the metallic skeleton as a square-based pyramid capped on one triangular face and on adjacent edge by two further Co^{II} centres. Numerically, complexes **35** (Fig 15) and **36** have a *NDk-m* symbol **3,3,4,5,5M7-1**. The two compounds can be derived from the structure of the mineral $Co(OH)_2$, allowing for some distortion in the lattice.
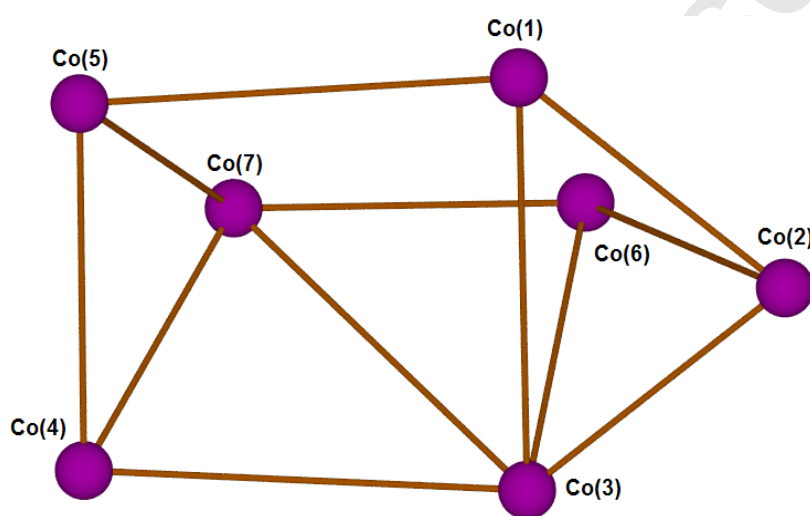
**Fig. 15.** The simplified core **3,3,4,5,5M7-1** of **35** (TAWJOQ). Colour code: Co^{II} pink.

The second motif in Co_7 chemistry is shown in Fig 16. Complex $[Co^{II}_7(\mu_4\text{-O})_2(O_2CMe)_8(NCO)_2(HNPEt_3)_4]$ (**37**) (LILQIG) was prepared from the reaction of $Co(O_2CMe)_2$ with $Me_3SiNPEt_3$ at 180 °C and subsequent crystallization from Et_2O [125]. The complex is a blue, moisture-sensitive material. The core can be described as two $\{Co^{II}_4(\mu_4\text{-O})\}^{6+}$ tetrahedra sharing a common apex. The Co^{II} atoms adopt three different coordination geometries: tetrahedral, tbp and octahedral. From the topological point of view, Co(2), Co(3) and Co(4) are 3-c.n., while Co(1) is 6-c.n.. Thus the binodal complex can be represented as **3,6M7-2**. The same motif is also found in complex $[Co^{II}_7(\mu_3\text{-OH})_2(bhqe)_3(H_2O)_6]$ (**38**) [126]. The CC was obtained through the solvothermal generation of 1,2-bis(8-hydroxyquinolin-2-yl)ethane-1,2-diol (H_4bhqe) from 2-(hydroxymethyl)quinolin-8-ol (H_2hmq), by an in situ C-C coupling

31

Edited Feb 6

reaction in EtOH also containing Co(NO$_3$)$_2$ 6H$_2$O and Et$_3$N (Scheme 9). The key factor of the structure

is that the average value of the Co^{II}-O(R)-Co^{II} angle is ~95°, and this leads to ferromagnetic coupling and

SMM behaviour (T_B = ~3 K)
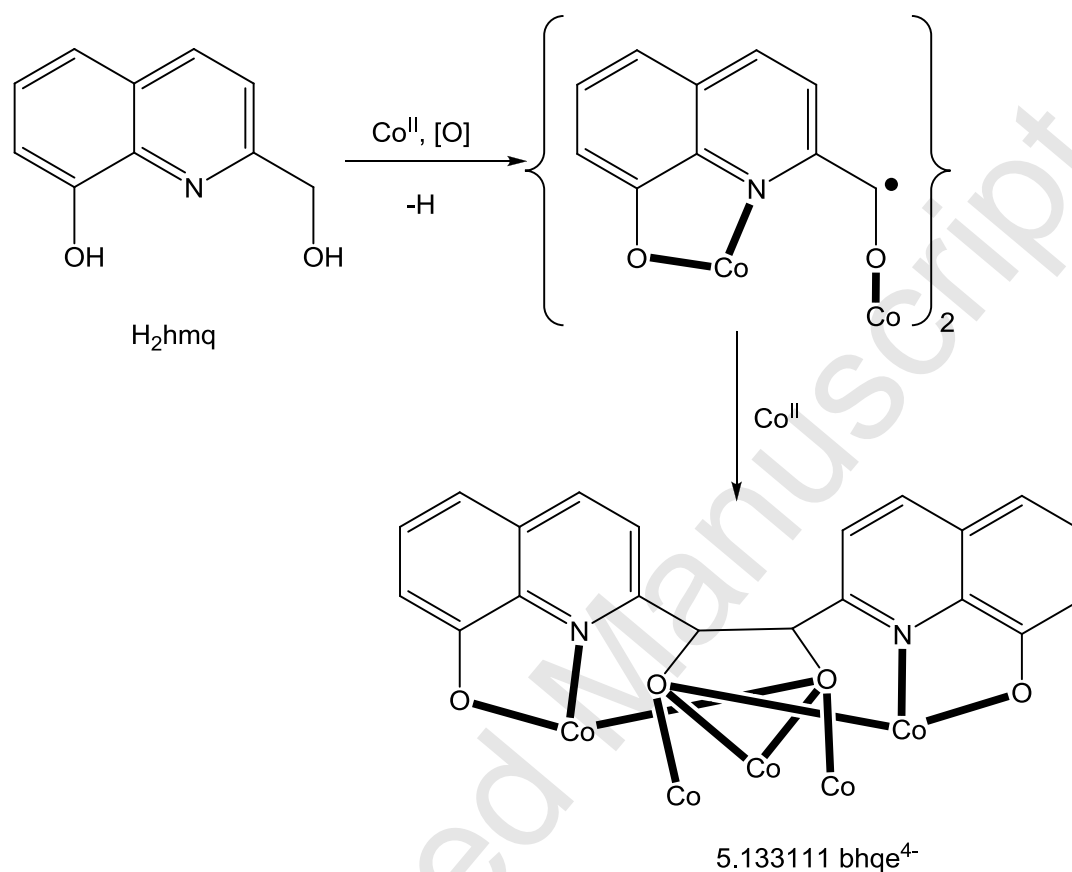
Scheme 9. The proposed simplified mechanism that leads to the μ_5-bhqe^{4-} ligand that is present in **38**.
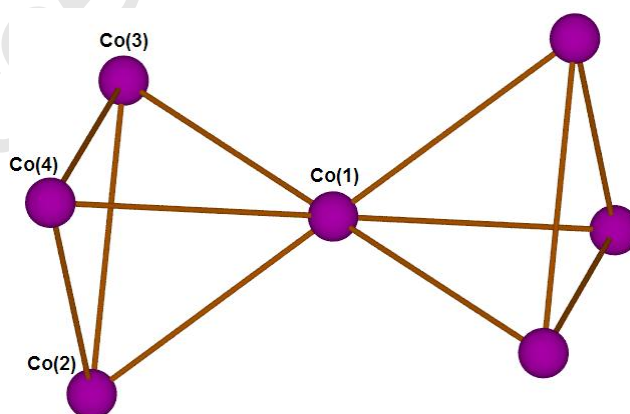
Fig. 16. The simplified core **3,6M7-2** that is present in compound **37** (LILQIG). Colour code: Co^{II} pink.

32

Edited Feb 6

The third motif is present in the cation $[Co^{II}_3Co^{III}_4(\mu_4\text{-}O)_3(\mu_3\text{-}O)(piv)_9(Hpiv)(H_2O)_3(MeCN)_2]^+$ (**39**) (UMAKAU) [100] which consists of a $\{Co^{III}_4O_4\}^{4+}$ heterocubane and three Co^{II} caps on three of the oxide atoms. The caps are five-coordinate, while the cubane sites are six-coordinate. The electrospray mass spectrum (positive ion) of the salt containing the cation **39** gives a single peak at *m/z* 1507; this comes from a heptanuclear fragment of the cation $[M^+ - 2piv - 2H_2O - 2MeCN]$. The CC presented in **39** has the *NDk-m* symbol **3,5,6M7-1**, see Fig. 17.
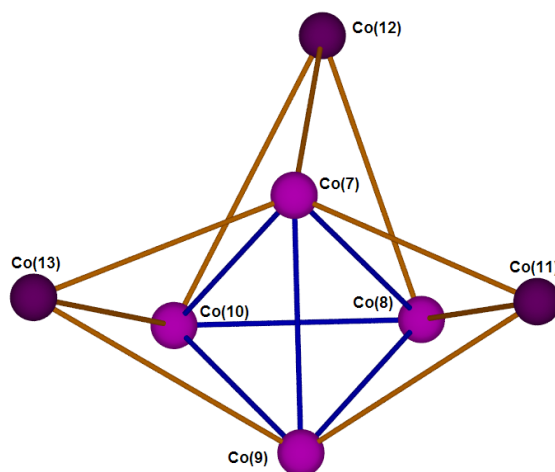
Fig. 17. The simplified core **3,5,6M7-1** that is present in the cation **39** (UMAKAU). Colour code: Co^{II} pink, Co^{III} mauve.

A rather peculiar motif is present in the heptanuclear complex $[Co^{II}_7(\mu_3\text{-}OH)_2(\mu\text{-}Cl)_2(piv)_2(L)_4Cl_4(MeCN)_4]$ (**40**) (EKUZOZ) [90], where HL is 3-one-6-(3,5-dimethylpyrazolyl-1-yl)-1,2,4,5-tetrazine. In the structure of the complex two $\{Co^{II}Cl_2(MeCN)\}$ units are attached to the main Co^{II}_5 skeleton (Fig. 18) through coordination to the carbonyl oxygen atom of L^-. Thus, there are no monoatomic bridges that link the $\{Co^{II}Cl_2(MeCN)\}$ units with the main core and the numerical representation of this CC is **2,4M5-1(0)$_2$.**

33

Edited Feb 6
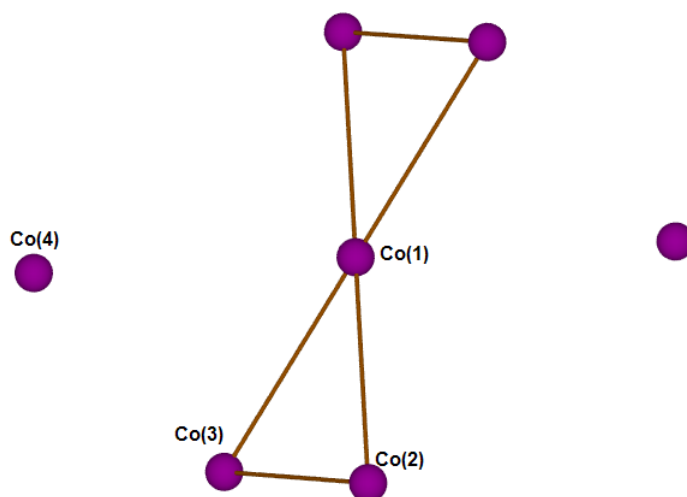
Fig. 18. The simplified core **2,4M5-1(0)₂** that is present in **40** (EKUZOZ). Colour code: Co^{II} pink.

Table 1

Chemical formulae, selected structural features and magnetic summary for wheel-shaped or disc-like Co$_7$ clusters comprising a central Co ion (Co+Co$_6$) with symbol **3,6M7-1.**

Complex[a]	μ₃-X bridge	Co-(μ₃-X)-Co(°)	Co-(μ-Ψ)-Co[c,d](°)	Magnetic behaviour	Ref.
[Co$^{II}_7$(OMe)$_3$(N$_3$)$_9$(bzp)$_6$]$^{2+}$(**41**)	MeO⁻, N₃⁻	93.2 – 95.3	99.1	F / SMM	[127]
[Co$^{II}_7$(N$_3$)$_6$(hdeo)$_6$]$^{2+}$(**42**)	N₃⁻	96.2 – 98.6	107.5	F / SMM	[128]
[Co$^{II}_7$(OMe)$_6$(immp)$_6$]$^{2+}$(**43**)	MeO⁻	95.4 – 99.0	102.9	F	[129]
[Co$^{II}_7$(OH)$_6$(L^1)$_6$]$^{2+}$(**44**)	OH⁻	96.4 – 98.6	102.6	F	[130]
[Co$^{II}_7$(OMe)$_6$(L^1)$_6$]$^{2+}$(**45**)	MeO⁻	94.4 – 98.2	102.7	F	[130]
[Co$^{II}_7$(N$_3$)$_6$(L^1)$_6$]$^{2+}$(**46**)	N₃⁻	94.9 – 98.8	104.2	F / SMM	[130]
[Co$^{II}_6$Co^{III}(thme)$_2$(piv)$_8$Br$_2$]⁻ (**47**)	RO⁻	95.2 – 101.2	85.1	F	[131]
[Co$^{II}_3$Co$^{III}_4$(OMe)$_6$(L^2)$_6$] (**48**)	RO⁻	89.4 – 101.5	103.9	F	[132]
[Co$^{II}_4$Co$^{III}_3$(HL^3)$_6$(NO$_3$)$_3$(H$_2$O)$_3$]$^{2+}$(**49**)	RO⁻	95.3 – 97.7	105.2	F / SMM	[133]
[Co$^{II}_4$Co$^{III}_3$(O$_2$CMe)$_3$(dea)$_6$]$^{2+}$(**50**)	RO⁻	94.4 – 97.9	106.8	F	[134]

[a] Counterions and solvate molecule have been omitted.
[b] R is a part of the polydentate ligand.
[c] Mean value.
[d] Ψ is most often a bridging donor atom coming from the polydentate ligand.
Abbreviations : bzp, 2-benzoylpyridine; H₂dea, diethanolamine; F, ferromagnetic exchange interactions; Hdeo, 2-hydroxy-[1,2-di(pyridinyl)ethane-1-one; Himmp, 2-iminomethyl-6-methoxy-phenol; HL^1, 2-methoxy-6-[(methylimino)methyl]phenol; HL^2, 1,1,1-trifluoro-7-hydroxy-4-methyl-5-aza-hept-3-en-2-

34

Edited Feb 6

one; H_3L^3, 2-amino-2-(hydroxymethyl)propane-1,3-diol; SMM, single-molecule magnet; H_3thme, 1,1,1-tris(hydroxymethyl)ethane.

The planar Co_7 disc is the most magnetically studied structural type in Co^{II}-based SMMs. The molecules, cations or anions possess a wheel-shaped structure comprising a central Co ion, linked to six peripheral Co ions by atoms provided by six μ_3-X bridges. Each μ_3-X group bridges the central Co ion with two peripheral metals (and also a pair of them on the rim). The six metals on the ring are held together by organic ligands and six X groups. The metallic skeleton describes a centred hexagon of six edge-sharing triangles. The skeleton can also be regarded as six defective cubanes (cubanes missing the fourth metal vertex) arranged in a circular manner, each sharing two faces. Simplifying the core, each peripheral metal ion is a 3-c.n., while Co(1) is connected to all peripheral Co atoms being a $6 - $ c.n. Thus the binodal cluster has the *NDk-m* symbol **3,6M7-1**.

The Co_7 discs have been synthesized with a variety of ligands and different in oxidation states (Co^{II}_7, $Co^{II}_6Co^{III}$, $Co^{II}_4Co^{III}_3$ and $Co^{II}_3Co^{III}_4$). Since most of the Co_7 CCs with the wheel-shaped topology have been recently reported [127–134], we have listed the structurally *and* magnetically characterized complexes of this type in Table 1 for a convenient comparison of their formulae and pertinent magnetic data; an analogous summary has been reported by Kurmoo and co-workers [27].

It should be mentioned at this point that the wheel-shaped or disc-like structural motif observed in the complexes of Table 1 is not confined to Co chemistry; it has also been observed in other heptanuclear 3d-metal CCs, most of which are mixed valent [71, 135 – 138], but also as a structural subunit in an 1D $\{Co^{II}_4Co^{III}_3\}_n$ coordination polymer [108].

35

Edited Feb 6
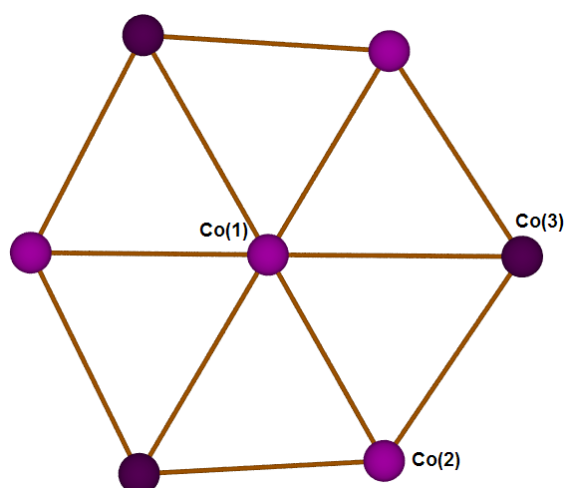
Fig. 19. The simplified core **3,6M7-1** that is present in Co_7 discs.

Perusal of Table 1 shows that only four, out of the ten structurally and magnetically characterized Co_7 clusters, belonging to the wheel-shaped group have SMM properties [139]. Whether slow magnetic relaxation is observed and to what extent appears to be very sensitive to the overall composition, structure and symmetry of the Co_7 unit. Since Murrie has recently reviewed the SMM properties of Co_7 discs in an excellent manner, we refer the interested reader to this tutorial review [7]. We devote here a few sentences on the interesting SMM properties of complex $[Co^{II}_4Co^{III}_3(HL^3)_6(NO_3)_3(H_2O)_3](NO_3)_2$ [133] containing the cation **49** (Table 1), where H_3L^3 is 2-amino-2-(hydroxymethyl)propane-1,3-diol ("tris", Scheme 10). The magnetic data can be understood by considering ferromagnetic coupling of the four effective spin $S' = 1/2$ carriers, leading to an effective $S' = 2$ ground state. Single-crystal magnetization vs applied field hysteresis loops show magnetic hysteresis below 0.5 K, which is temperature and sweep rate dependent, confirming SMM behaviour. The coercive field is very small, no doubt due to the very fast tunnelling. Due to weak intermolecular interactions, the first step in the hysteresis loop (attributed to quantum tunnelling) is shifted ± 30 mT from zero field. This suggests a very small antiferromagnetic exchange bias between cations at about 30 mT. The closest intercluster Co   Co distance is just over 10 Å. However, there is a H-bonding interaction between the free OH groups of the tris ligands on adjacent cations **49** [7].

36
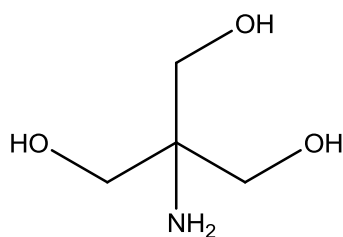
$$H^3L_3$$

Scheme 10. The "tris" ligand used for the preparation of the salt containing the cation **49**.

5.4. Co_8

Oxidation of $Co(O_2CPh)_2$ in MeCN with aqueous H_2O_2 leads to a dark emerald-green solution from which $[Co^{II}_4Co^{III}_4(\mu_4\text{-}O)_4(O_2CPh)_{12}(MeCN)_3(H_2O)]$ (**51**) (LETYOY10) can be isolated. The molecule has idealized T_d symmetry [140]. The structure consists of a central $\{Co^{III}_4O_4\}^{4+}$ cubane unit, with each $\mu_3\text{-}O^{2-}$ ion becoming μ_4 by attachment to a Co^{II} centre to give a $\{Co_8(\mu_4\text{-}O)_4\}^{12+}$ core; the cubane unit is thus bridging the four Co^{II} atoms. As seen in Fig. 20, the clusters are binodal with the *NDk-m* **3,6M8-1**. ^{1}H NMR spectra recorded in $(CD_3)_2CO$, CD_2Cl_2 or CD_3OD show only one set of paramagnetically-shifted benzoate resonances suggesting effective T_d solution symmetry and retention of the core on dissolution [140]. The same structural motif, but with no linking of the internal Co_4 unit with the external metal ions is present in other Co_8 CCs [141-143]; the topology remains the same but has a *NDk-m* symbol **3M4-1(0)$_4$**. For example, dihydroxyfumaric acid, $HOOC\text{-}C(OH)=C(OH)\text{-}COOH$, in the presence of $Co(O_2CMe)_2$ in aqueous solution, undergoes a sequence of oxidation and benzilic acid rearrangement to give complex $[Co^{II}_8(C_4O_7)_4(H_2O)_{12}]$ (**52**). The ligand is the trisubstituted methoxide ion $^-OC(CO_2^-)_3$, a previously undocumented oxyanion of carbon, which generates the cubane inner core of a highly symmetrical octanuclear complex [142, 143]. Besides providing the μ_3 component of the cubane unit, the $C_4O_7^{4-}$ provides a carboxylate donor for each of the three Co^{II} centres bridged by its alkoxide centre, i.e. it acts as a "three-strap cubane-generating ligand". The geometry of the Co^{II} atoms within the cubane is trigonal prismatic, whereas the four outer sites are distorted octahedral. This complex displays

37

Edited Feb 6

frequency dependent out-of-phase signals in the ac susceptibility to 1500 Hz, revealing a U_{eff} value of

20.5K [143]; not all molecules in the sample are undergoing the same relaxation process.
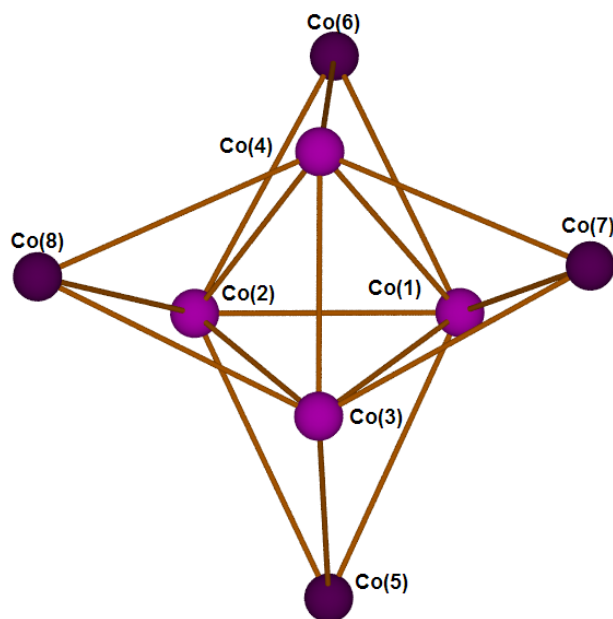
**Fig. 20**. The simplified core **3,6M8-1** that is present in **51**. Colour code: Co^{II} pink, Co^{III} mauve.

The second motif found in Co_8 chemistry corresponds to compound $[Co^{II}_8O_2(L)_6]$ (**53**) (XESKIP)

reported by Saalfrank et al in 2001 [144], where L is a bis-bidentate ligand depicted in Scheme 11. The

topological representation of this compound can be considered as a join of two tetrahedra with the *NDk-m*

symbol being **3,4M8-1**.
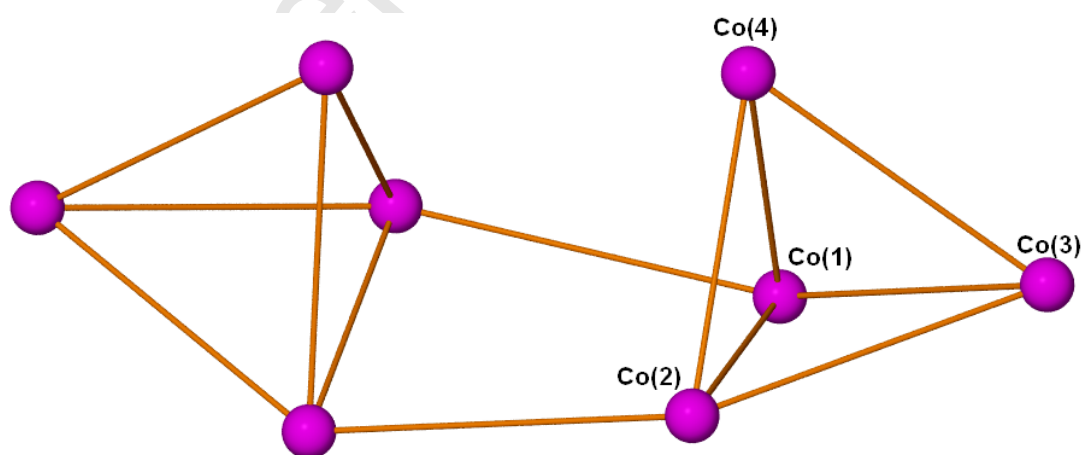
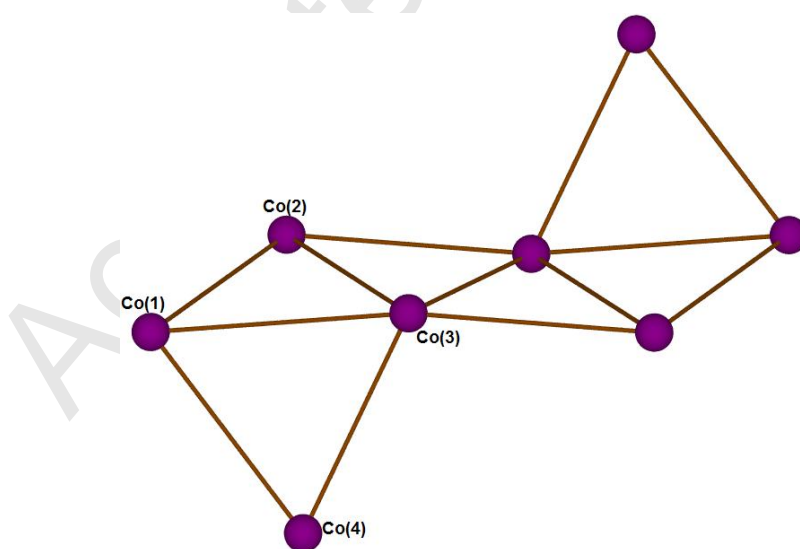**Fig. 21**. The simplified core **3,4M8-1** that is present in **53** (XESKIP). Colour code: Co^{II} pink.

38

Edited Feb 6
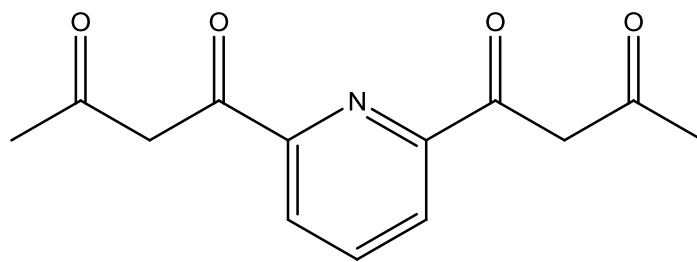

Scheme 11. The ligand L used for the preparation of compound **53**.

The third motif within the Co_8 family of CCs can be found by decoration of complex $[Co^{II}_8(\mu_3-$OH$)_4(\mu$-OH$)_2($piv$)_8($L$)_2($Hpiv$)_4($H$_2$O$)_2]$ (**54**) (LICYOM) [107]. The complex was prepared from the 2:2:1 reaction between 2,4,4,5,5-pentamethyl-4,5-dihydro-1H-imidazole-1-oxyl (Im-Me), 2,4,4,5,5-pentamethyl-4,5-dihydro-1H-imidazole-3-oxide-1-oxyl (NIT-Me) and $[Co^{II}_4Co^{III}_2O_2($piv$)_{10}($THF$)_3($H$_2$O$)]$ [118]. An impressive, metal-ion mediated transformation of the organic radicals used to L$^-$ takes place during the reaction (Scheme 12). The polymetallic matrix serves for fixation and kinetic stabilization of the resulting ligand. The simplified metallic core of **54** is shown in Fig. 22. Co(4) is 2 – c.n., Co(1) and Co(2) are 3 – c.n. and finally Co(3) is 5-c.n., and thus the tetranodal cluster can be presented as **2,3,3,5M8-1**.
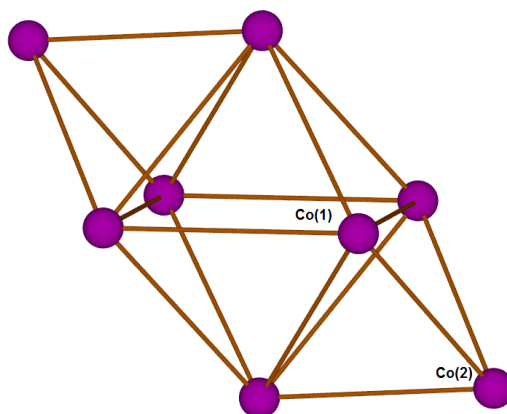

Fig. 22. The simplified core **2,3,3,5M8-1** that is present in **54** (LICYOM). Colour code: Co^{II} pink.

39

Edited Feb 6
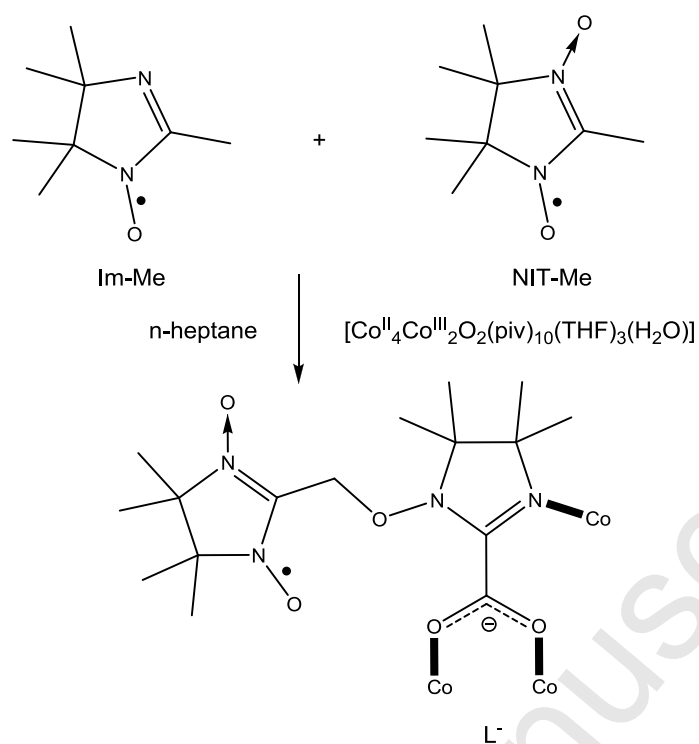
Scheme 12. The transformation of the organic radicals Im-Me and NIT-Me into the coordinated ligand L$^-$ during the preparation of **54**.

In 1966, Blake reported the synthesis of [Co$^{II}_8$(μ_4-O)$_2$(piv)$_{12}$] (**55**) (ZZZWQS) [145]. The decorated motif can be considered as an octahedron capped by two further Co^{II} atoms at two opposite faces (Fig. 23). Topologically, Co(2) is 3 – c.n. and Co(1) is 5 – c.n., therefore the binodal cluster can be represented as **3,5M8-1**. This motif is also found in other compounds [146-148], for example in [Co$^{II}_8$(μ_4-O)$_2$(O$_2$CN^{i}Pr$_2$)$_{12}$] (**56**) (MOGWEK). Mass spectral data indicate an exceptional stability of **56** in toluene [148].

40

Edited Feb 6

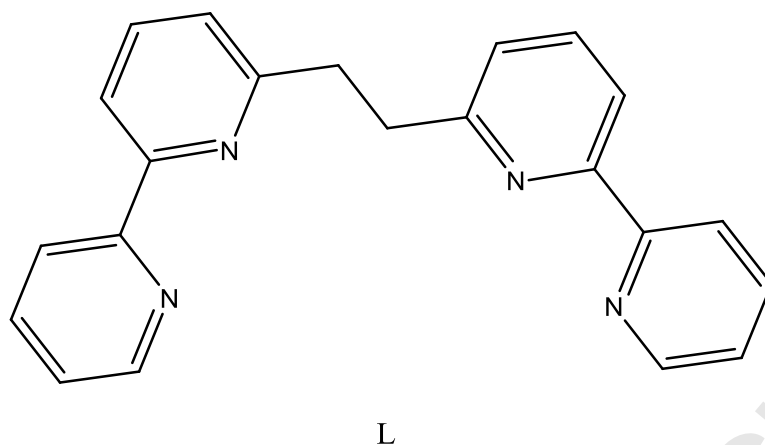**Fig. 23.** The simplified core **3,5M8-1** that is present in **55** (ZZZWQS) and related complexes. Colour code: Co^{II} pink.

Reaction of "cobalt(III) acetate" [149] and NH_4PF_6 in MeOH over one week at room temperature gave dark green $(NH_4)[Co^{III}_8(\mu\text{-}OMe)_{16}(O_2CMe)_8](PF_6)$ (**57**) (PAQFAO) [150]. The molecule has a highly symmetric toroidal shape. The Co^{III} atoms are situated at the vertices of a near regular planar octagon. Each pair of metal ions is bridged by a 2.11 $MeCO_2^-$ ligand and two stereochemically distinct 2.1 methoxy ligands, one MeO$^-$ on either side of the Co$_8$ plane. The NH_4^+ ion is situated at the centre of the molecule, with the nitrogen atom in the Co$_8$ plane. Topological analogues of **57** have been reported in the chemistry of other 3d-metals, e.g. V^{IV}/^{V} [151] and Cu^{II} [152]. Each Co^{III} is a 2-c.n. and the *NDk-m* symbol is **2M8-1** see Fig. 24.
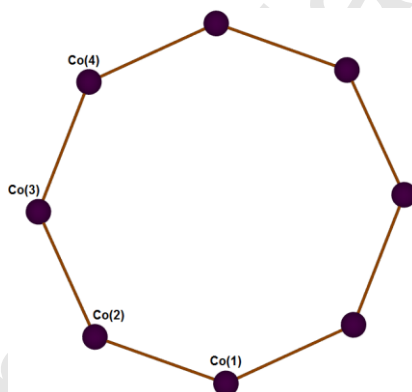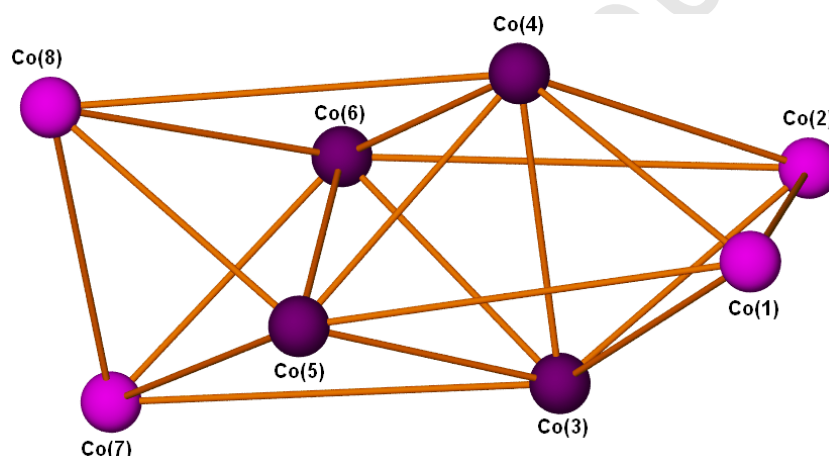

Fig. 24. The simplified core **2M8-1** that is present in **57** (PAQFAO). Colour code: Co^{III} mauve.

Addition of aqueous H_2O_2 to a solution of $Co(O_2CMe)_2$ $4H_2O$ and 1,2-bis(2,2'-bipyridyl-6-yl)ethane (L, Scheme 13), followed by addition of LiClO$_4$, allows isolation of $[Co^{II}_4Co^{III}_4(\mu_3\text{-}OH)_4(\mu_4\text{-}O)_4(O_2CMe)_6(L)_2](ClO_4)_2$ (**58**) (TOKDOM) [153]. The core comprises three face-sharing cubane units, and magnetic susceptibility studies confirm the paramagnetic nature of the compound and the presence of high-spin Co^{II} atoms. Simplifying the metallic skeleton (Fig. 25), Co(1), Co(2), Co(7) and Co(8) are 4 – c.n. while the rest are 6 – c.n.; thus the binodal cluster can be presented as **4,6M8-1**. A similar core is found in $[Co_8(\mu_4\text{-}O)_4(\mu_3\text{-}OMe)_4(OH_n)_4(O_2CMe)_6]$ (**59**) (RUQTAY), where n = 1 or 2 [154]; the X-ray structure of the latter is of poor quality.

41

L

Scheme 13. The ligand L used for the preparation of **58**.

Fig. 25. The simplified core **4,6M8-1** that is present in **58** (TOKDOM). Colour code: Co^{II} pink, Co^{III} mauve.

Complex $[Co^{II}_8(L)_4(EtOH)_3]$ (**60**) (VEHMAX) was prepared from the reaction of $Co(O_2CMe)_2 \cdot 4H_2O$ and H_4L (Scheme 14) in $EtOH/CHCl_3$. All Co^{II} centres are five-coordinate [155]. The discrete octanuclear structure is present in $MeOH/CHCl_3$ as confirmed by ESI mass spectroscopy. The $\chi_M T$ product shows a continuous decrease with decreasing T, suggesting antiferromagnetic exchange interactions between the Co^{II} atoms. The magnetic susceptibility obeys the Curie-Weiss law above 40 K with a Weiss constant θ of -39 K and a Curie constant of 19.7 cm^3Kmol^{-1}. For the topological description Co(1), Co(2), Co(3) and Co(4) are 2 – c.n. while the rest are 4 – c.n., and thus the *NDk-m* symbol is **2,4M8-1**, see Fig. 26. The same motif is found in a 3D Co^{II} coordination polymer reported recently [156].

42

Edited Feb 6
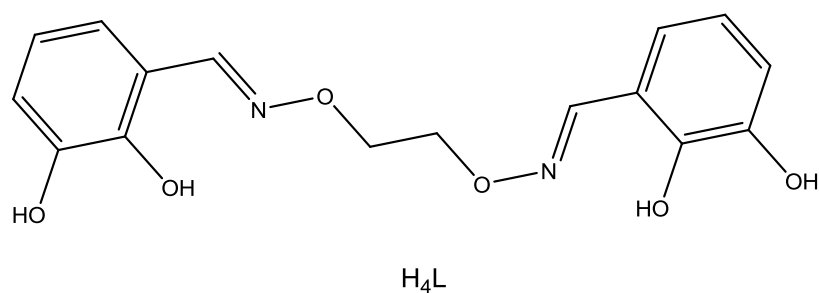
Scheme 14. The ligand H_4L used for the preparation of **60**.
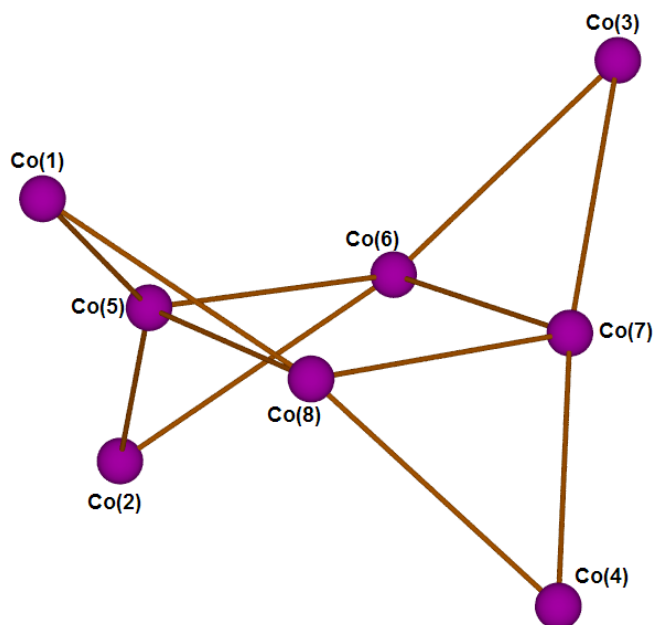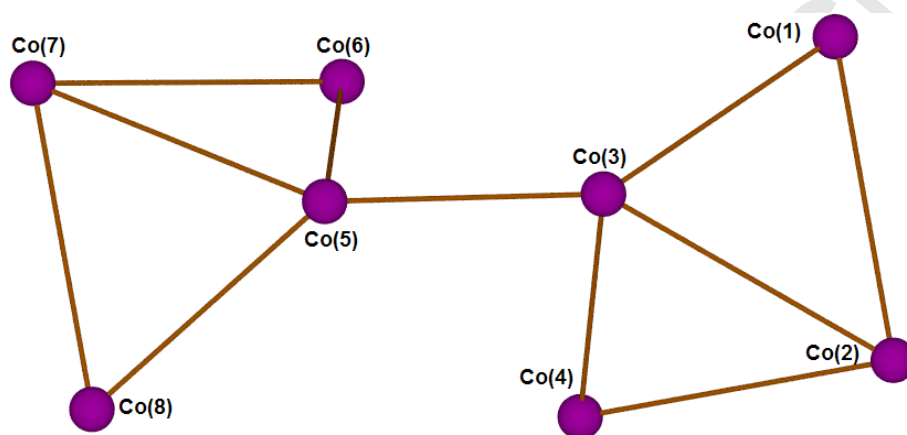

Fig. 26. The simplified core **2,4M8-1** that is present in **60** (VEHMAX). Colour code: Co^{II} pink.

A final motif in Co_8 chemistry is depicted in Fig. 27. It has been observed in the anionic CC [Et_3NH] [$Co^{II}_8(O_3PPh)_2(chp)_{10}(NO_3)_3(Hchp)_2$] (**61**) (SAVBAT) isolated from the $Co(NO_3)_2 \cdot 6H_2O$ / Hchp / $PhPO_3H_2$ / Et_3N reaction mixture in MeCN [114, 157]. The structure is irregular. Two phosphonate P atoms and four Co^{II} atoms lie on the vertices of a central trigonal prism. The final four Co^{II} atoms lie above the triangular faces of the prism. The phosphonates both show the 4.211 coordination mode. The decorated core of **61** has four 2 – c.n., [Co(1), Co(4), Co(6) and Co(8)], two 3 – c.n., [Co(2) and Co(7)], while Co(3) and Co(5) are 4 – c.n. The *NDk-m* symbol is **2,3,4M8-1**. The Et_3NH^+ cation forms a H bond to the chelating nitrato groups from neighbouring {Co_8} cluster anions, leading to a 1D chain forming in the crystal. The ac data are unusual, displaying frequency-dependent maxima in both χ'_M and χ''_M between 4 and 6 K, although the χ''_M signal is around one-tenth of the height of χ'_M. This

43

suggests that only a fraction of the magnetization is relaxing slowly [7]. The in-depth analysis [114] suggests that some Co_8-based samples (there are some differences from sample to sample) are better described as unusual examples of single-chain magnets. Compound **61** would have a higher energy barrier than that of the Mn^{III}_6 SMM [40] *if* the slow relaxation was due to a component of the crystal which is a SMM. This illustrates a "classical" problem in SMM research: the complication provided by intermolecular interactions. Excluding these interactions and the possibility that single-chain magnets are being formed will require better control of crystal packing than can currently be achieved.

Fig. 27. The simplified core **2,3,4M8-1** that is present in **61** (SAVBAT). Colour code: Co^{II} pink.

5.5. Co_9

The simplified core shown in Fig. 28 was observed in complexes $[Co^{II}_9(\eta^1:\mu_4-X)_2(O_2CMe)_8\{(py)_2CO_2\}_4]$ [X=OH, **62** (JAXSOQ); X=N$_3$, **63** (IBEZIY)], prepared and studied by a collaboration between the groups of Escuer and one of the authors of this review [158, 159]. The $(py)_2CO_2^{2-}$ ligand is the dianion of the *gem*-diol derivative, $(py)_2C(OH)_2$, of di-2-pyridyl ketone, $(py)_2CO$ (Scheme 15) [69 – 71]. Complex **62** was prepared [158] from the 2:1 reaction of $Co(O_2CMe)_2\cdot 4H_2O$ and $(py)_2CO$ in refluxing MeCN. Complex **63** was prepared from the reaction represented by Eq. (2) [159,160] :

Edited Feb 6

$$[Co^{II}{}_9(\eta^1:\mu_4\text{-}OH)_2(O_2CMe)_8\{(py)_2CO_2\}_4] \ + 2NaN_3 \xrightarrow[\text{T}]{\text{DMF}}$$

$$[Co^{II}{}_9(\eta^1:\mu_4\text{-}N_3)_2(O_2CMe)_8\{(py)_2CO_2\}_4] \ + 2NaOH \quad (2)$$
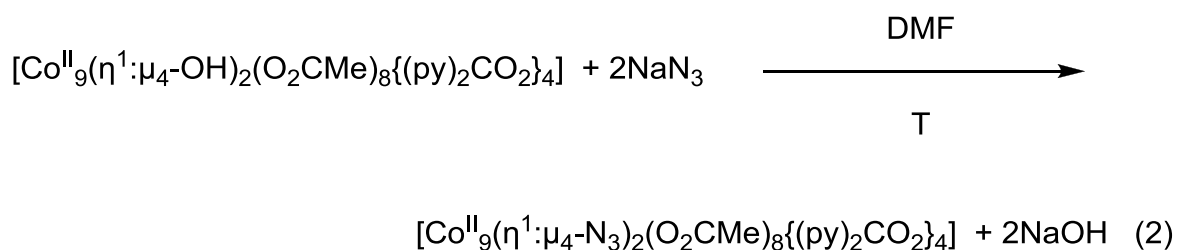
The above reaction is just an example of our general strategy [160 – 163] to increase the ground state S value of 3d-metal CCs. This strategy involves substitution of bridging hydroxy ligands, which most often propagate antiferromagnetic exchange interactions, by end-on ($\eta^1:\mu_x$, x=2,3,4) azido ligands which are good ferromagnetic couplers for a wide variety of M-N-M angles.
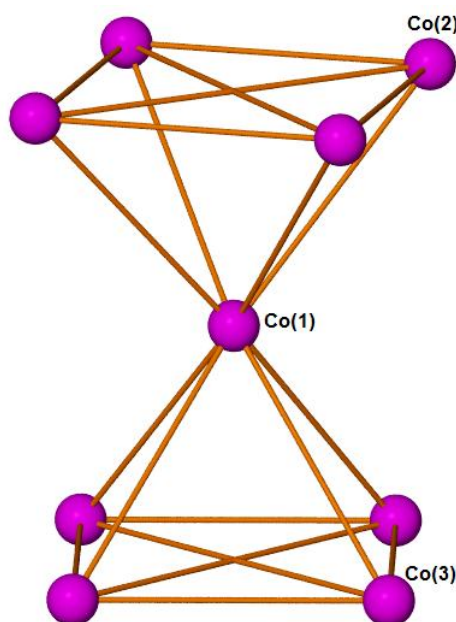
Fig. 28. The simplified core **4,8M9-1** that is present in **62** (JAXSOQ) and **63** (IBEZIY). Colour code: Co^{II} pink.

The X-ray structures of the complexes reveal that the nine Co^{II} atoms adopt a topology of two square pyramids sharing the common apex [Co(1)]. Each base is capped by one $\eta^1:\mu_4$-X$^-$ group (X=OH, N_3). The oxygen atoms of the 5.3311 $(py)_2CO_2{}^{2-}$ ligands are placed in the centre of the triangular faces of the pyramids, and bridge the central Co^{II} atom with two Co^{II} atoms of the base of each pyramid. A salient feature of the structures is the coordination number 8 of the central metal, which is extremely rare in Co^{II}

45

Edited Feb 6

chemistry [9, 82-85, 164]. The complexes are binodal with the *NDk-m* symbol **4,8M9-1**. Complex **62** exhibits an overall antiferromagnetic coupling, which is associated to dominant antiferromagnetic exchange in the Co^{II}_4 square bases of the CC giving a total *S* value in the ground state equivalent to one isolated local spin. In contrast, the data for **63** are associated to ferromagnetic coupling mediated by the end-on azido bridges giving a total ground-state *S* value of seven times that of the local spins (assuming antiferromagnetic coupling between the central Co^{II} atom and the Co^{II} atoms in the two squares), leading to a ferrimagnetic system.

$(py)_2CO$ 5.3311 $(py)_2CO_2^{2-}$
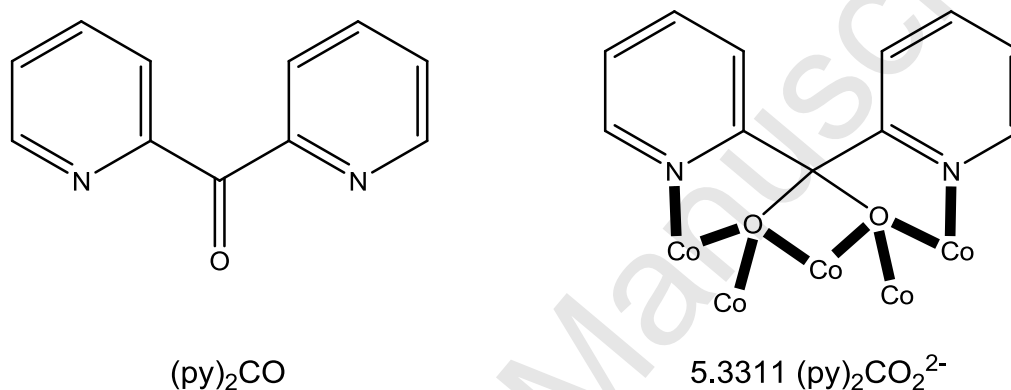
Scheme 15. Di-2-pyridyl ketone (left) and the coordinated dianion (with the Harris notation) $(py)_2CO_2^{2-}$ (right); the latter is present in compounds **62** and **63**.

A second core motif found in Co_9 chemistry was reported by Ovcharenko's group in 2007 [107]. The simplified core shown in Fig. 29 is found in various solvated forms of complex $[Co^{II}_9(\mu_3\text{-}OH)_2(piv)_{12}(L')_2]$ (**64**) (LICYUS), where L'^{2-} is the dianionic ligand shown in Scheme 16 and generated in situ from the reaction of $[Co^{II}_4Co^{III}_2(piv)_{10}(THF)_3(H_2O)]$ [118] and NIT-Me (Scheme 12). The enneanuclear decorated core consists of 2-, 3- and 6-c.n., with the *NDk-m* symbol is **2,3,3,6M9-1** .

46

Edited Feb 6
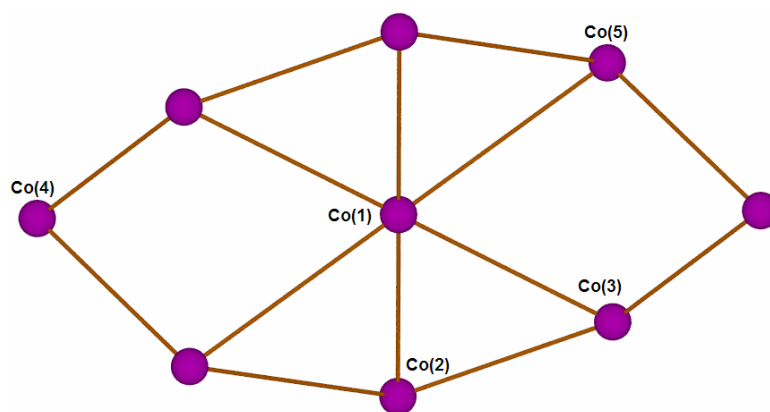
Fig. 29. The simplified core **2,3,3,6M9-1** that is present in **64** (LICYUS). Colour code: Co^{II} pink.
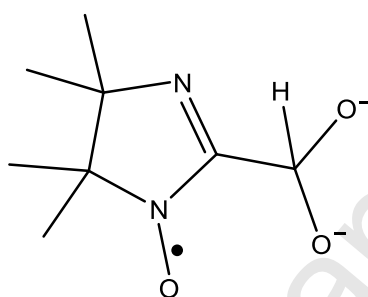
L'^{2-}

Scheme 16. The in situ formed L'^{2-} during the preparation of **64**.

In 2001, the synthesis and X-ray structure of another enneanuclear Co^{II}/piv^- complex were reported. The decorated core of $[Co^{II}_9(\mu_3\text{-}OH)_6(piv)_{12}(Me_2CO)_4]$ (**65**) (MUFTEM) [165] is shown in Fig. 30. The CC is trinodal with the *NDk-m* symbol **2,3,8M9-1**. The core of **65** is similar to that of complexes **62** and **63**.
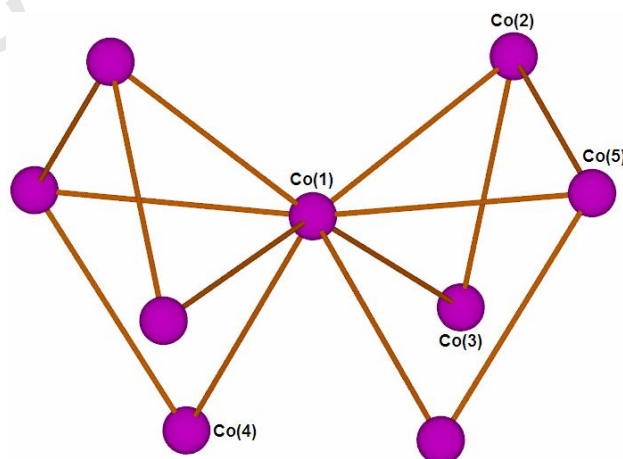
Fig. 30. The simplified core **2,3,8M9-1** that is present in **65** (MUFTEM). Colour code: Co^{II} pink.

47

Edited Feb 6

The reaction of "Co(OH)$_2$" with two equivalents of Hchp at 130 ^{o}C under N$_2$ gave a paste, which, after drying in vacuum, could be crystallized from EtOAc to give pink crystals of [Co$^{II}_9$(chp)$_{18}$] (**66**) (ROJFUR) [166]. The cage has crystallographic D_{3d} symmetry and the central cobalt [Co(1) in Fig. 31] lies on both a 3-fold axis [which also passes through Co(3)] and a 2-fold axis. The molecule contains four adamantane units. Two of them share Co(1) as a common vertex; two additional units share the basal planes [Co(2) and symmetry equivalents] with Co(3) [and symmetry equivalent] as vertex. The decorated core of **66** can be considered as two trigonal pyramids sharing on a common apex. The trinodal CC found in **66** can be represented as **3,4,6M9-1**.
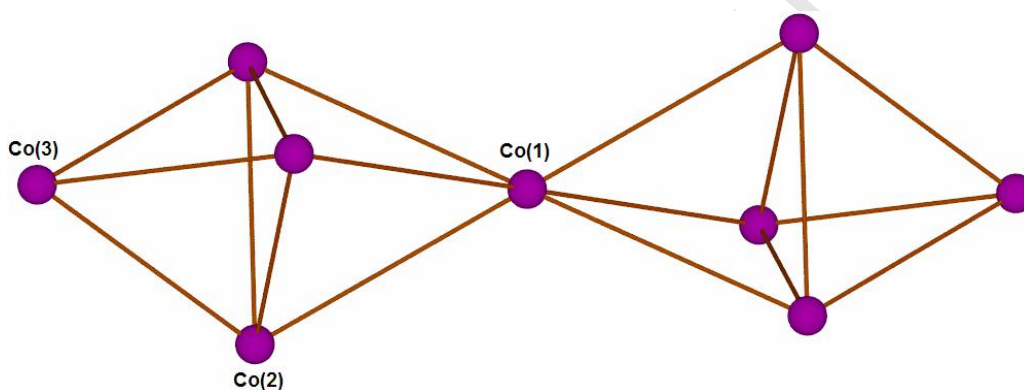
Fig. 31. The simplified core **3,4,6M9-1** that is present in **66** (ROJFUR). Colour code: Co^{II} pink.

In 2009, the group of Tao reported the remarkable mixed-valence CC [Co$^{II}_5$Co$^{III}_4$(μ_4-Cl)(HL)$_4$(L)$_4$Cl]·(**67**) (IGOYAF) [167] where H$_3$L is (*E*)-2-2((1,3-dihydroxy-2-methylpropan-2-ylimino)methyl) phenol. The complex was prepared using Co(OAc)$_2$ · 4H$_2$O under solvothermal conditions in EtOH at 140 ^{o}C for 24h in the presence of SmCl$_3$ 6H$_2$O. The molecule contains a square pyramidal Co$^{II}_5$ unit with a motif similar to that reported for **13** [103], formed through μ_4-Cl$^-$ and μ_3-alkoxy bridges. The pentanuclear unit is surrounded by four peripheral Co^{III} atoms at the basal plane of the square pyramid through μ-alkoxy atoms. The coordination modes of the HL^{2-} and L^{3-} ligands are illustrated in Scheme 17. Numerically, the core of **67** can be described as a trinodal cluster with the *NDk-*

48

Edited Feb 6

m symbol **1,4,5M9-1,** see Fig 32. The $Co^{II}\cdots Co^{II}$ exchange interactions within the Co^{II}_5 unit are both ferro- and antiferromagnetic ($D = +6.0$ cm^{-1}, $g = 2.30$) [167].

2.2111 HL^{2-}

4.3211 L^{3-}
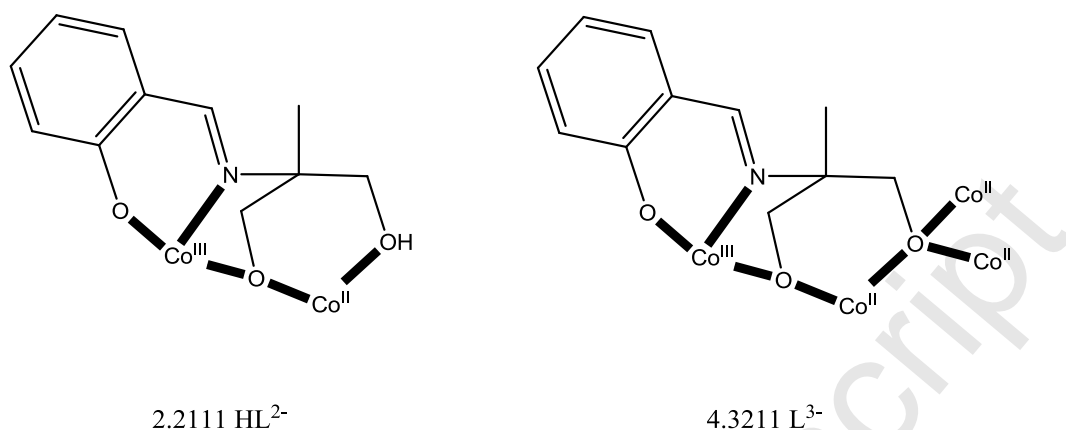
Scheme 17. The coordination modes of HL^{2-} and L^{3-} in **67** and the Haris notation that describes these modes.
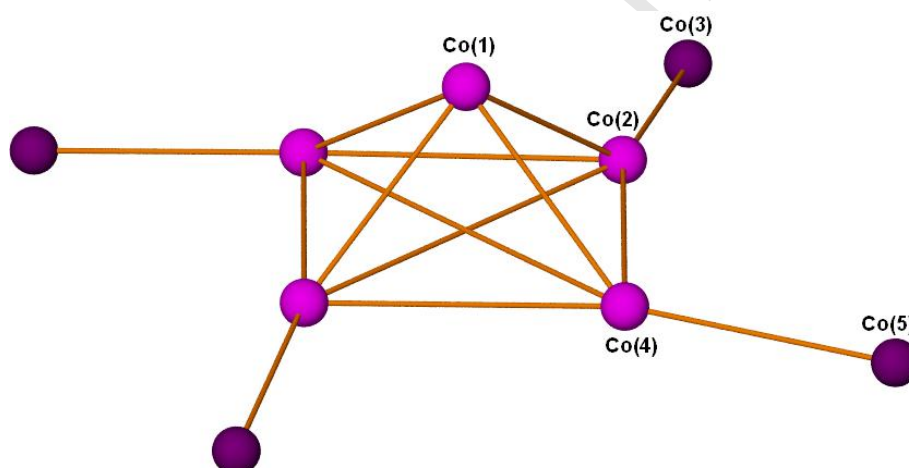
Fig. 32. The simplified core **1,4,5M9-1** that is present in **67** (IGOYAF). Colour code: Co^{II} pink, Co^{III} mauve.

5.6.   *Co$_{10}$*

In a now classical paper on the structural chemistry of Co and Ni CCs [168] the group of Winpenny reported-amongst others- the decanuclear complexes $[Co^{II}_{10}(\mu_3\text{-OH})_6(O_2CPh)_7(mhp)_6\text{-}(Hmhp)_3Cl(MeCN)]$ (**68**) (TOTYIK), $[Co^{II}_{10}(\mu_3\text{-OH})_6(piv)_7(mhp)_6(Hmhp)Cl(MeCN)_3]$ (**69**) (HUDQUS) and $[Co^{II}_{10}(\mu_3\text{-OH})_4(piv)_6(chp)_{10}(EtOH)_2]$ (**70**), (HUDRIH) where Hmhp is 6-methyl-2-pyridone. In **68**

49

Edited Feb 6

and **69** the ten metal ions describe a centered-tricapped-trigonal prism. The molecules contain six μ_3-OH$^-$ ligands around the central Co^{II}, and the exterior is coated with pyridonate and carboxylate ligands. Compound **70** contains a metal core based on an incomplete centred-tetraicosahedron; it can also be described as a centred-pentacapped trigonal prism missing two edge vertices. Compounds **68** and **69** possess a similar decorated motif (Fig. 33, left), while **69** possesses a slightly different motif (Fig. 33, right). Compounds **68** and **69** can be described as trinodal clusters with the *NDk-m* **4,5,9M10-1**, while compound **70** is a five − nodal cluster with the *NDk-m* symbol **3,4,5,5,9M10-1**. The same motifs are observed in other Co$^{II}_{10}$ clusters [119,170], e.g. [Co$^{II}_{10}$(μ_3-OH)$_6$(*o*-MeBz)$_7$(chp)$_6$(*n*-C$_3$H$_7$OH)$_5$] (*o*-MeBz) (**71**) (AHOZOM) and [Co$^{II}_{10}$(μ_3-OH)$_6$(*p*-^{t}BuBz)$_8$(mhp)$_6$(Hmhp)$_2$(MeCN)$_2$] (**72**) (AHOZUS) [169], where *o*-MeBz$^-$ is 2-methylbenzoate and *p*-^{t}BuBz is 4-*tert*butylbenzoate.
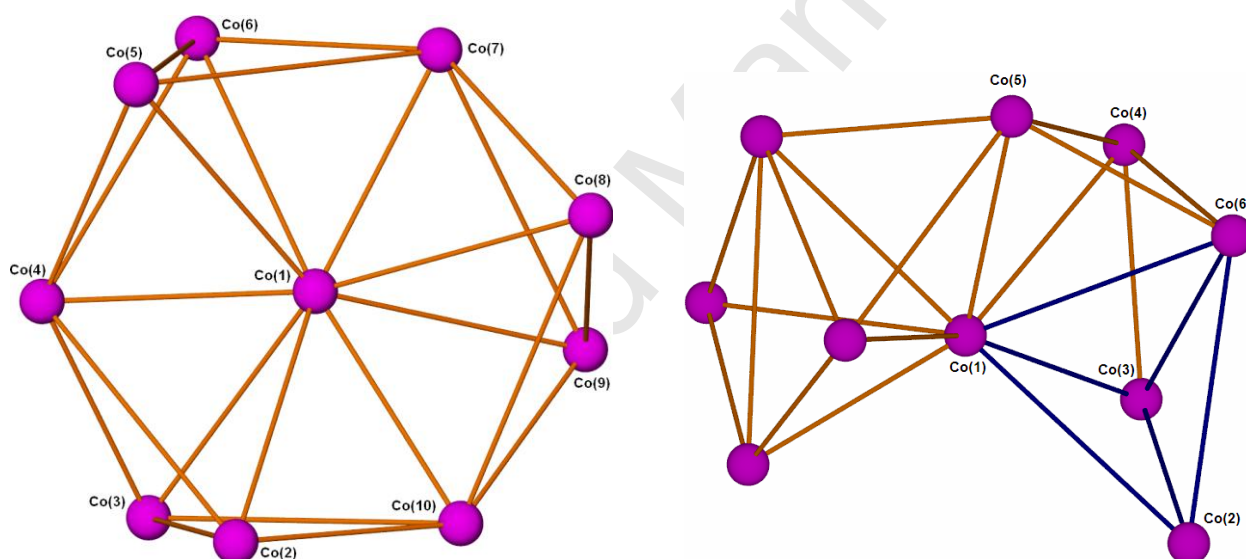
Fig. 33. The simplified core of **68**(TOTYIK), **69** (HUDQUS) and **71** (AHOZOM) (**4,5,9M10-1,** left) and **70** (HUDRIH) and **72** (AHOZUS) (**3,4,5,5,9M10-1**, right). Colour code: Co^{II} pink.

A somewhat similar motif is observed in [Co$^{II}_9$Co^{III}(μ_3-OH)$_6$(HCO$_3$)$_3$(O$_2$CCPh$_3$)$_6$(mhp)$_6$(Hmhp)$_3$] (**73**) (MARGIV) [171]. X-ray analysis reveals a centred-tricapped-trigonal prism which lies on a crystallographic C_3 axis; however, the capping metal ions are found on the edges of the prism rather than the faces, as in the structures of **68**, **69** and **71**. At the centre of the cage there is the Co^{III} site. The requirement for formation of HCO$_3^-$ (from atmospheric CO$_2$) explains the long crystallization times (4

50

Edited Feb 6

months) and low yield (~5%) of this reaction. Another description of the decorated core (Fig. 34) is a as two tetrahedra sharing the Co^{III} site, while three Co^{II} atoms [Co(3) and symmetry equivalents] are each attached to the common apex and two metal ions belonging to two different tetrahedra. Finally, the trinodal cluster has the *NDk-m* symbol **3,4,9M10-1**.
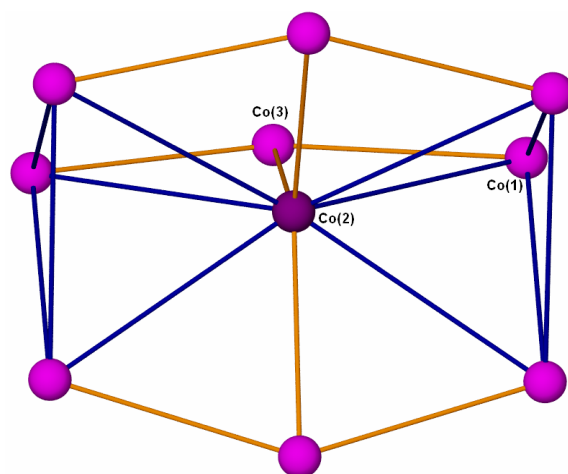
Fig. 34. The simplified core **3,4,9M10-1** that is present in **73** (MARGIV). Colour code: Co^{II} pink, Co^{III} mauve.

The next motif in Co_{10} chemistry has been observed in complex $[Co^{II}_{10}(piv)_{14}(L')_2(L'')_2(Hpiv)_2]$ (**74**) (LICXOL) [107], another product from the fertile $[Co^{II}_4Co^{III}_2(piv)_{10}(THF)_3(H_2O)]$/Im-Me (Scheme 12) reaction system. L'^{2-} is the in situ formed ligand shown in Scheme 16, while the structural formula of L''^- (also formed in situ) is illustrated in Scheme 18. The decorated core of **74** (Fig. 35) can be considered as a fusion of six triangles, sharing alternately three edges and two nodes. The CC has the *NDk-m* symbol **2,3,3,4M10-1**.
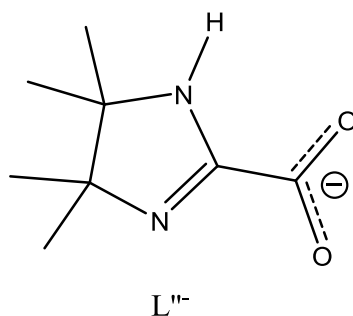
Scheme 18. The in situ formed ligand L'''^- during the preparation of **74**.

51

Edited Feb 6
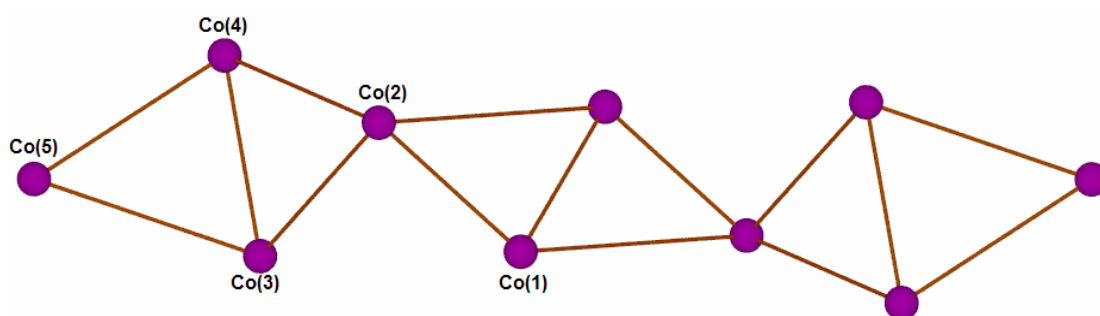
Fig. 35. The simplified core **2,3,3,4M10-1** that is present in **74** (LICXOL). Colour code: Co^{II} pink.

If ethylenediphosphonic acid reacts with $Co(BF_4)_2$ $6H_2O$ and Hchp in the presence of Et_3N in MeCN, the decanuclear complex $[Co^{II}_{10}(\mu_3\text{-}OH)_2(O_3PCH_2CH_2PO_3)(chp)_{14}]$ (**75**) (TIWGIQ), can be made [114]. The 10 Co^{II} and 2 P sites of the molecule lie on the vertices of an octahedron that is capped on 4 faces and 2 edges. Both PO_3^{2-} end groups of the diphosphonate show a 5.211 binding mode, but two Co sites are bound at both PO_3^{2-} groups. The overall binding mode of the diphosphonate is 8.221221. The binding mode of the chp⁻ ligands is variable. Of the seven crystallographically unique chp⁻ groups, five show the 2.21 mode, one the 3.21 mode and one the chelating 1.11 mode. The decorated core of **75** can be described (Fig. 36) as a four-nodal complex with the *NDk-m* symbol **2,3,4,5M10-1**. The compound shows a steady decrease in $\chi_M T$ as T falls.
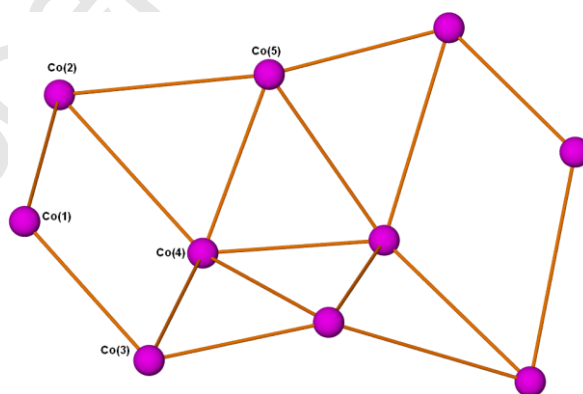
Fig. 36. The simplified core **2,3,4,5M10-1** that is present in **75** (TIWGIQ). Colour code: Co^{II} pink.

Solvothermal reaction, in 1:1:1 ratio, of $[Co^{II}(dmp)_2(H_2O)_2]$ (Hdmp=dipivaloylmethane), H_3tmp [1,1,1-tris(hydroxymethyl)propane, $EtC(CH_2OH)_3$] and adamantyl carboxylic acid ($AdCO_2H$) in MeOH

52

Edited Feb 6

at 150 ^{o}C yields $[Co^{II}_{10}(\mu_6\text{-}O)(O_2CAd)_2(tmp)_4(dpm)_4(AdCO_2H)_{0.5}(MeOH)_{3.5}(H_2O)_{1.5}]$ (**76**) (LOKZIV) [172] The core consists of four edge-sharing $\{Co^{II}_4(\mu_3\text{-}OR)_4\}^{4+}$ cubane units centred around a μ_6 oxide. The metal ions define a tetrahedron with each $\{Co_6\}$ face bound by a fully deprotonated tmp^{3-} ligand (6.333 binding in Harris notation) and diketonates chelating the vertices. The structure is sensitive to changes in ligands and solvents. The use of the more constrained, cyclohexane-based triol H$_3$cht (*cis,cis*-1,3,5-cyclohexanetriol), in place of H$_3$tmp, results in the distorted $\{Co_{10}\}$ cage $[Co^{II}_{10}(\mu_6\text{-}O)(\mu_3\text{-}OH)(O_2CAd)_3(cht)_2(dpm)_4(Hcht)_2(EtOH)_3]$ (**77**) (LOKZOB) [169]. In this case, one of the four edge-sharing cubanes has a missing edge and the supertetrahedron has an opened face. Adopting our topological approach, the two compounds are decorated binodal CCs with the *NDk-m* symbol **3,7M10-1**, see Fig. 37. However, this motif has a different numerical representation compared to Mn$_{10}$ supertetrahedron motifs [2,3] due to the presence of a μ_6-O^{2-} group in the Co$^{II}_{10}$ complexes, which offers three additional links (blue lines in Fig 37). Complex **76** exhibits unusual magnetization dynamics (slow magnetic relaxation at temperatures up to 12 K have been detected) associated with the regular supertetrahedral $\{Mn_{10}\}$ structure, supporting a model [173] proposed by the same authors (McInnes' group) for a completely analogous supertetrahedral Ni$^{II}_{10}$ cluster to account for slow relaxation in the absence of any significant energy barrier from either high anisotropic spins or intermolecular interactions.

53
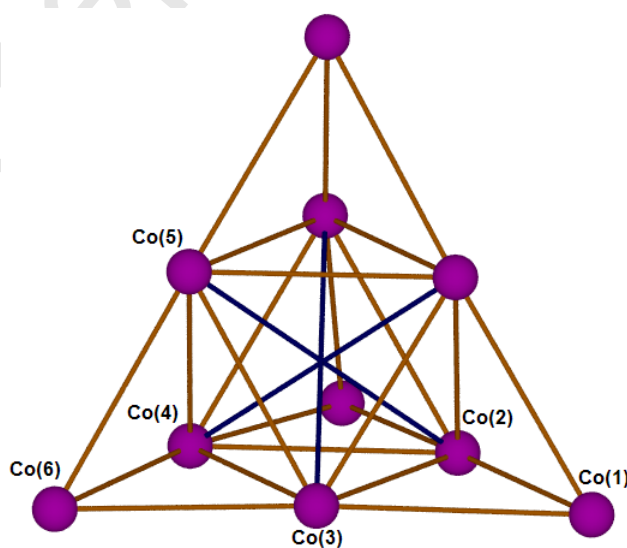
Edited Feb 6

Fig. 37. The simplified core **3,7M10-1** that is present in **76** (LOKZIV)and **77** (LOKZOB). Colour code: Co^{II} pink.

5.7. Co_{11}

Undecanuclearity is extremely rare in Co chemistry and only two examples have been reported [114]. The $Co(BF_4)_2 \cdot 6H_2O/FPO_3H_2/Hchp/Et_3N$ reaction system in MeCN has led to $[Co^{II}_{11}(\mu_3-F)(PO_4)(chp)_{18}]$ (**78**) (TIWGAI). The fluorido ligand presumably derives from either BF_4^- or FPO_3^{2-}, and the phosphate from hydrolysis of FPO_3^{2-}. The identity of **77** led to an examination of the $Co(BF_4)_2 \cdot 6H_2O/H_3PO_4/Hchp/Et_3N$ reaction system in MeCN, which gave the isostructural compound $[Co^{II}_{11}(\mu_3-OH)(PO_4)(chp)_{18}]$ (**79**) (TIWGOW); reaction with pyrophosphonic acid ($H_2O_3POPO_3H_2$) instead of phosphoric acid also led to **79**. The structures have approximately 3-fold symmetry. They contain a central PO_4^{3-}, showing a 9.3222 binding mode. The nine Co^{II} centres bound to the phosphate form a triangle bound to the μ_3-O atom of the phosphate above six Co^{II} centres with a "chair" conformation; this array could be considered an icosahedron missing one triangular face. The 10th and 11th Co^{II} centres cap the triangle and chair, respectively. The CCs possess the decorated motif depicted in Fig. 38. Compounds **78** and **79** are four-nodal clusters with the *NDk-m* symbol **2,3,3,4,4,5M11-1**.
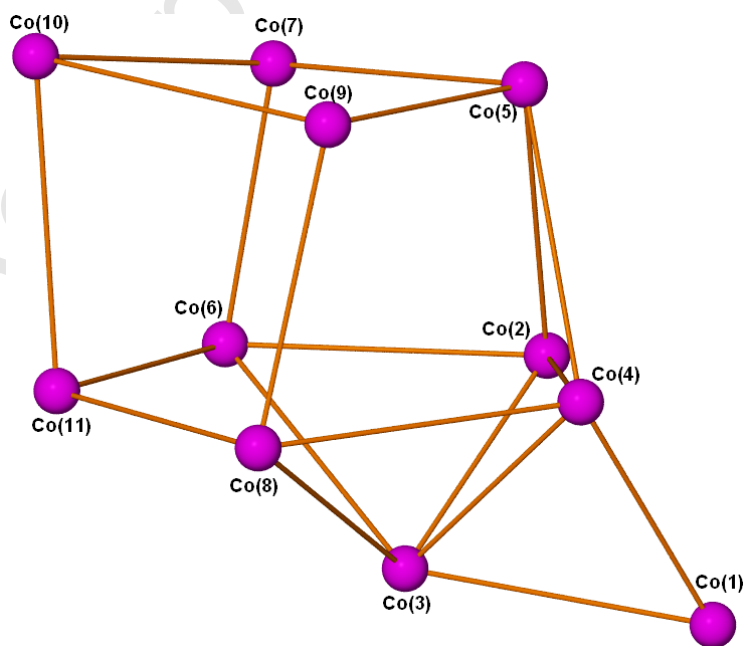
Edited Feb 6

Fig. 38. The simplified core **2,3,3,4,4,5M11-1** that is present in **78** (TIWGAI) and **79** (TIWGOW). Colour code: Co^{II} pink.

5.8. Co_{12}

In 1983, Garner and co-workers reported the synthesis and characterization of the dodecanuclear CC $[Co^{II}_{12}(\mu_3\text{-OH})_6(O_2CMe)_6(mhp)_{12}]$, (**80**) (BUTKOQ) [174]. The decorated core of **80** is shown in Fig. 39 (left). The trinodal complex has the *NDk-m* symbol **3,5,5,9M12-1**. A comparison of the decorated cores of **80** and the decanuclear Co^{II} complexes **68**, **69** (Fig 39, right) shows that the core of **80** can be derived from the core of **68** and **69** by adding the Co(2) and Co(3) nodes in the former, which can be proved by a graph comparison through TOPOS. Since the three CCs contain the $OH^-/RCO_2^-/mhp^-$ bridging donor set, it seems that use of bulkier carboxylates (piv^-, $PhCO_2^-$ vs $MeCO_2^-$) leads to a lower nuclearity in this specific reaction system. Moreover, the comparison of the Point Symbols $(4^3)_2(3^5.4^4.5)_6(3^6.4^4)_3(3^{15}.4^{15}.5^6)$ [**80**] and $(3^5.4)_6(3^6.4^4)_3(3^{15}.4^{15}.5^6)$ [**68,69**] for the two types of complexes, without any assistance of a core scheme, clearly provides a strong evidence that the two cores are related.
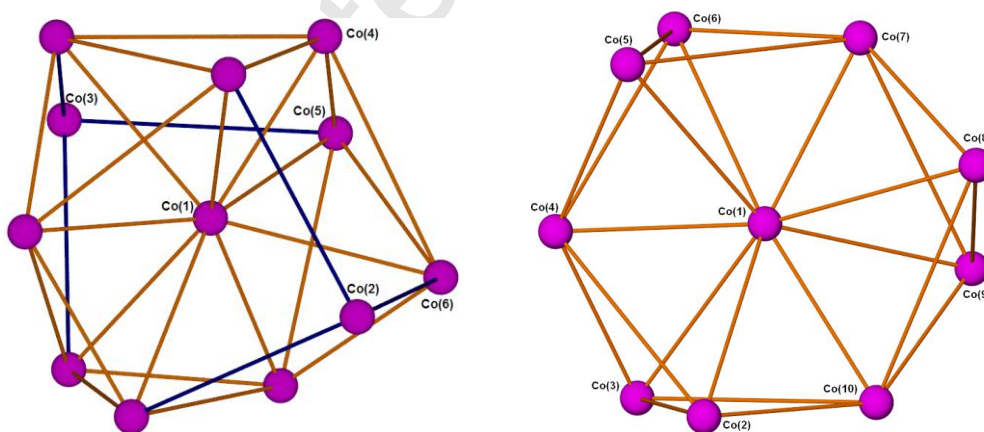
Fig. 39. The simplified core of **3,5,5,9M12-1** of **80** (BUTKOQ) (left), and **4,5,9M10-1** of **68** and **69** (right). Colour code: Co^{II} pink.

55

Edited Feb 6

The wheel motif (Fig. 40) is the second motif in Co_{12} chemistry [175-177]. A typical example is $[Co^{II}Cl(^tBu_3SiS)]_{12}$ (**81**) (IVATEE) [175] which shows weak antiferromagnetic exchange interactions. Its topological representation is **2M12-1**.
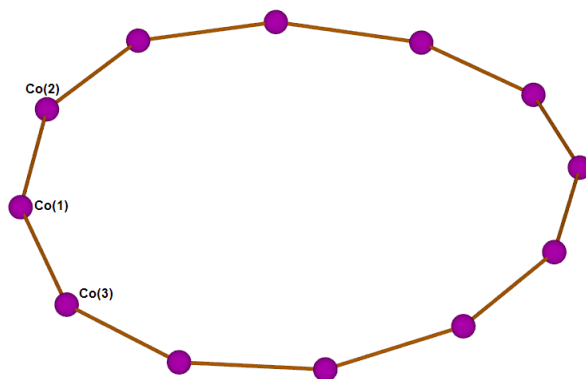
Fig. 39. The simplified core **2M12-1** that is present in **81** (IVATEE). Colour code: Co^{II} pink.

Complex $[Co^{II}_{12}(\mu_3\text{-}OH)_4(\mu\text{-}Cl)_2(chp)_{18}(Hchp)_2(MeOH)_2]$ (**82**) (TAWJIK) [123] has an unusual motif. The authors described the dodecanuclear species as containing two $\{Co^{II}_4(\mu_3\text{-}OR)(\mu_3\text{-}OH)_2Cl\}^{4+}$ non-ideal cubane units linked by a central eight-membered ring involving four Co^{II} atoms (two are part of the cubes) and four μ-O atoms derived from chp$^-$ ligands. The remaining two Co^{II} sites are at the periphery of the molecule. Two tetrahedra are connected through Co(6) and its symmetry equivalent, while Co(1) (and its symmetry equivalent) is placed in the plane of the triangle formed by Co(2), Co(3) and Co(5), see Fig. 41. The decorated core of **82** can be represented as a trinodal cluster with the *NDk-m* symbol **2,4,4,4,5,5M12-1**.
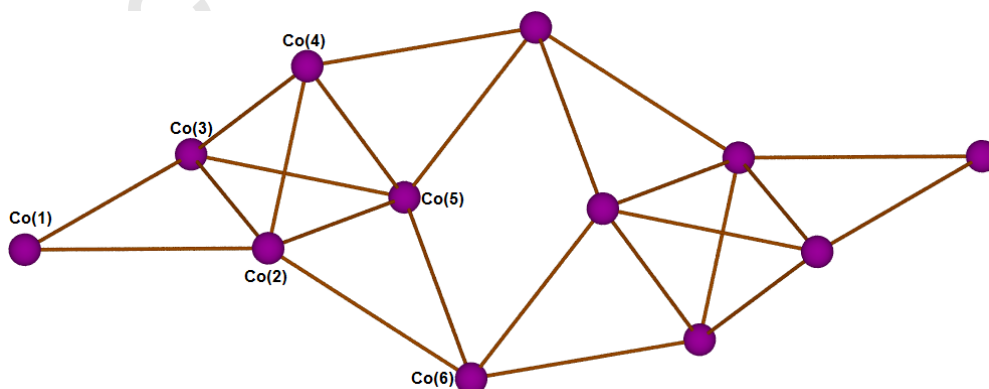
Fig. 41. The simplified core **2,4,4,4,5,5M12-1** that is present in **82** (TAWJIK). Colour code: Co^{II} pink.

56

Edited Feb 6

The $Co(BF_4)_2$ $6H_2O/NapCH_2PO_3H_2/Hchp/Et_3N$ reaction system in MeCN, where Nap is naphthylmethyl group, has yielded complex $[Co^{II}_{12}(\mu_3\text{-}OH)_2(\mu\text{-}OH)(O_3PCH_2Nap)(BO_3H)(chp)_{18}(H_2O)]$ (**83**) (TIWDUZ) [114]. This has a very irregular structure. There is a 7.331 hydrogenborate(-2) group at the centre of the structure derived from hydrolysis of BF_4^-. Two {Co$_4$} fragments are attached to the μ_3-O atoms of the BO_3H^{2-}; both are heavily distorted and incomplete heterocubanes [Co(2), Co(6), Co(7), Co(12) and Co(4), Co(5), Co(9), Co(10) in Fig. 42]. The phosphonate has the 4.211 binding mode in the structure. The 18 chp$^-$ ligands show four modes: 9 show the 2.21 mode, 5 the 2.11 mode, 3 the 3.21 mode and 1 the terminal 1.10 mode. There are two four-coordinate cobalt sites [Co(3) and Co(12)] and two five-coordinate cobalt sites [Co(1) and Co(11)], with the remainder six-coordinate. Simplifying the metallic core (Fig. 42), a 12-nodal CC is formed with the *NDk-m* symbol **2,2,3,3,3,4,4,4,4,5,5,5M12-1**. Complex **83** shows an increase of the $\chi_M T$ product below 20 K, but no out-of-phase signals were detected above 1.8 K [114].
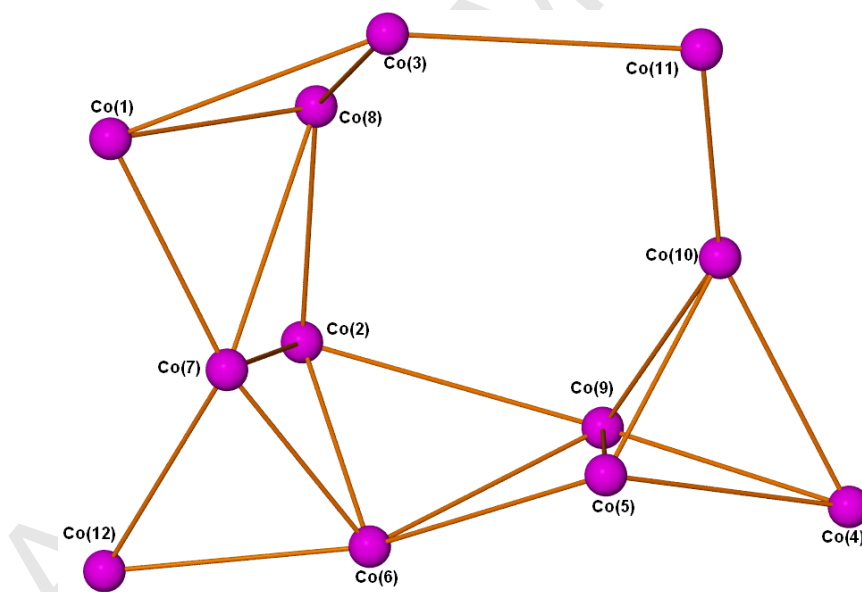
Fig. 42. The simplified core **2,2,3,3,3,4,4,4,4,5,5,5M12-1** that is present in **83** (TIWDUZ). Colour code: Co^{II} pink.

Reaction of $Co(ClO_4)_2$ $6H_2O$ with (1*H*-benzimidazol-2-yl)methanol (HL), NaN$_3$ and triethanolamine (H$_3$tea) in MeOH has led to cluster $[Co^{II}_9Co^{III}_3(\mu_3\text{-}O)_3(\mu_{1,1,1}\text{-}N_3)(\mu_{1,1}\text{-}N_3)_3(L)_{15}](ClO_4)_2 \cdot H_3$tea (**84**) [178]. The complex has a disc-like structure in which the Co centres are

Edited Feb 6

almost coplanar. The L⁻ ligands adopt the 2.210 and 3.310 coordination modes (Scheme 19). The topological analysis (Fig. 43) shows that Co(1) is a 6-c.n., Co(2) is a 4 – c.n., while Co(3) and Co(4) are 3 – c.n.; thus the symbol of the cluster is **3,4,6M12-2** (the topologically non-equivalent type **3,4,6M12-1** does not occur in the Co chemistry, but was observed with Mn [80]). Both ferromagnetic coupling through the μ_3-O_L and μ-O_L pathways and antiferromagnetic coupling through the $\mu_{1,1,1}$-N_3^- pathway result in a ferrimagnetic behaviour of **84** [178].

2.210   3.310
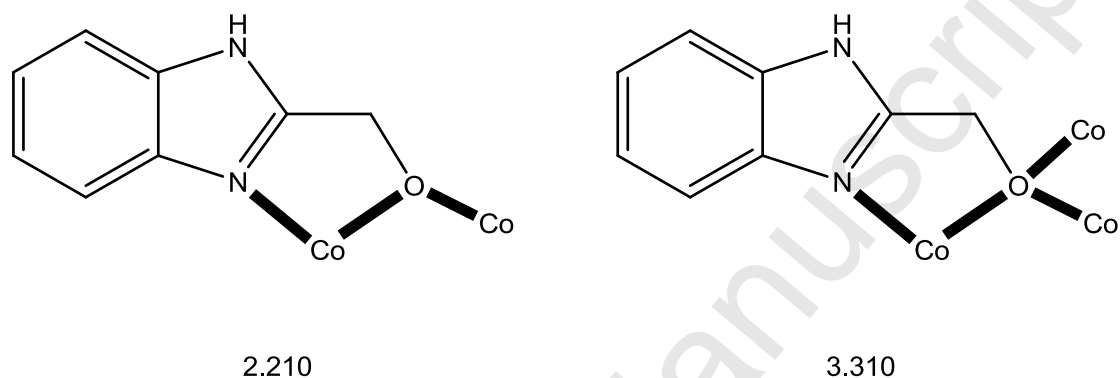
Scheme 19. The coordination modes of the L⁻ ligands that are present in **84** and the Harris notation that describes their modes.
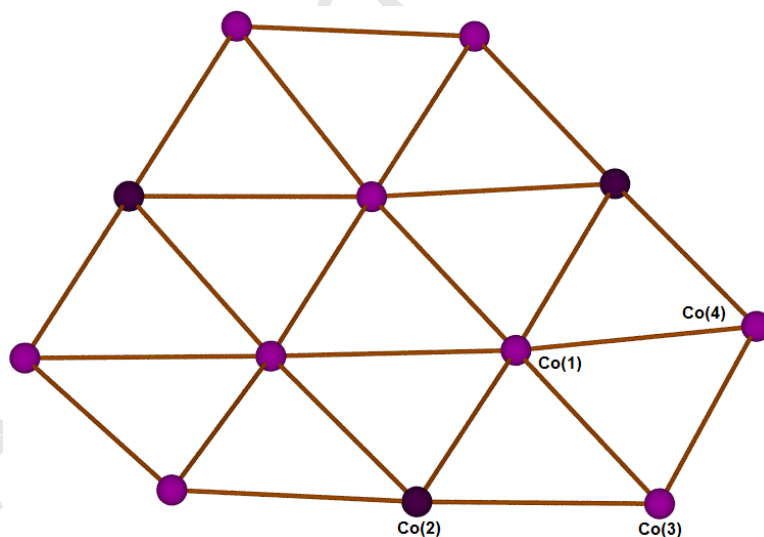
Fig. 43. The simplified core **3,4,6M12-2** that is present in **84**. Colour code: Co^{II} pink, Co^{III} mauve.

The last motif that has been observed in Co_{12} chemistry is found in complexes $[Co^{II}_{12}(\mu_3\text{-}OH)_{12}(\mu_3\text{-}CO_3)(O_2CMe)_9(trans\text{-}tachH)_6](ClO_4)_7$ (**85**) (VEXYED) [179] and $[Co^{II}_{12}(\mu_6\text{-}NO_3)(O_2CMe)_6\text{-}(L)_{12}(EtOH)_6]$ $(NO_3)_5$ (**86**) (VEZVIG) [180]. This motif is based on three cubane units that are found in a

58

Edited Feb 6

triangular arrangement (Fig. 44). In both cases a central planar ion (CO_3^{2-}, NO_3^-) bridges the faces of the three $\{Co^{II}_4(OR)_4\}$ cubanes. The clusters are binodal with the *NDk-m* symbol **3,4M12-1**.
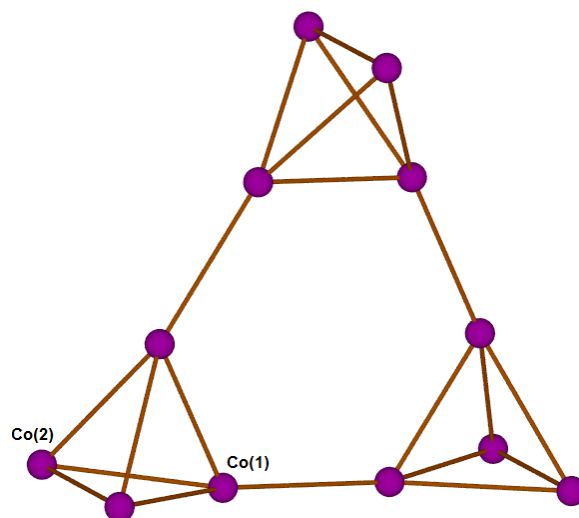
Fig. 44. The simplified core **3,4M12-1** that is present in **85** (VEXYED) and **86** (VEZVIG). Colour code: Co^{II} pink.

Complexes **84** and **85** demonstrate in an excellent manner the use of templating (μ_3-CO_3^{2-} or μ_6-NO_3^-) and multifunctional ligands to facilitate the directed assembly of cubane building blocks to form $\{Co^{II}_{12}\}$ CCs. Central to the synthesis of **85** is the aliphatic triamine ligand *cis,trans*-1,3,5-triaminocyclohexane (*trans*-tach). This ligand is particularly versatile due to the rigidity of its cyclohexane backbone which prevents the interaction of all three amino donor groups with one single metal centre and a bis(axial)-mono(equatorial) type of coordination of the amino groups is invariably observed upon coordination to open-shell transition-metal ions. In **85**, the *trans*-tach$^+$ cationic group acts as a bidentate chelating ligand while the protonated *trans* amine group anchors the complex into a supramolecular H-bonded network. Electrospray mass spectrometry data clearly show envelopes corresponding to the $\{Co_{12}\}$ intact cluster species. The $\chi_M T$ vs T graph for **85** continually decrease towards lower temperatures and any intramolecular coupling is masked by dominating single-ion anisotropy zero-field splitting contributions typical for high-spin Co^{II} centres in distorted octahedral ligand fields, see Part 4.3 of this review.

59

Edited Feb 6

The ligand L$^-$ in **86** is the anion of (1*H*-benzimidazol-2-yl)methanol, also used to prepare **84**, and it adopts the 3.310 mode (Scheme 19) being responsible for the construction of the cubane unit. Complex **86** was prepared from an one-pot solvothermal reaction from Co(NO$_3$)$_2$ 6H$_2$O and Co(O$_2$CMe)$_2$ 4H$_2$O. The μ_6-nitrato ligand is unprecedented, in contrast to the well-documented μ_3-bridging mode of the isoelectronic CO$_3^{2-}$ group [171, 181-183]. Magnetic studies are indicative of a relatively strong ferromagnetic intracubane Co^{II} Co^{II} interactions and weak ferromagnetic intercubane coupling. Compound **86** is a SMM with a U_{eff} value of 15.0 K (10.4 cm^{-1}) and a pre-exponential term of $\tau_0 = 1.94$ x 10^{-7} s [180].

5.9. *Co$_{13}$*

If the solid Co(OH)$_2$/PhPO$_3$H$_2$/Hchp (3:1:6) reaction mixture is heated to above the melting point of Hchp, the purple paste that results could be dissolved in a range of solvents. Crystals of [Co$^{II}_{13}$(μ_3-OH)$_3$(O$_3$PPh)$_2$(chp)$_{19}$(H$_2$O)$_2$(EtOAc)$_2$] (**87**) (RAKTEC) form in moderate yield from EtOAc, while crystals of [Co$^{II}_{13}$(μ_3-OH)$_3$(O$_3$PPh)$_2$(chp)$_{19}$(H$_2$O)$_2$(Hchp)$_2$] (**88**) (RAKTOM) form in poor yield from MeCN/Et$_2$O [184]. The crystallization of two very similar cages from different solvents suggests that the cages are formed during the initial reaction, rather than forming during crystallization. Complex **87** could also be prepared [114] from the Co(ClO$_4$)$_2$ · 6H$_2$O/PhPO$_3$H$_2$/Hchp/Et$_3$N reaction mixture in MeCN followed by extraction of the resulting oil (after solvent removal) with EtOAc. The structures are highly irregular and essentially identical, differing in the replacement of the two terminal EtOAc ligands in **87** by Hchp ligands in **88**. Each PhPO$_3^{2-}$ group binds to five Co^{II} centers adopting a 5.221 mode. The 19 chp$^-$ ligands in the cage adopt four different modes (2.21, 2.20, 3.21 and 3.31). The complexes have the some decorated motif (Fig. 45). Topologically, the cages consist of 2-, 3-, 4- and 5- c.n. and the *NDk-m* symbol is **2,3,3,3,3,3,4,4,4,4,5,5,5M13-1**.

60

Edited Feb 6
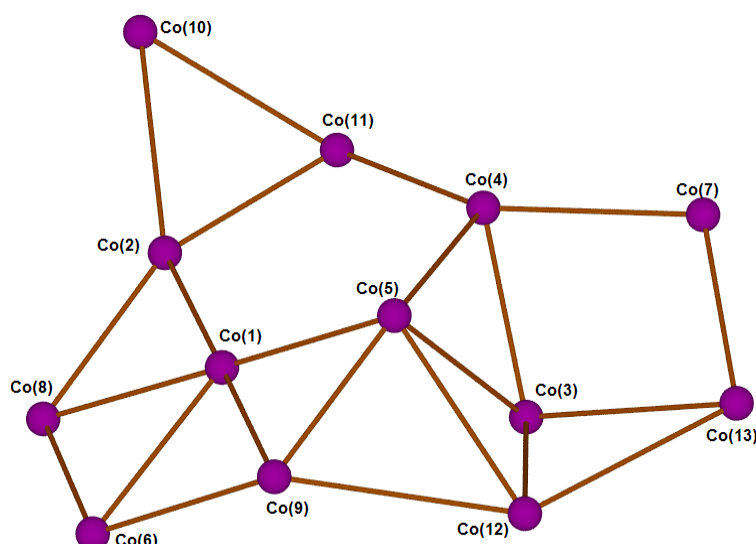
Fig. 45. The simplified core **2,3,3,3,3,3,4,4,4,4,5,5,5M13-1** that is present in **87** (RAKTEC) and **88** (RAKTOM). Colour code: Co^{II} pink.

A second Co_{13} motif has been observed in complex $[Co^{II}_{13}(\mu_3\text{-}OH)_2(phth)_2(chp)_{20}]$ (**89**) (TAWJUW) [123,124], where phth^{2-} is the doubly deprotonated phthalate ligand. The centrosymmetric cage is extremely irregular. The asymmetric unit contains a square-based pyramid consisting of Co(2), Co(3), Co(5) and Co(6) within the square base and Co(4) at the vertex of the pyramid (Fig. 46).
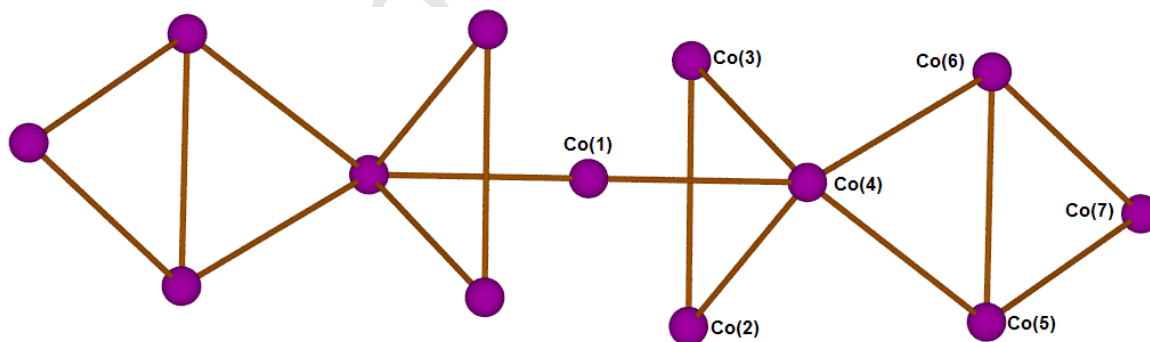
Fig. 46. The simplified core **2,2,3,5M13-1** that is present in **89** (TAWJUW). Colour code: Co^{II} pink.

The Co(5) Co(6) edge of the pyramid is capped by Co(7), and the triangular face Co(2)Co(3)Co(4) is capped by Co(1) which (owing to the inversion centre at this metal ion) caps the triangular faces of the two symmetry-equivalent pyramids. **89** is a four-nodal CC with a total symbol of **2,2,3,5M13-1**. Five of

61

Edited Feb 6

the seven unique metal sites in **89** could be matched with sites in **34** and **35**. Fig. 47 illustrates this comparison with a superposition of the metal sites in **89** and **35**.
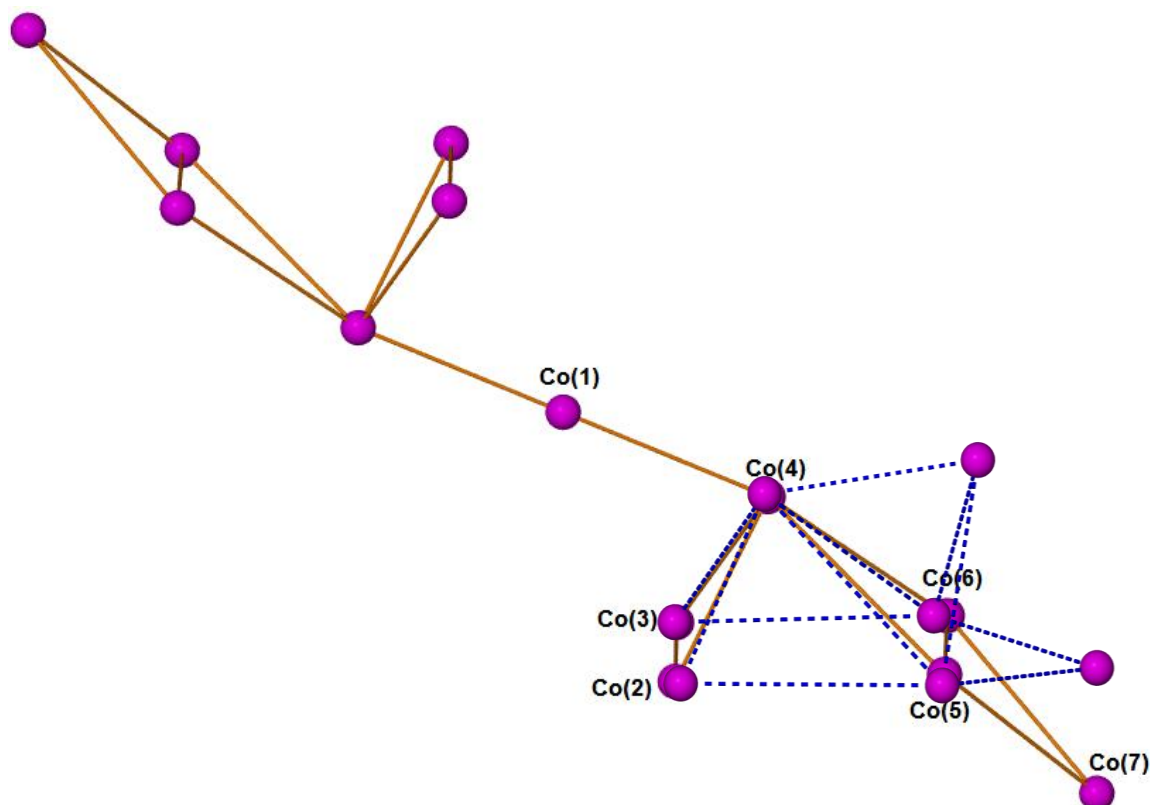
Fig. 47. A similar figure that exist in ref. [121] showing the superposition of the metal cores of complex **89** (shown as yellow lines) and **35** (shown as dotted blue lines) [121]

The third Co_{13} motif has been observed in the nanoscale complex $[Co^{II}_{13}(\mu_3\text{-OH})_{12}(\mu_3\text{-}O)_3(O_2CMe)_{10}(trans\text{-tachH})_6](O_2CMe)_4$ (**90**) (XITYIJ) [185]. Structurally, the cation of **90** represents a replacement of the carbonate dianion in the dodecanuclear cation of **85** by a five-coordinate $\{CoO_3(O_2CMe)\}^{5-}$ unit. The authors were able to show by using electrospray measurements that the cation of **90** can be converted into the cation of **85** via the addition of K_2CO_3. Mass spectrometry and other synthetic studies have demonstrated that the $\{Co_{13}\}$ represents a common unit in the construction of the $\{Co_{12}\}$ species and that species are present in solution without the need for sophisticated terminal ligands. Topologically, in both **85** (Fig. 44) and **90** (Fig. 48) there are three metal tetrahedra (originating from the three cubane units) in a triangular arrangement; in the case of **90**, a 13th node is present in the middle and the trinodal Co_{13} CC can be presented as **3,5,6M13-1**.

62

Edited Feb 6
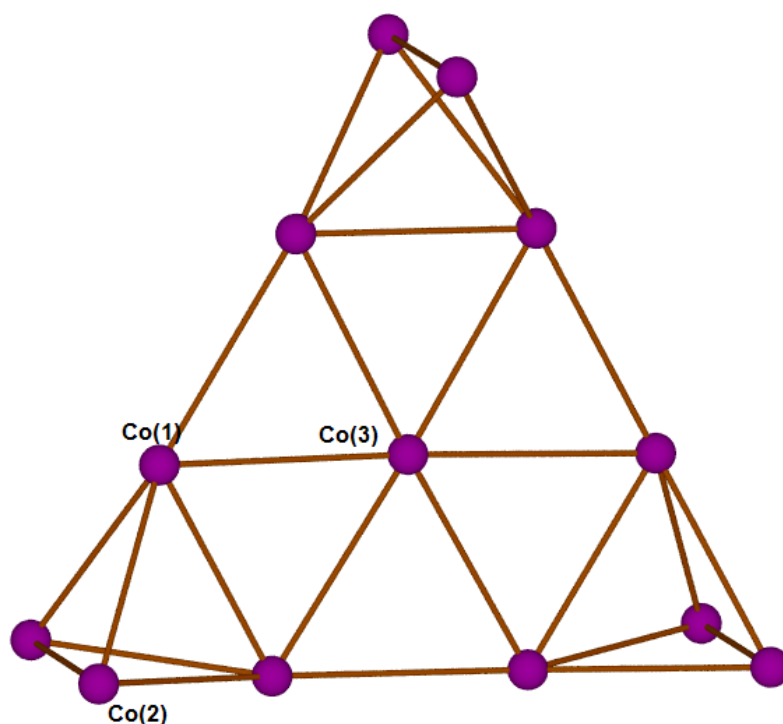
Fig. 48. The simplified core **3,5,6M13-1** that is present in **90** (XITYIJ). Colour code: Co^{II} pink.

The last Co$_{13}$ motif has been observed in $[Co^{II}_{13}(mosao)_8(Hmosao)_6]\cdot(ClO_4)_4\cdot$(**91**) (AGUFEO) prepared [186] by a solvothermal reaction, where H$_2$mosao is 3-methoxysalicylaldoxime. The cation is disc-like consisting of 14 face-sharing distorted defective cubanes. The oximate ligands adopt the coordination modes shown in Scheme 20. Topologically, Co(8) is a 2 – c.n., Co(1), Co(2), Co(6), Co(12) and Co(13) are 3 – c.n., while Co(5) and Co(11) are also 3 – c.n.; Co(3) and Co(9) are 4 – c.n. and finally Co(4), Co(7) and Co(10) are 5 – c.n., see Fig. 49. Thus, the *NDk-m* symbol of the CC is **2,3,3,3,3,4,5,5M13-1**. Electrospray ionization mass spectrometry strongly suggests that the {Co$_{13}$} cluster is present in MeCN solution. Variable-temperature magnetic susceptibility studies reveal antiferromagnetic behaviour; the odd number of spins results in a remaining effective magnetic moment at 2 K.

63

Edited Feb 6
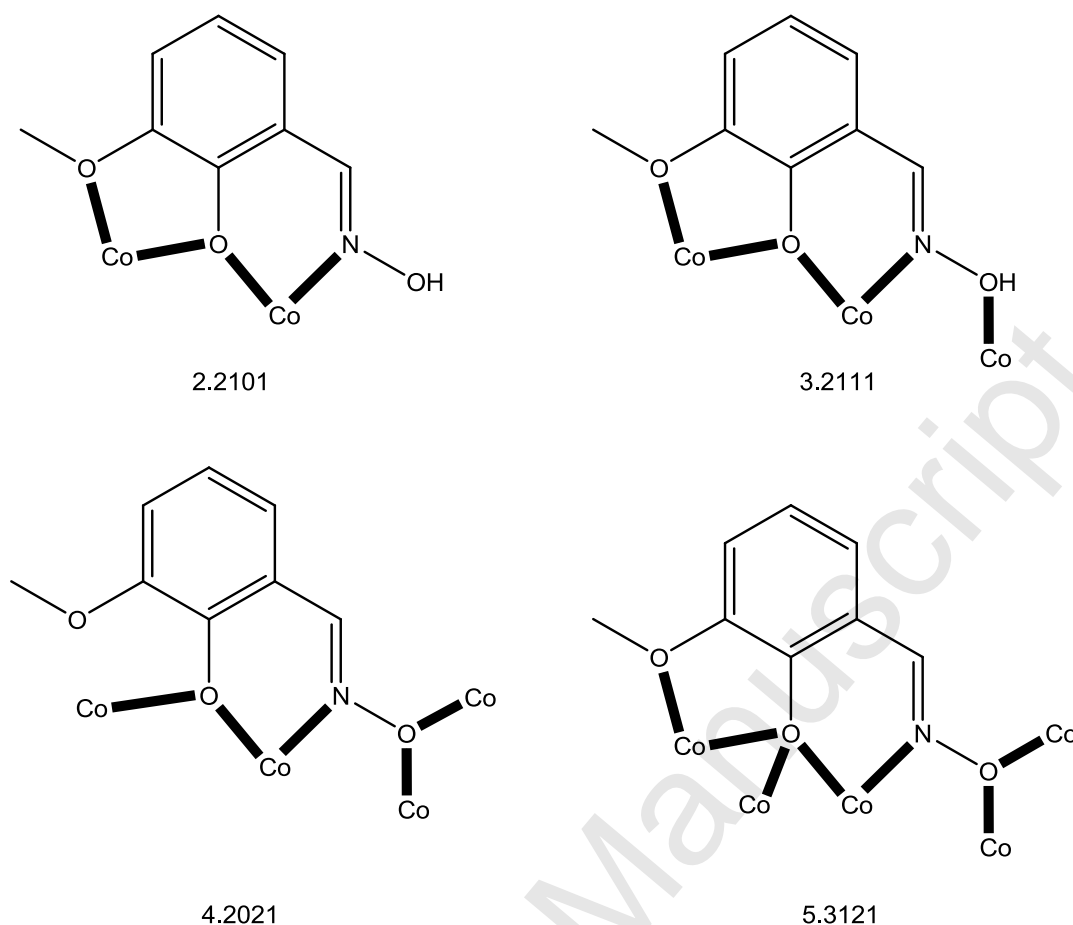
Scheme 20. The coordination modes of the Hmosa$^-$ and mosa^{2-} ligands that are present in complex **91** and the Harris notation that describes these modes.
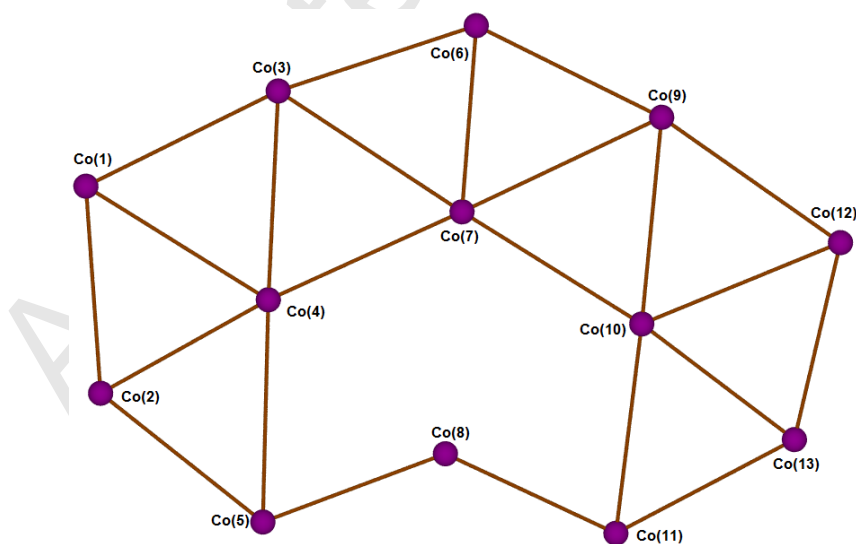
Fig. 49. The simplified core **2,3,3,3,3,4,5,5M13-1** that is present in **91** (AGUFEO). Colour code: Co^{II} pink.

Edited Feb 6

5.10. Co₁₄

The first Co_{14} motif, shown in Fig. 50, has been observed in cobalt pivalate chemistry [93, 100, 119]. Typical examples are $[Co^{II}_8Co^{III}_6(\mu_5\text{-}O)_2(\mu_3\text{-}O)_2(\mu_3\text{-}OH)_{12}(piv)_{14}(Hpiv)_2(H_2O)_6(MeCN)_2]$ (**92**) (EYUHOV) and $[Co^{II}_8Co^{III}_6(\mu_5\text{-}O)_2(\mu_3\text{-}O)_2(\mu_3\text{-}OH)_{12}(piv)_{14}(Hpiv)_3(H_2O)_8]$ (**93**) (UMAKEY) [100]. The molecules contain four cubane units sharing two Co-O edges and two metal vertices [Co(3) and its symmetry equivalent], and two further Co vertices [Co(7) and its symmetry equivalent]. The complexes are most probably formed from "dimerization" of a heptanucelar CC, rather than by stepwise addition of Co^{II} atoms. This suggests that as the complexes grow bond formation between CCs becomes a process competing with metal ion-addition by metal ion growth. This is unsurprising, and similar to growth of colloids of metals or metal oxides. From the topological point of view, **92** and **93** can be considered as pentanodal with the *NDk-m* symbol **2,3,6,6,9M14-1**. Co^{III}_{14} analogues have also been isolated [93, 119].
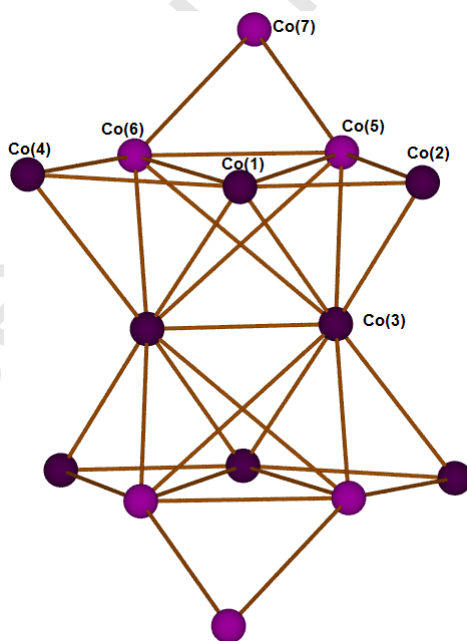
Fig. 50. The simplified core **2,3,6,6,9M14-1** that is present in **92** (EYUHOV) and **93** (UMAKEY). Colour code: Co^{II} pink, Co^{III} mauve.

65

Edited Feb 6

The most common cluster is observed in the products from the general Co(Ψ)$_2$ 6H$_2$O/RPO$_3$H$_2$/Hchp/Et$_3$N reaction system in MeCN (Ψ=ClO$_4$, BF$_4$), [Co$^{II}_{14}$(μ_3-OH)$_2$(μ_3-X)$_2$(O$_3$PR)$_2$(chp)$_{20}$(H$_2$O)$_2$] (where X = OH for perchlorate and X = F for tetrafluoroborate as starting materials), was found for five different phosphonates – R; **94** for R = CH$_2$Ph, **95** for R = Me, **96** for R = Et, **97** for R = *n*-octyl and **98** for R=H (**94** and **96** contain X=OH, whereas **95**, **97**, **98** contain X = F) [114]. In the case of **98**, a further two terminal Hchp ligands are attached to the core. The structures of the tetradecanuclear complexes are all similar, differing only in the X group and in the alkyl group on the phosphonate. In each case, the molecules lie on an inversion centre. The seven Co^{II} atoms in the asymmetric unit lie in a plane, with four of the centres [Co(3), Co(5), Co(6), Co(7); Fig. 51] surrounding a fifth [Co(4)], bridged through μ_3-OH$^-$ atoms in an array similar to the repeating pattern found in Co(OH)$_2$, and also found at the core of large CCs, e.g. {Fe$_{19}$} [187]. The other two Co^{II} sites in the asymmetric unit [Co(1) and Co(2)] are attached to this pentametallic fragment through the phosphonates. The phosphonates also bridge to the second half of the molecule, which is symmetry equivalent to the first half. The structure has a distinct "step", quantified by considering the angle between the mean plane of the seven Co^{II} centres in the asymmetric unit and the Co(1)Co(2)Co(1')Co(2') section, which is 56.4°. The two phosphonates therefore disrupt the planar "Co(OH)$_2$" structure and link together two planes. The phosphonates adopt the 5.221 mode. The chp$^-$ ligands coat the exterior of the CC and show a variety of ligation modes (2.21, 2.11, 1.11). Topologically, the cluster can be described with the *NDk-m* symbol **3,3,3,4,4,4,5M14-1**, see Fig. 51.
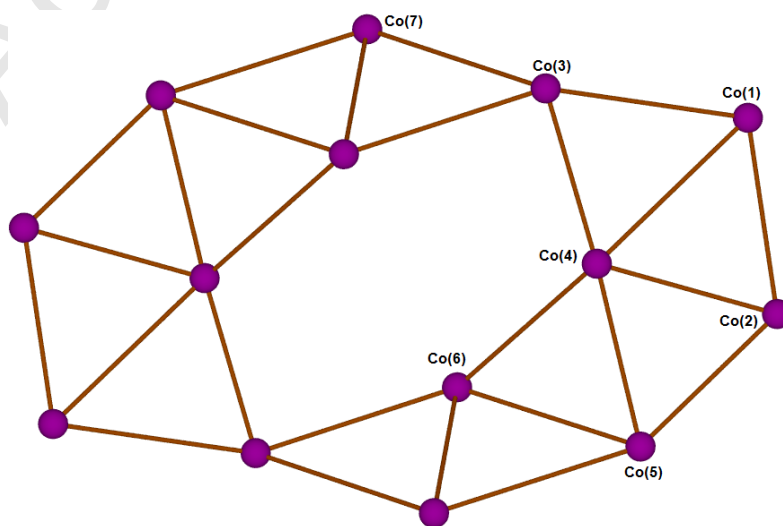
Edited Feb 6

Fig. 51. The simplified core **3,3,3,4,4,4,5M14-1** that is present in **94 – 98** (TIWDOT, TIWFAH, TIWFIP, TIWFUB, TIWGEM). Colour code: Co^{II} pink.

5.11. Co_{15}

This nuclearity is known only for the cationic complex $[Co^{II}_{15}(L)_6(H_2O)_{24}](trans$-E) (**99**) (WUHJAL) [188]. The Co^{II} atoms are held together by six tetra-anions of *N*-(phosphonomethyl)iminodiacetic acid $[N(CH_2CO_2H)_2(CH_2PO_3H_2), H_4L]$ and charge-balanced with one hexa-anion of *trans*-1,2,3,4,5,6-cyclohexanehexacarboylic acid $[C_6H_6(CO_2H)_6, trans$-$H_6E]$. The complex was prepared hydrothermally. The authors describe the 15 metal ions as arranged in alternating $Co/Co_3/Co_7/Co_3/Co$ layers along a pseudo 3-fold axis. The Co_3 triangles are staggered with respect to each other, while the middle Co_7 layer is a close-packed centred hexagon. Each L^{4-} ligand coordinates to 8 Co^{II} atoms, with the phosphonate group adopting the 5.221 mode and the two carboxylate groups exhibiting 2.20 and 3.21 modes. Using our improved topological approach [80], **99** has the *NDk-m* symbol **1,4,6M13-1(0)$_2$**. The nonzero plateau in the $\chi_M T$ vs T at 5 - 10 K reflects a non diamagnetic ground state for **99**, as expected. The data clearly suggest antiferromagnetic coupling between the Co^{II} centres. The complex is a weak SMM.

67
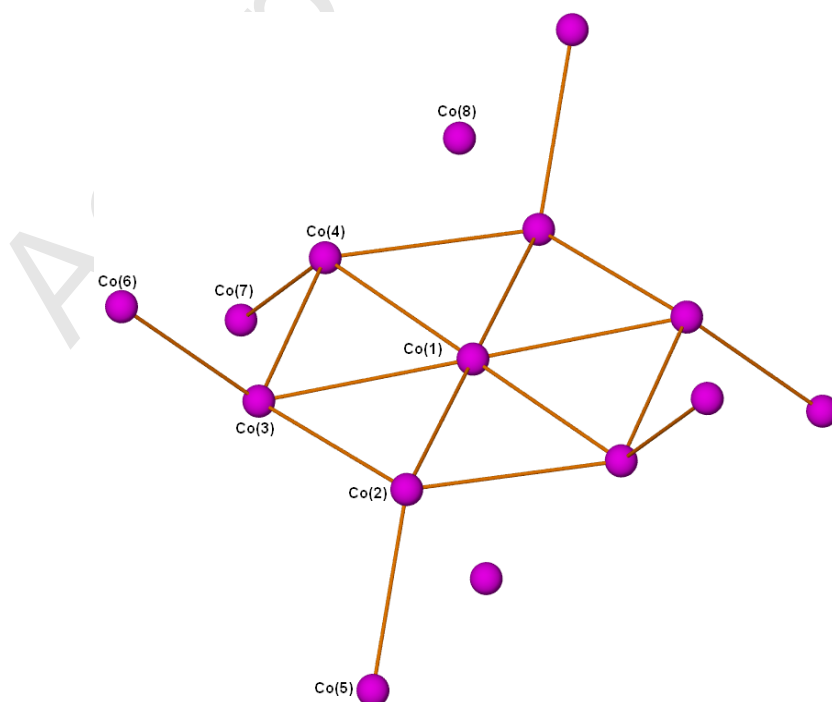
Edited Feb 6

Fig. 52. The simplified core the *NDk-m* symbol **1,4,6M13-1(0)$_2$** that is present in **99** (WUHJAL). Colour code: Co^{II} pink.

A key structural feature in **99** is the presence of 24 peripheral aqua ligands. Such labile ligands are potential targets for ligand exchange with polydentate linkers in order to build extended structures. The authors achieved [188] the hierarchical assembly of the hexacationic clusters of **99** into a 3D network by linking them using the *cis* enantiomer of H$_3$E^{3-}; the formula of the coordination polymer is $\{[Co^{II}_{15}(L)_6(cis\text{-}H_3E)_2(H_2O)_{18}](H_2O)_{12}\}_n$ (**100**) (WUHJEP). Each *cis*-H$_3$E^{3-} ligand uses the three deprotonated carboxylic groups at positions 1, 2 and 4 to coordinate *via* one of the O atoms to peripheral Co^{II} atoms from three different clusters, simultaneously replacing coordinated H$_2$O molecules. Each Co$_{15}$ building block is, in turn, coordinated by six *cis*-H$_3$E^{3-} ligands that replace six aqua ligands per **99** and link the building blocks in a network. It should be pointed out that the Co$_{15}$ building block in the network of **100** is exactly the same {Co$_{15}$} cluster characterized in **99** minus six coordinated H$_2$O molecules.

5.12. Co$_{19}$

Along with the supertetrahedral cluster **76**, McInnes and coworkers reported in 2008 the synthesis, structure and preliminary magnetic results of $[Co^{II}_{19}(\mu_6\text{-}O)_2(\mu_3\text{-}OH)_2(O_2CPh)_4(cht)_6(dbm)_6(Hcht)_2(EtOH)_2]$ (**101**) (LOKZUH), where Hdbm is dibenzoylmethane [172]. Compound **101** consists of two identical supertetrahedral subunits sharing the Co(1) vertex. The subunits are similar to those for **76** and **77** (Fig. 37). The benzoate groups were not present in the reaction mixture, arising from degradation of dbm$^-$ [189]. For **101**, $\chi_M T$ has approximately double the room-temperature value for the Co$^{II}_{10}$ complexes **76** and **77**, decreasing continuously with decreasing *T*. No divergence occurs in FC or ZFC curves down to 2 K, although there is a significant rise in χ''_M as temperatures approaching 2 K. Clearly, lower temperature measurements are required before any valid conclusion can be made for this complex. A numerical comparison with complex $[Mn^{II}_7Mn^{III}_{12}(\mu_4\text{-}O)_8(\eta^1:\mu_3\text{-}N_3)_8(HL)_{12}(MeCN)_6]Cl_2$ [3, 28], where H$_3$L is 2,6-bis(hydroxymethyl)-4-methylphenol, possessing an analogous motif, shows a difference due to

68

Edited Feb 6

the presence of two μ_6-O^{2-} groups in **101** which offers six additional links (blue lines in Fig. 53). The Co_{19} cluster is trinodal with the *NDk-m* symbol **3,6,7M19-1**.
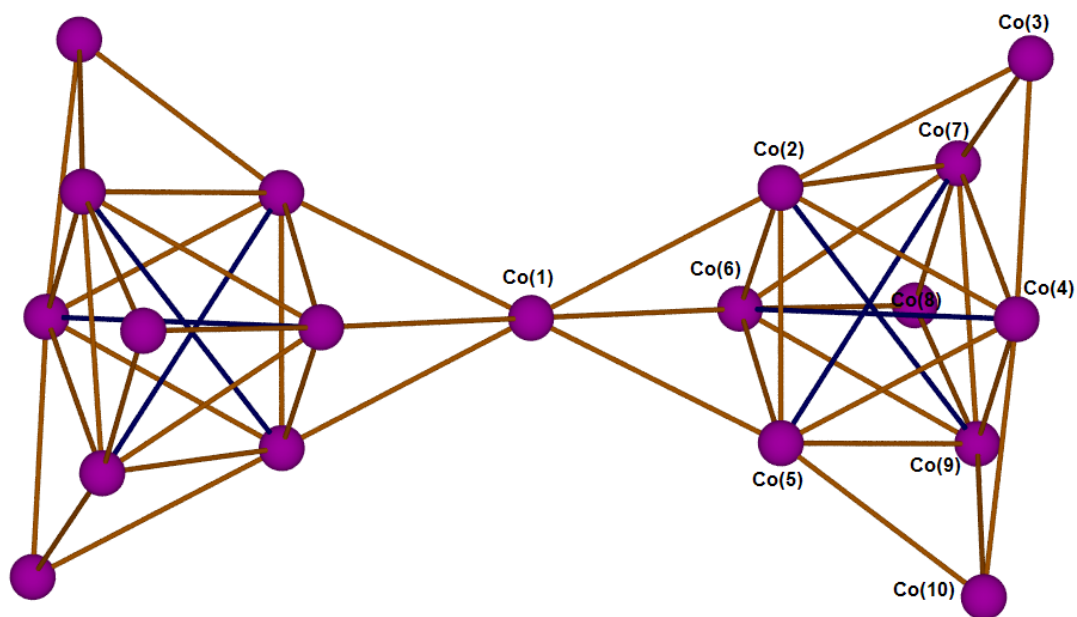
Fig. 53. The simplified core **3,6,7M19-1** that is present in **101** (LOKZUH). Colour code: Co^{II} pink.

5.13. Co_{20}

Two different Co_{20} CCs have been reported in the literature [114, 190]. Boudalis' group studied the coordination chemistry of di-2,6-(2-pyridyl)pyridine or (2,6-pyridine-yl)bis(2-pyridyl)methanone, (py)CO(py)CO(py) [191], see Scheme 21. The ligand can potentially be found in metal complexes in the diketo, partly or completely hydrolyzed/solvolyzed forms, thus providing a variety of possibilities for CC synthesis [70]. In the course of such studies, reaction of excess $Co(O_2CMe)_2$ $4H_2O$ with (py)CO(py)CO(py) in hot DMF gave [187] $[Co^{II}_{20}(\mu_3$-OH$)_6(O_2CMe)_{22}(HL)_4(DMF)_2]$ (**102**) (ECAJUO), where H_4L is the bis(*gem*-diol) form of the ligand. The core consists of a central double cubane having two missing vertices connected to two warped $\{Co_6O_6\}$ rings through two $\{Co_2O_4\}$ moieties. The triply deprotonated ligands adopt the 6.3221111 and 5.2220111 modes (Scheme 21). Our topological analysis shows that the icosanuclear complex consists of 2-, 3-, 4-, and 5-c.n. and the *NDk-m* symbol is

69

Edited Feb 6

2,2,2,2,3,4,4,4,5,5M20-1, see Fig. 54. The complex exhibits superparamagnetic relaxation, but no maxima in the χ''_M vs T curves at various frequencies were observable down to 1.9 K.
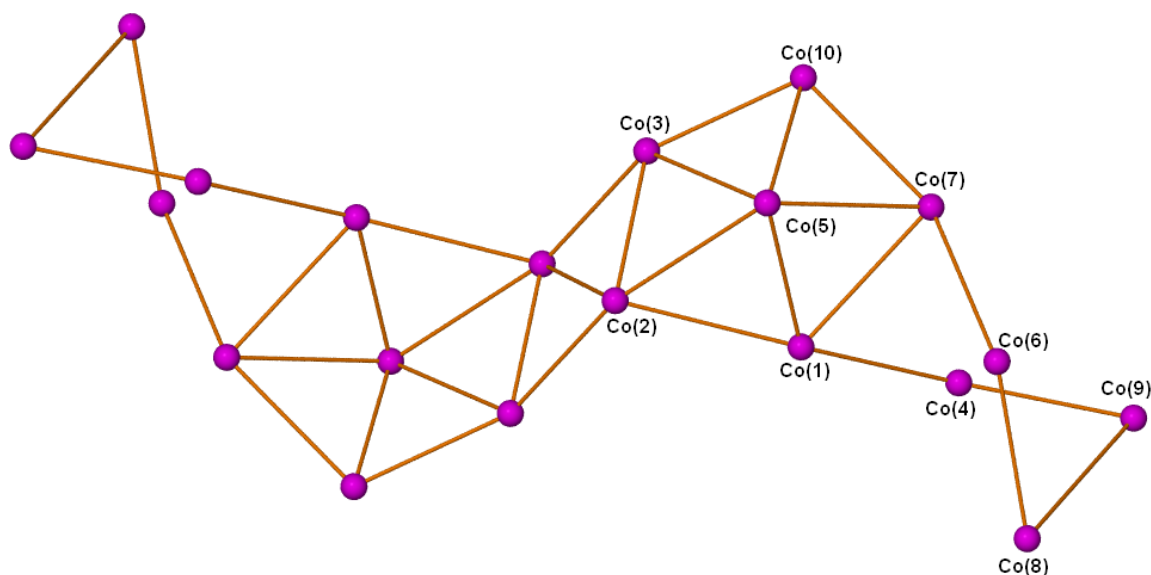
Fig. 54. The simplified core **2,2,2,2,3,4,4,4,5,5M20-1** that is present in **102** (ECAJUO). Colour code: Co^{II} pink.

(py)CO(py)CO(py)

5.2220111 HL^{3-}

6.3221111 HL^{3-}

70
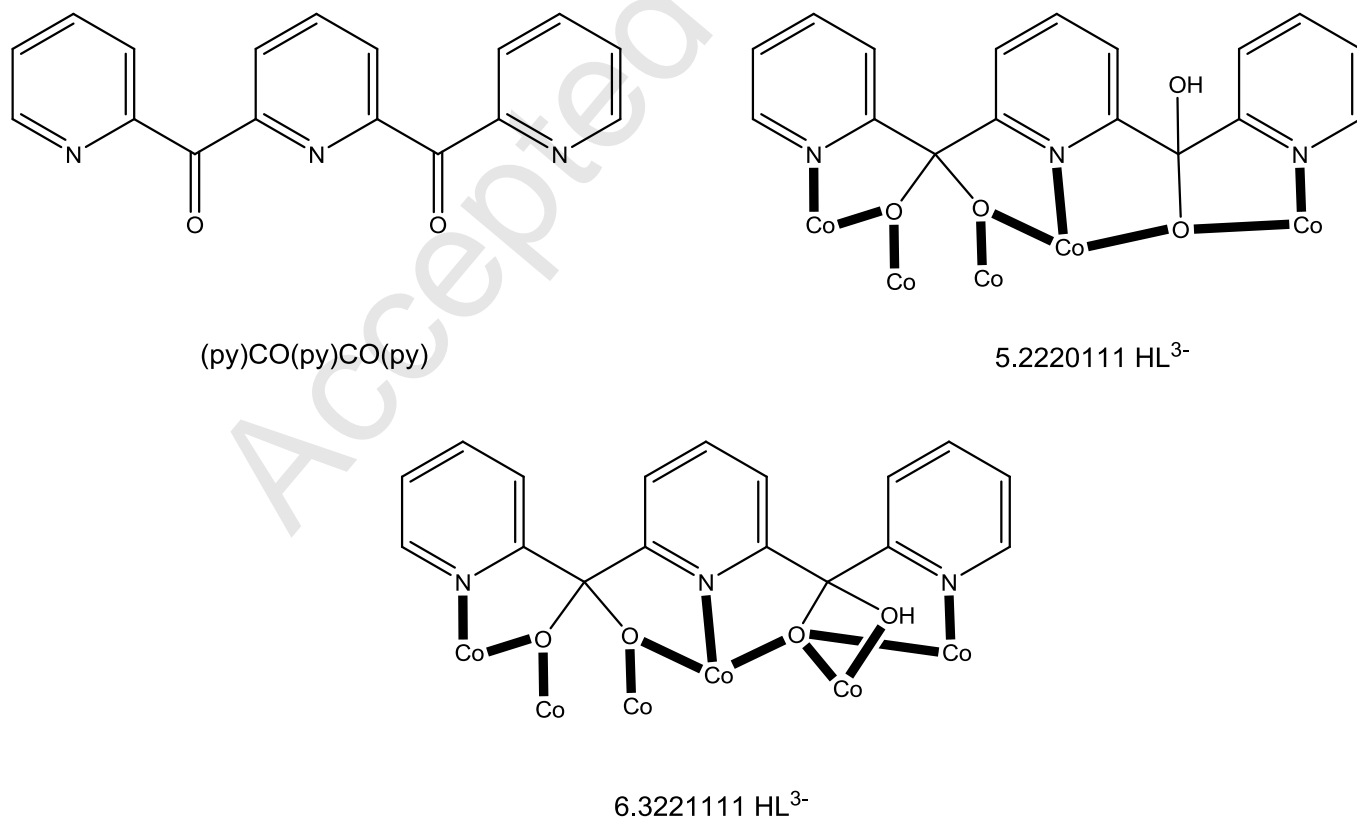
Edited Feb 6

Scheme 21. The ligand di-2,6-(2-pyridyl)pyridine (top left) and the coordination modes (Harris notation) of the trianionic ligands [derived from the bis(*gem*-diol) derivative of the diketo ligand] that are present in **102**.

The second example of a Co_{20} CC comes from the study of the general $Co^{II}/RPO_3H_2/Hchp$ reaction system in Winpenny's group. In studies of cobalt pivalate complexes, it has been found [100] that the nuclearity of the compound formed could be influenced by the addition of hydrogen peroxide. When a few drops of $H_2O_2(30\%)$ were added to the reaction mixture that gives the anionic Co^{II}_8 cluster **61**, the solution turns dark brown. The crystals that result from this procedure contain a centrosymmetric icosanuclear complex $[Co^{II}_{18}Co^{III}_2(\mu_3\text{-O})_2(\mu_3\text{-OH})_4(O_3PPh)_4(chp)_{26}(H_2O)_6]$ (**103**) (TIWFEL) [114], with a structure related to the tetradecanuclear CCs **94 – 98**. The resemblance is most clear around Co(4) [Fig. 55]; as in **94** (Fig. 51), for example, for other Co^{II} sites [Co(1), Co(2), Co(3) and Co(8)] are attached to this site through μ_3-O atoms, creating a planar array similar to that of $Co(OH)_2$. The big difference arises in the centre of the molecule, where Co(9), Co(10) and their symmetry equivalents are found. Both the bridging oxides and the Co^{III} centres arise from the use of H_2O_2 [100, 114]. Both crystallographically independent phosphonate ligands show the 5.221 coordination mode. The 13 unique chp⁻ ligands show six(!) binding modes (2.21, 3.31, 3.21, 2.11, 1.10, 1.11). The decorated core can be described in terms of a central unit consisting of two fused edge-sharing tetrahedra, each of which is linked to one pentanuclear "open" disc through a common vertex; Co(5) is attached to the disc and Co(6) is linked to Co(5). The CC can be described as **1,2,3,3,3,3,3,5,5,5M20-1**.

71

Edited Feb 6
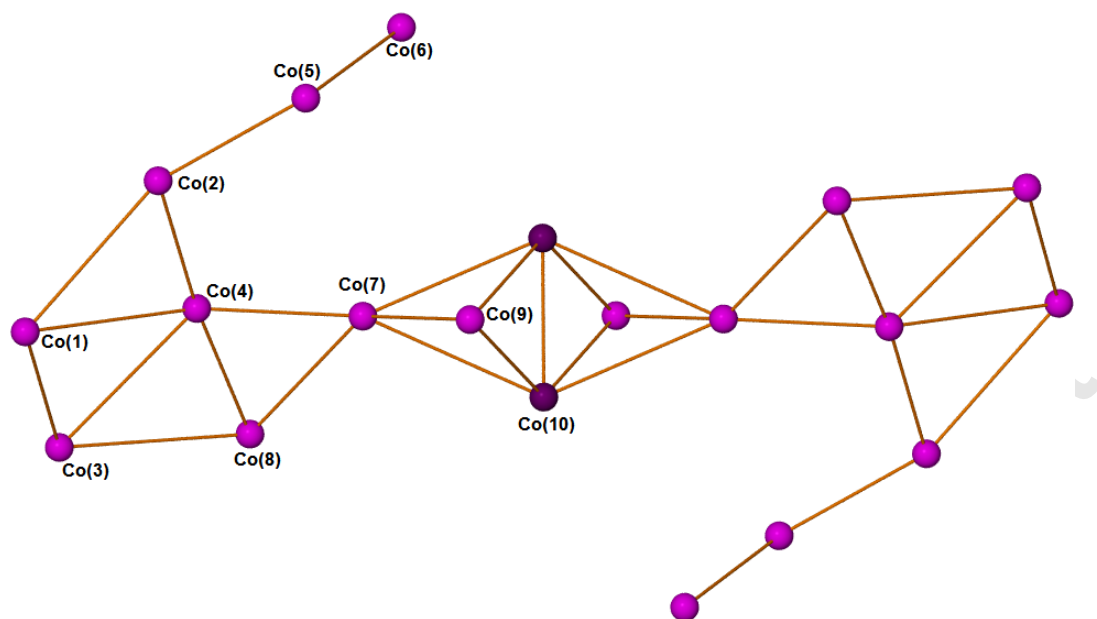
Fig. 55. The simplified core **1,2,3,3,3,3,3,3,5,5,5M20-1** that is present in **103** (TIWFEL). Colour code: Co^{II} pink, Co^{III} mauve.

5.14.   Co$_{24}$

Until 2009, complex [Co$^{II}_{24}$(μ_3-OH)$_{14}$(μ-OH)$_4$(μ_3-OMe)$_2$(μ_3-Cl)$_2$(mhp)$_{22}$Cl$_4$] (**104**) (RIYYAZ) [192] was the highest-nuclearity CC in Co chemistry. This was prepared by the reaction of CoCl$_2$ with two equivalents of Na(mhp) in MeOH for 24 h at room temperature, followed by evaporation to dryness and dissolution of the resulting paste in EtOAc. The synthesis is reproducible; however the yield was reported to vary between 5 and 20% depending on the exact H$_2$O content of the ethyl acetate used. The structure is based on defective {Co$^{II}_3$(OH)$_4$}$^{2+}$ cubane units (one metal corner is missing), and in some cases with one of the hydroxide vertices occupied by methoxy or chlorido groups. Preliminary magnetic studies indicated a high-spin ground state and the possibility of superparamagnetic behaviour [192]. The topological analysis of **104** (Fig. 56) leads to a CC whose *NDk-m* symbol is **2,3,3,3,4,4,4,5,6,6,6,7M24-1.**

72

Edited Feb 6
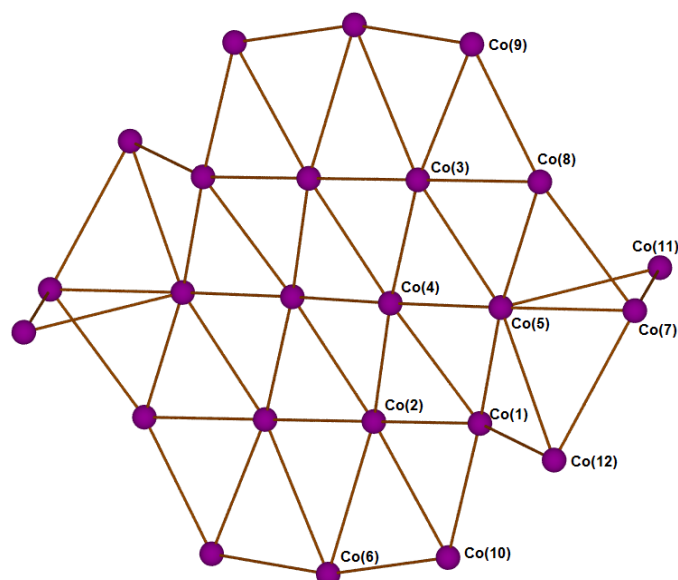
Fig. 56. The simplified core **2,3,3,3,4,4,4,5,6,6,6,7M24-1** that is present in **104** (RIYYAZ). Colour code: Co^{II} pink.

5.15. Co_{32}

In 2009, the solvothermal synthesis and characterization of the second highest-nuclearity cobalt CC [$Co^{II}_{24}Co^{III}_8(\mu_3\text{-}O)_{24}(TC4A)_6(H_2O)_{24}$] (**105**), where H_4TC4A is *p-tert*-butylthiacalix[4]arene, were reported [193]. Three isomers of **105** were structurally characterized. The diameter of the spherical units ($C_{butyl} \cdots C_{butyl}$) is ~ 23.4Å and that of the inner inorganic core (Co $\cdots$ Co) is ~ 10.6Å. The spherical molecules (nanospheres) can be thought to be assembled by six {$Co^{II}_4(TC4A)$}$^{4+}$ subunits around a {Co^{II}_8} cube subunit. The calixarenes capping the six faces of the cube exhibit a unique octahedral arrangement. In two isomers the calixarene-capped {Co_{32}} spherical units are arranged into a body-centred cubic lattice, while they are assembled in a cubic closest packing pattern in the third isomer. The CC can be thought of as a sodalite-type Co^{II}_{24} cage encapsulating a Co^{III}_8 cube. Topologically (Fig. 57), a a binodal complex has the *NDk-m* symbol **5,6M32-1**. As T is lowered, the $\chi_M T$ value decreases gradually to a minimum of 6.27 cm^{3}mol^{-1}K at 2 K. The χ_M^{-1} follows the Curie-Weiss law with Curie constant $C =$ 87.96 cm^{3}Kmol^{-1} and Weiss constant $\theta = $ -71 K, which indicates an antiferromagnetic exchange interaction between the high-spin Co^{II} centres. The compound shows no SMM behaviour above 2 K.

73

Edited Feb 6

MALDI-TOF mass spectrometry indicates that the structure (with loss of aqua ligands) is retained in solution.
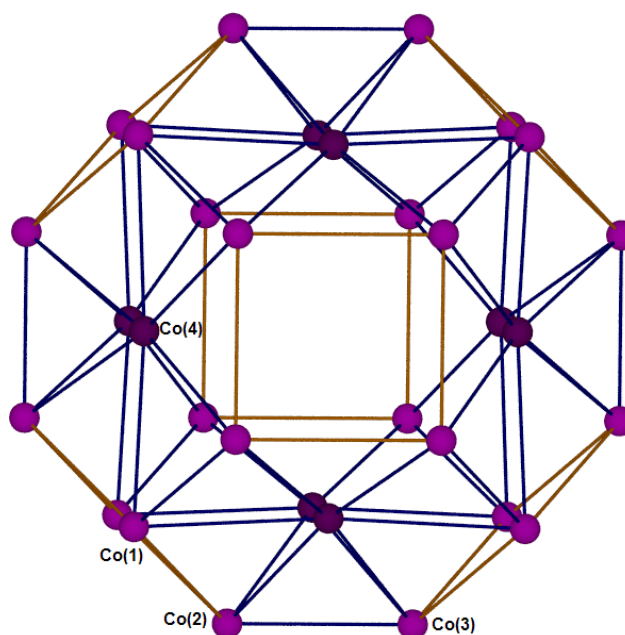
Fig. 57. The simplified core **5,6M32-1** that is present in **105** (WUMLUM, WUMMAT, WUMMEX). Colour code: Co^{II} pink, Co^{III} mauve.

5.16. Co_{36}

The highest-nuclearity Co CC known to date is $[Co^{II}_{32}Co^{III}_{4}(\mu_5\text{-}O)_4(\mu_3\text{-}O)_4(\mu_3\text{-}OH)_{16}(piv)_{36}(dcpz)_2(Hdcpz)_4(Hpiv)_4(H_2O)_{16}(MeCN)_6]$ (**106**) (CUDXEF) [194]. It was prepared by the reaction of $[Co^{II}_2(\mu\text{-}OH_2)(piv)_4(Hpiv)_4]$ with 2,3-dicarboxypyrazine (H$_2$dcpz, Scheme 22) in MeCN. The molecule is almost rhombohedral, but distortion arises from the capping of two additional faces. Because of the capped faces, the overall shape is a distorted, axially compressed octahedron, with equatorial edges lengths of ~3 and ~2 nm, and axial edges of ~2 and ~3 nm. These dimensions are of the same order of magnitude as those of the smallest nanoparticles. The overall arrangement can be understood as an inner Co_{12} subcore consisting of four fused cubane-type units, clamped by two identical Co_{12} wings. Adopting our topological approach, the decorated core of **106** is depicted in Fig. 58 (upper). There is a main

74

Edited Feb 6

$\{Co^{II}_{20}Co^{III}_{4}\}$ central unit and four $\{Co^{II}_{3}\}$ triangles which are not linked to the main unit by monoatomic bridges. The numerical representation is **(2M3-1)$_4$(1,2,2,3,3,4,4,5,5,6,6,8M24-1)**. Applying the TOPOS procedure of searching for common subgraphs [195] to a fragment of the central unit of **106** and the decorated tetradecanuclear core of **93** (Fig. 58, lower left and right) one can reveal that the former has been built up from the core of the latter. The continuous decrease in $\chi_M T$ with decreasing T for **106** is indicative of dominant antiferromagnetic exchange interactions; however orbital contributions can not be ignored and will also influence the overall profile. Below 5 K, $\chi_M T$ reaches a plateau with a value of 30.8 cm^{3}mol^{-1}K. The extrapolation of $\chi_M T$ at 0K gives a value of 32 cm^{3}Kmol^{-1}, confirming a magnetic $S = 6$ ground state in agreement with dc susceptibility data. No out-of –phase signal is observed down to 2 K.
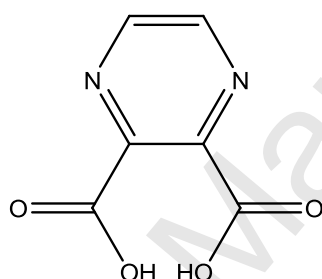
Scheme 22. The 2,3- dicarboxypyrazine ligand used for the preparation of **106**.

75

Edited Feb 6
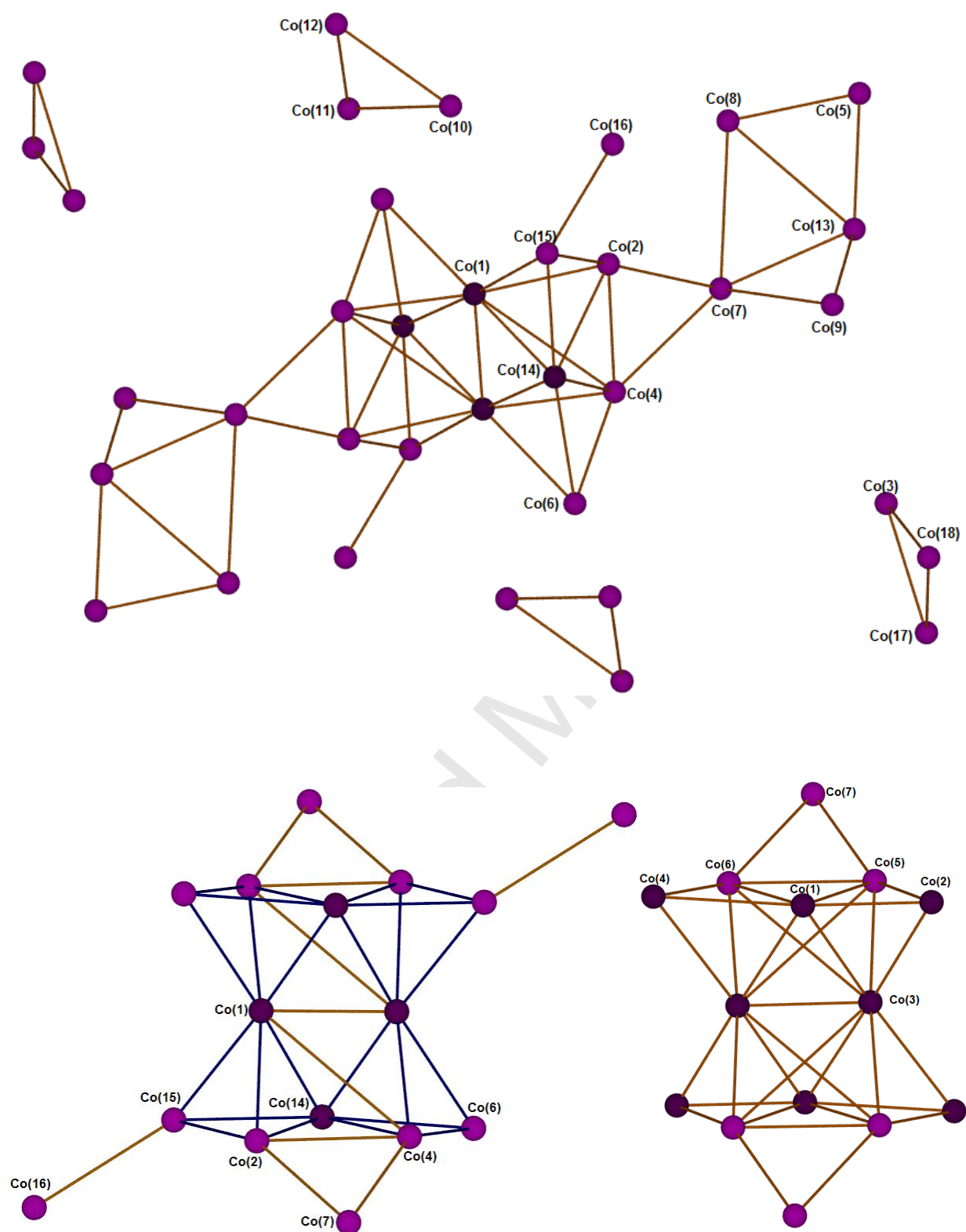
Fig. 58. The simplified core **(2M3-1)₄(1,2,2,3,3,4,4,5,5,6,6,8M24-1)** that is present in **106** (CUDXEF) (upper) and comparison of a 16 atoms fragment of the central unit of **106** (lower left) and the tetradecanuclear core **2,3,6,6,9M14-1** of **93** (lower right). Colour code: Co^{II} pink, Co^{III} mauve.

Edited Feb 6

6.   Conclusions and prognosis for the future

In this review we have analyzed aspects of the synthetic, reactivity, structural and magnetic chemistry of Co CCs with nuclearities higher than 4. Using the TOPOS program package that supports this method we identify 284 entries and 105 different topologies for polynuclear Co CCs. In the present database all Co CCs are collected and illustrated in such a way that they can be searched by cluster topological symbol and nuclearity, compound name, dimensionality and Refcode. We hope that our survey illustrates what is possible in this area through simple coordination chemistry. The research described has something for everyone: from smart synthetic inorganic chemistry to Co complexes with aesthetically pleasant structures, and from high-spin molecules to SMMs. The immense structural diversity of many of the complexes stems from the ability of the ligands to exhibit a great variety of coordination modes. Employment of a second or even a third organic, e.g. a carboxylate or phosphonate, or inorganic, e.g. the azido group, ligand in this chemistry gives an extraordinary structural flexibility in the resulting mixed-ligand systems ("blends"). The diversity of structures for a given ligand system is sometimes remarkable and, with the exception of cobalt/pivalate and cobalt/pyridonate/phosphonate complexes, has prevented up to now any guiding principles being proposed. Most of the clusters do not seem to correspond in a straightforward manner to polyhedral archetypes or to fragments of common Co minerals, but display a richness of nuclearities and topologies that is intriguing. The wide employment of our improved topological approach [2-5, 80] to categorizing cluster topologies seems to give a significant tool in understanding that some structural motifs of higher nuclearity clusters are built up from motifs of CCs with lower nuclearity. This benefit will undoubtedly open new horizons in synthetic cluster chemistry and help scientists understand relationships between structural motifs and magnetic properties. From the magnetism point of view, only few Co^{II}-based SMMs have been studied below 1.8 K. It seems that each one displays different behaviour as a function of the applied magnetic field. It is quite clear that

77

Edited Feb 6

Co^{II}-based SMMs show a very high prevalence of fast tunnelling at zero field and this effect often destroys coercivity in the hysteresis loops.

The research area of the chemistry and magnetism of Co CCs will undoubtedly continue to expand, given the recent nature of the majority of references in this review. We believe that new ligand systems will be used and new synthetic routes will be developed which will result in the discovery of unknown nuclearities and novel structural motifs. Research at the time of submission of this review reveals exciting Co CCs, e.g. a nestlike C_4-symmetric Co$^{II}_{24}$ metallamacrocycle sustained by *p-tert*-butylsulfonylcalic[4]arene and 1,2,4-triazole [196]. According to Murrie [7], there is enormous need for new research into polynuclear Co^{II}-based SMMs. The interplay of quantum tunnelling and weak intermolecular interactions should be further investigated. Both the precise nature of the magnetic exchange and the orientation of the local zero-field splitting tensors and how they contribute to the cluster anisotropy are questions that should be answered; such answers will require the frequent use of HFEPR, inelastic neutron scattering and other sensitive techniques. We also predict that more than the currently existing Co^{II}/4f -metal CCs will be synthesized in the quest of SMMs and magnetic refrigerants with improved properties.

At the beginning of the second decade of the twenty-first century, it is still true to say that Co remains a firm favourite for traditional Werner-type coordination chemistry. However, Co coordination compounds are appearing in greater diversity than before. Although the basic synthetic routes established for decades have remained as entry points into Co chemistry, the application of theses routes with a wider range of ligand systems and the development of more "boutique" reagents has expanded what is possible to encompass some of what was previously considered impossible [85]. It is difficult to predict the paths of Co chemistry that will travel in the next decades. Since Co remains today an excellent centre for coordination chemistry, it is not dangerous to say that the research on Co CCs is still in its childhood, and we do believe that the future promises many more new and exciting Co clusters that will attract scientists from the chemistry and physics communities.

78

Edited Feb 6

Acknowledgment

References

[1]   For an in-depth discussion on the various meanings of the term "cluster" in several areas of inorganic chemistry, see: M. H. Chisholm, Polyhedron 17 (1998) 2773.

[2]   G. E. Kostakis, A. K. Powell, Coord. Chem. Rev. 253 (2009) 2686.

[3]   G. E. Kostakis, A. M. Ako, A. K. Powell, Chem. Soc. Rev. 39 (2010) 2238.

[4]   G. E. Kostakis, I. J. Hewitt, A. M. Ako, V. Mereacre, A. K. Powell, Phil. Trans. R. Soc. A 368 (2010) 1509.

[5]   G. E. Kostakis, A. K. Powell, Chem. Eur. J. 16 (2010) 7983.

[6]   O. Kahn, Molecular Magnetism, VCH Publishers, New York, 1993.

[7]   M. Murrie, Chem. Soc. Rev. 39 (2010) 1986.

[8]   K. Isele, F. Gigon, A. F. Williams, G. Bernardinelli, P. Franz, S. Decurtins, Dalton Trans. (2007) 332.

[9]   M. Kurmoo, Chem. Soc. Rev. 38 (2010) 1353.

[10]   F. A. Cotton, R. A. Walton, C. A. Murillo, Multiple Bonds Between Metal Atoms, Springer-Verlag, New York, 2005.

[11]   R. A. Coxall, S. G. Harris, D. K. Henderson, S. Parsons, P. A. Tasker, R. E. P. Winpenny, J. Chem. Soc., Dalton Trans. (2000) 2349.

[12]   R. E. P. Winpenny, in : J. A. McCleverty, T. J. Meyer (Eds.), Comprehensive Coordination Chemistry II, vol. 7, Elsevier, Amsterdam, 2004, pp. 125 -175.

79

Edited Feb 6

[13]   E. K. Brechin, Chem. Commun. (2005) 5141 (Feature Article).

[14]   T. C. Stamatatos, G. Christou, Phil. Trans. R. Soc. A 366 (2008) 113.

[15]   See the various perspectives and articles in: E. K. Brechin (Ed.) Dalton Trans. 39 (2010) 4655 –
         5038 (a themed issue on Molecular Magnets).

[16]   C. E. Anson, A. Eichhöfer, I. Issac, D. Fenske, O. Fuhr, P. Sevillano, C. Persau, D. Stalke, J.
         Zhang, Angew. Chem., Int. Ed. 47 (2008) 1326.

[17]   A. Müller, E. Beckmann, H. Bögge, M. Schmidtmann, A. Dress, Angew. Chem. Int. Ed. 41
         (2002) 1162.

[18]   Z. – M. Zhang, S. Yao, Y. – G. Li, R. Clérac, Y. Lu, Z. – M. Su, E. – B. Wang, J. Am. Chem. Soc.
         131 (2009) 14600.

[19]   X. – J. Kong, Y. P. Ren, W. – X. Chen, L. – S. Long, Z. Zheng, R. – B. Huang, L. S. Zheng,
         Angew. Chem. Int. Ed. 47 (2008) 2398.

[20]   A. J. Tasiopoulos, A. Vinslava, W. Wernsdorfer, K. A. Abboud, G. Christou, Angew. Chem. Int.
         Ed. 43 (2004) 2117.

[21]   R. A. Grant, D. J. Filman, S. E. Finkel, R. Colter, J. M. Hogle, Nat. Struct. Biol. 5 (1998) 294.

[22]   For a minireview, see: E. C. Theil, M. Matzapetakis, X. Liu, J. Biol. Inorg. Chem. 11 (2006) 803.

[23]   J. Barber, J. W. Murray, Coord. Chem. Rev. 252 (2008) 233.

[24]   C. J. Mullins, V. L. Pecoraro, Coord. Chem. Rev. 252 (2008) 416.

[25]   Y. Umena, K. Kawakami, J. R. Shen, N. Kamiya, Nature 473 (2011) 55.

[26]   J. S. Kanady, E. Y. Tsui, M. W. Day, T. Agapie, Science 333 (2011) 733.

[27]   I. J. Hewitt, J. – K. Tang, N. T. Madhu, R. Clérac, G. Buth, C.E. Anson, A. K. Powell, Chem.
         Commun. (2006) 2650.

[28]   A. M. Ako, I. J. Hewitt, V. Mereacre, R. Clérac, W. Wernsdorfer, C. E. Anson, A. K. Powell,
         Angew. Chem. Int. Ed. 45 (2006) 4926.

[29]   R. Sessoli, H. L. Tsai, A. R. Schake, S. Wang, J. B. Vincent, K. Folting, D. Gatteschi, G.
         Christou, D. N. Hendrickson, J. Am. Chem. Soc. 115 (1993) 1804.

80

Edited Feb 6

[30]   R. Sessoli, D. Gatteschi, A. Caneschi, M. A. Novak, Nature 365 (1993) 141.

[31]   J. D. Rinehart, J. R. Long, Chem Sci, 2 (2011) 2078.

[32]   R. Sessoli, D. Gatteschi, J. Villain, Molecular Nanomagnets, Oxford University Press, Oxford, UK, 2006.

[33]   M. Murrie, D. J. Price, Annu. Rep. Prog. Chem. Sect. A : Inorg. Chem. 103 (2007) 20.

[34]   G. Aromí, E. K. Brechin, Struct. Bonding (Berlin) 122 (2006) 1.

[35]   R. Bagai, G. Christou, Chem. Soc. Rev. 38 (2009) 1011.

[36]   D. Gatteschi, R. Sessoli, Angew. Chem., Int. Ed. 42 (2003) 268.

[37]   R. Bircher, G. Chaboussant, C. Dobe, H. U. Güdel, S. T. Ochsenbein, A. Sieber, O. Waldmann, Adv. Funct. Mater. 16 (2006) 209.

[38]   J. S. Miller, Dalton Trans. (2006) 2742 (Perspective).

[39]   O. Waldmann, Inorg. Chem. 46 (2007) 10035.

[40]   C. J. Milios, A. Vinslava, W. Wernsdorfer, S. Moggach, S. Parsons, S. P. Perlepes, G. Christou, E. K. Brechin, J. Am. Chem. Soc. 129 (2007) 2754.

[41]   L. Bogani, W. Wernsdorfer, Nature Mater. 7 (2008) 179.

[42]   A. Affronte, J. Mater. Chem. 19 (2009) 1731.

[43]   M. N. Leuenberger, D. Loss, Nature 410 (2001) 789.

[44]   A. Ardavan, O. Rival, J. J. L. Morton, S. J. Blundell, A. M. Tytyshkin, G. A. Timco, R. E. P. Winpenny, Phys. Rev. Lett. 98 (2007) 057201-1.

[45]   P. C. E. Stamp, A. Gaita – Ariňo, J. Mater. Chem. 19 (2009) 1718.

[46]   A. Mannini, F. Pineider, P. Sainctavit, C. Danieli, E. Otero, C. Sciancalepore, A. M. Talarico, M. – A. Arrio, A. Gornia, D. Gatteschi, R. Sessoli, Nature Mater. 8 (2009) 194.

[47]   A. Candini, S. Klyatskaya, M. Ruben, W. Wernsdorfer, M. Affronte, Nano Lett. 11 (2011) 2634.

[48]   M. Evangelisti, E. K. Brechin, Dalton Trans. 39 (2010) 4672 (Perspective).

[49]   E. Warburg, Ann. Phys. Chem. 13 (1881) 141.

[50]   P. Debye, Ann. Phys. 386 (1926) 1154.

81

Edited Feb 6

[51]   T. Feder, Phys Today 62 (2001) 21.

[52]   R. Shaw, E. H. Laye, L. F. Jones, O. M. Low, C. Talbot − Eeckelaers, Q. Wei, C. J. Milios, S. Teat, M. Helliwell, J. Raftery, M. Evangelisti, M. Affronte, D. Collison, E. K. Brechin, E. J. L. McInnes, Inorg. Chem. 46 (2007) 4968.

[53]   M. Manoli, A. Collins, S. Parsons, A. Candini, M. Evangelisti, E. K. Brechin, J. Am. Chem. Soc. 130 (2008) 11129.

[54]   S. Nayak, M. Evangelisti, A. K. Powell, J. Reedijk, Chem Eur. J. 16 (2010) 12865.

[55]   M. Evangelisti, A. Candini, M. Affronte, E. Pasca, L. J. de Jongh, R. T. W. Scott, E. K. Brechin, Phys. Rev. B 79 (2009) 104414.

[56]   G. Karotsis, S. Kennedy, S. J. Teat, C. M. Beavers, D. A. Fowler, J. J. Morales, M. Evangelisti, S. J. Dalgarno, E. K. Brechin, J. Am. Chem. Soc. 132 (2010) 12983.

[57]   S. K. Langley, N. F. Chilton, B. Moubaraki, T. Hooper, E. K. Brechin, M. Evangelisti, K. S. Murray, Chem Sci. 2 (2011) 1166.

[58]   M. Evangelisti, O. Roubeau, E. Palacios, A. Camón, T. N. Hooper, E. K. Brechin, J. J. Alonso, Angew. Chem. Int. Ed. 50 (2011) 6606.

[59]   Y. – Z. Zheng, M. Evangelisti, R. E. P. Winpenny, Chem Sci. 2 (2011) 99.

[60]   J. W. Sharples, Y. – Z. Zheng, F. Tuna, E. J. L. McInnes, D. Collison, Chem. Commun. 47 (2011) 7650.

[61]   Y. – Z. Zheng, M. Evangelisti, R. E. P. Winpenny, Angew. Chem. Int. Ed. 50 (2011) 3692.

[62]   J. N. Rebilly, T. Mallah, Struct. Bonding (Berlin) 122 (2006) 103.

[63]   J. R. Long, in: P. Yang (Ed.), Chemistry of Nanostructured Materials, World Scientific Publishing, Hong Kong, 2003, pp. 291 – 316.

[64]   N. G. Pschirer, D. M. Ciurtin, M. D. Smith, U. H. F. Bunz, H. C. zur Loye, Angew. Chem. Int. Ed. 41 (2002) 583.

[65]   L. Carlucci, G. Ciani, D. M. Prosperpio, S. Rizzato, Chem. Commun. (2000) 1319.

[66]   R. E. P. Winpenny, J. Chem. Soc., Dalton Trans. (2001) 1 (Perspective).

82

Edited Feb 6

[67]   A. Baniodeh, I. J. Hewitt, V. Mereacre, Y. Lan, G. Novitchi, C. E. Anson, A. K. Powell, Dalton Trans. 40 (2011) 4080.

[68]   H. Xiang, Y. Lan, H. − Y. Li, L. Jiang, T. − B. Lu, C. E. Anson, A. K. Powell, Dalton Trans. 39 (2010) 4737.

[69]   G. S. Papaefstathiou, S. P. Perlepes, Comments Inorg. Chem. 23 (2002) 249.

[70]   T. C. Stamatatos, C. G. Efthymiou, C. C. Stoumpos, S. P. Perlepes, Eur. J. Inorg. Chem. (2009) 3361 (Microreview).

[71]   A. J. Tasiopoulos, S. P. Perlepes, Dalton Trans. (2008) 5537 (Perspective).

[72]   C. J. Milios, T. C. Stamatatos, S. P. Perlepes, Polyhedron 25 (2006) 134 (Report).

[73]   C. J. Milios, S. Piligkos, E. K. Brechin, Dalton Trans. (2008) 1809 (Perspective).

[74]   For a review, see: R. W. Saalfrank, H. Maid, A. Scheurer, Angew. Chem. Int. Ed. 47 (2008) 2.

[75]   S. L. Heath, A. K. Powell, Angew. Chem. Int. Ed. 31 (1992) 191.

[76]   D. Fenske, C. Persau, S. Dehnen, C. E. Anson, Angew. Chem. Int. Ed. 37 (1998) 1460.

[77]   For a review, see: S. R. Batten, R. Robson, Angew. Chem. Int. Ed. 37 (1998) 1460.

[78]   M. O'Keeffe, M. A. Peskov, S. J. Ramsden, O. M. Yaghi, Acc. Chem. Res. 41 (2008) 1782.

[79]   V. A. Blatov, IUCr CompComm Newsletter, 7 (2006) 4; http://www.topos.ssu.samara.ru.

[80]   G. E. Kostakis, V.A. Blatov, D.M. Proserpio, Dalton Trans., DOI:10.1039/C2DT12263D.

[81]   E.V. Alexandrov, V.A. Blatov, A.V. Kochetkov, D.M. Proserpio, CrystEngComm, 13 (2011) 3947.

[82]   D. A. Buckingham, in: R. B. King (Ed.), Encyclopedia of Inogranic Chemistry, vol. 2, Wiley, New York, 1994, pp. 712 − 731.

[83]   F. A. Cotton, G. Wilkinson, C. A. Murillo, M. Bochmann, Advanced Inorganic Chemistry, 6th ed., Wiley, New York, 1999.

[84]   A. B. P. Lever, Inorganic Electronic Spectroscopy, 2nd ed., Elsevier, Amsterdam, 1984.

[85]   P. V. Bernhardt, G. A. Lawrance, in: J. A. McCleverty, T. J. Meyer (Eds.), Comprehensive Coordination Chemistry II, vol. 6, Elsevier, Amsterdam, 2004, pp. 1 − 145.

83

Edited Feb 6

[86] R. Boča, Coord. Chem. Rev. 248 (2004) 757.

[87] A. Abragam, B. Bleaney, Electron Paramagnetic Resonance of Transition Ions, Clarendon, Oxford, UK, 1970.

[88] A. V. Palii, B. S. Tsukerblat, E. Coronado, J. M. Clemente – Juan, J. J. Borrás – Almenar, Inorg. Chem. 42 (2003) 2455, and refs cited therein.

[89] U. Englert, J.Strahle, Z.Naturforsch.,B:Chem.Sci. 42 (1987) 959.

[90] A. E. Malkov, I. G. Fomina, A. A. Sidorov, G. G. Aleksandrov, I. M. Egorov, N. I. Latosh, O. N. Chupakhin, G. L. Rusinov, Y. V. Rakitin, V. M. Novotortsev, V. N. Ikorskii, I. L. Eremenko, I. I. Moiseev, J.Mol.Struct. 656 (2003) 207.

[91] Y. Wei, H. Hou, Y. Fan, Y. Zhu, Eur. J. Inorg. Chem. (2004) 3946.

[92] H. – C. Chang, N. Nishida, S. Kitagawa, Chem. Lett. 34 (2005) 402.

[93] S. E. Nefedov, T. O. Denisova, Zh. Neorg. Khim. (Russ.). Russ. J. Inorg. Chem. 51 (2006) 946.

[94] A. Ferguson, A. Parkin, M. Murrie, Dalton Trans. (2006) 3627.

[95] C. Floriani, R. Henzi, F. Calderazzo, J. Chem. Soc., Dalton Trans. (1972) 2640.

[96] S. – J. Shieh, C. – C. Chou, G. – H. Lee, C. – C. Wang, S. – M. Peng, Angew. Chem. Int. Ed. 36 (1997) 56.

[97] C. – Y. Yeh, C. – H. Chou, K. – C. Pan, C. – C. Wang, G. – H. Lee, Y. O. Su, S. – M. Peng J.Chem.Soc., Dalton Trans. (2002) 2670.

[98] C. – C. Wang, W. – C. Lo, C. – C. Chou, G. – H. Lee, J. – M. Chen, S. – M. Peng, Inorg. Chem. 37 (1998) 4059.

[99] B. Zhuang, P. Yu, L. Huang, L. He, G. Pan, Polyhedron 16 (1997) 1425.

[100] G. Aromi, A. S. Batsanov, P. Christian, M. Helliwell, A. Parkin, S. Parsons, A. A. Smith, G. A. Timco, R. E. P. Winpenny, Chem. Eur. J. 9 (2003) 5142.

[101] C. J. Matthews, L. K. Thompson, S. R. Parsons, Z. Xu, D. O. Miller, S. L. Heath, Inorg. Chem. 40 (2001) 4448.

84

Edited Feb 6

[102] T. Kajiwara, R. Shinagawa, T. Ito, N. Kon, N. Iki, S. Miyano, Bull. Chem. Soc. Jpn. 76 (2003) 2267.

[103] F. Klöwer, Y. Lan, J. Nehrkorn, O. Waldmann, C. E. Anson, A. K. Powell, Chem. Eur. J. 15 (2009) 7413.

[104] H. Kumagai, Y. Oka, S. Kawata, M. Ohba, K. Inoue, M. Kurmoo, H. Okawa, Polyhedron 22 (2003) 1917.

[105] T. Shiga, H. Oshio, Polyhedron 26 (2007) 1881.

[106] T. C. Stamatatos, A. K. Boudalis, K. V. Pringouri, C. P. Raptopoulou, A. Terzis, J. Wolowska, E. J. L. McInnes, S. P. Perlepes, Eur. J. Inorg. Chem. (2007) 5098.

[107] E. Fursova, O. Kuznetsova, V. Ovcharenko, G. Romanenko, V. Ikorskii, I. Eremenko, A. Sidorov, Polyhedron 26 (2007) 2079.

[108] K. G. Alley, R. Bircher, O. Waldmann, T. Ochsenbein, H. U. Güdel, B. Moubaraki, K. S. Murray, F. Fernandez-Alonso, B. F. Abrahams, C. Boskovic, Inorg. Chem. 45 (2006) 8950.

[109] V. Tudor, A. Madalan, V. Lupu, F. Lloret, M. Julve, M. Andruh, Inorg. Chim. Acta 363 (2010) 823.

[110] Y. Xie, Q. Liu, H. Jiang, J. Ni, Eur. J. Inorg. Chem. (2003) 4010.

[111] G. E. Lewis, C. S. Kraihanzel, Inorg. Chem. 22 (1983) 2895.

[112] C. Jocher, T. Pape, F. E. Hahn, Z. Naturforsch., B: Chem. Sci. 60 (2005) 667.

[113] R. Schmid, J. Beck, J. Strahle, Z. Naturforsch., B: Chem. Sci. 42 (1987) 911.

[114] S. Langley, M. Heliwell, R. Sessoli, S. J. Teat, R. E. P. Winpenny, Inorg. Chem. 47 (2008) 497.

[115] K. S. Gavrilenko, S. V. Punin, O. Cador, S. Golhen, L. Ouahab, V. V. Pavlishchuk, J.Am.Chem.Soc. 127 (2005) 12246.

[116] E. V. Pakhmutova, A. A. Sidorov, I. G. Fomina, G. G. Aleksandrov, V. M. Novotortsev, V. N. Ikorskii, I. L. Eremenko, Russ. Chem. Bull. 52 (2003) 2013.

[117] M. A. Golubichnaya, A. A. Sidorov, I. G. Fomina, M. O. Ponina, S. M. Deomidov, S. E. Nefedov, I. L. Eremenko, I. I.Moiseev, Russ. Chem. Bull. 48 (1999) 1751.

85

Edited Feb 6

[118] A. A. Sidorov, M. E. Nikiforova, E. V. Pakhmutova, G. G. Aleksandrov, V. N. Ikorskii, V. M. Novotortsev, I. L. Eremenko, I. I. Moiseev, Russ. Chem. Bull. 55 (2006) 1851.

[119] T. O. Denisova, M. A. Golubnichaya, S. E. Nefedov, Russ. Chem. Bull. 52 (2003) 2612.

[120] I. G. Fomina, G. G. Aleksandrov, Z. V. Dobrokhotova, O. Y. Proshenkina, M. A. Kiskin, Y. A. Velikodnyi, V. I. Ikorskii, V. M. Novotortsev, I. L. Eremenko, Russ. Chem. Bull. 55 (2006) 1841.

[121] Q. Chen, M. – H. Zeng, L. – Q. Wei, M. Kurmoo, Chem. Mater. 22 (2010) 4328.

[122] C. – H. Chien, J. – C. Chang, C. – Y. Yeh, G. – H. Lee, J. – M. Fang, S. – M. Peng, Dalton Trans. (2006) 2106.

[123] E. K. Brechin, S. G. Harris, S. Parsons, R. E. P. Winpenny, Chem.Commun. (1996) 1439.

[124] E. K. Brechin, A. Graham, A. Parkin, S. Parsons, A. M. Seddon, R. E. P. Winpenny, J.Chem.Soc., Dalton Trans. (2000) 3242.

[125] H. Ackermann, R. Leo, W. Massa, K. Dehnicke, Z. Anorg. Allg. Chem. 626 (2000) 608.

[126] Q. Chen, M. – H. Zeng, Y. – L. Zhou, H. – H. Zou, M. Kurmoo, Chem. Mater. 22 (2010) 2114.

[127] Y. – Z. Zhang, W. Wernsdorfer, F. Pan, Z. – M. Wang, S. Gao, Chem.Commun. (2006) 3302.

[128] X. – T. Wang, B. – W. Wang, Z. – M. Wang, W. Zhang, S. Gao, Inorg. Chim. Acta 361 (2008) 3895.

[129] S. – H. Zhang, Y. Song, H. Liang, M. – H. Zeng, CrystEngComm 11 (2009) 865.

[130] Y. – L. Zhou, M. – H. Zeng, L. – Q. Wei, B. – W. Li, M. Kurmoo Chem. Mater. 22 (2010) 4295.

[131] M. Moragues-Canovas, C. E. Talbot-Eeckelaers, L. Catala, F. Lloret, W. Wernsdorfer, E. K. Brechin, T. Mallah, Inorg. Chem. 45 (2006) 7038.

[132] L. F. Chibotaru, L. Ungur, C. Aronica, H. Elmoll, G. Pilet, D. Luneau, J. Am. Chem. Soc. 130 (2008) 12445.

[133] A. Ferguson, A. Parkin, J. Sanchez-Benitez, K. Kamenev, W. Wernsdorfer, M. Murrie, Chem. Commun. (2007) 3473.

[134] V. Tudor, G. Marin, L. Floret, V. C. Kravtsov, Y. A. Simonov, M. Julve, M. Andruh, Inorg. Chim. Acta 361 (2008) 3446.

86

Edited Feb 6

[135] H. Oshio, N. Hashino, T. Ito, M. Nakano, F. Renz, P. Gutlich, Angew. Chem. Int. Ed. 42 (2003) 223.

[136] S. Koizumi, M. Nihei, T. Shiga, M. Nakano, H. Nojiri, R. Bircher, O. Waldmann, S. T. Ochsenbein, H. U. Güdel, F. Fernandez – Alonso, H. Oshio, Chem. Eur. J. 13 (2007) 8445.

[137] R. W. Saalfrank, A. Scheurer, R. Prakash, F. W. Heinemann, T. Nakajima, F. Hampel, R. Leppin, B. Pilawa, H. Rupp, P. Müller, Inorg. Chem. 46 (2007) 1586.

[138] A. M. Ako, O. Waldmann, V. Mereacre, F. Klöwer, I. J. Hewitt, C. E. Anson, H. U. Güdel, A. K. Powell, Inorg. Chem. 46 (2007) 756.

[139] The group of one of us (SPP) have recently prepared and characterize the SMM [Co$^{II}_6$Co^{III}(μ_3-OH)$_6$(L)$_6$](ClO$_4$)$_3$, where L$^-$ is the anion of 2-(pyridine-2-yl)pentane-2-ol-4-one, formed in situ through a crossed-aldol reaction of 2-acetylpyridine in acetone under basic conditions, see: A. Kitos, C. G. Efthymiou, C. Papatriantafyllopoulou, V. Nastopoulos, A. J. Tasiopoulos, M. Manos, W. Wernsdorfer, G. Christou, S. P. Perlepes, Polyhedron (2011), doi: 10.1016/j.poly.2011.02.013.

[140] K. Dimitrou, J. – S. Sun, K. Folting, G. Christou, Inorg.Chem. 34 (1995) 4160.

[141] D. – Q. Ma, S. Hikichi, M. Akita, Y. Moro-oka, J. Chem. Soc., Dalton Trans. (2000) 1123.

[142] B. Moubaraki, K. S. Murray, T. A. Hudson, R. Robson, Eur. J. Inorg. Chem. (2008) 4525.

[143] B. F. Abrahams, T. A. Hudson, R. Robson, J. Am. Chem. Soc. 126 (2004) 8624.

[144] R. W. Saalfrank, V. Seitz, F. W. Heinemann, C. Gobel, R. Herbst-Irmer, J. Chem. Soc., Dalton Trans. (2001) 599.

[145] A. B. Blake, Chem. Commun. (1966) 569.

[146] A. A. Sidorov, I. G. Fomina, M. O. Ponina, G. G. Aleksandrov, S. E. Nefedov, I. L. Eremenko, I. I. Moiseev, Russ. Chem. Bull., 49 (2000) 960.

[147] A. A. Sidorov, I. G. Fomina, S. S. Talismanov, G. G. Aleksandrov, V. M. Novotortsev, S. E. Nefedov, I. L. Eremenko, Russ. J. Coord. Chem., 27 (2001) 584.

[148] D. Belli Dell'Amico, C. Bradicich, F. Calderazzo, A. Guarini, L. Labella, F. Marchetti, A. Tomei, Inorg. Chem. 41 (2002) 2814.

87

Edited Feb 6

[149] U. Uemura, A. Spencer, G. Wilkinson, J. Chem. Soc., Dalton Trans. (1973) 2565.

[150] J. K. Beattie, T. W. Hambley, J. A. Klepetko, A. F. Masters, P. Turner, Chem. Commun. (1998) 45.

[151] Q. Chen, S. Liu, J. Zubieta, Inorg. Chem. 28 (1989) 4433.

[152] G. A. Ardizzoia, M. A. Angaroni, G. L. Monica, F. Cariati, M. Moret, N. Masciocchi, J. Chem. Soc., Chem. Commun. (1990) 1021.

[153] V. A. Grillo, Z. Sun, K. Folting, D. N. Hendrickson, G. Christou, Chem. Commun. (1996) 2233.

[154] J. K. Beattie, T. W. Hambley, J. A. Klepetko, A. F. Masters, P. Turner, Polyhedron 16 (1997) 2109.

[155] S. Akine, W. Dong, T. Nabeshima, Inorg. Chem. 45 (2006) 4677.

[156] L. Hou, W. – X. Zhang, J. – P. Zhang, W. Xue, Y. – B. Zhang, X. – M. Chen, Chem. Commun. 46 (2010) 6311.

[157] S. J. Langley, M. Helliwell, R. Sessoli, P. Rosa, W. Wernsdorfer, R. E. P. Winpenny, Chem. Commun. (2005) 5029.

[158] A. Tsohos, S. Dionyssopoulou, C. P. Raptopoulou, A. Terzis, E. G. Bakalbassis, S. P. Perlepes, Angew. Chem. Int. Ed. 38 (1999) 983.

[159] G. S. Papaefstathiou, S. P. Perlepes, A. Escuer, R. Vicente, M. Font-Bardia, X. Solans, Angew. Chem. Int. Ed. 40 (2001) 884.

[160] G. S. Papaefstathiou, A. K. Boudalis, T. C. Stamatatos, C. J. Milios, C. G. Efthymiou, C. P. Raptopoulou, A. Terzis, V. Psycharis, Y. Sanakis, R. Vicente, A. Escuer, J. - P. Tuchagues, S. P. Perlepes, Polyhedron 26 (2007) 2089.

[161] G. S. Papaefstathiou, A. Escuer, R. Vicente, M. Font-Bardia, X. Solans S. P. Perlepes, Chem. Commun. (2001) 2414.

[162] A. K. Boudalis, B. Donnadieu, V. Nastopoulos, J. M. Clemente – Juan, A. Mari, Y. Sanakis, J. – P. Tuchagues, S. P. Perlepes, Angew. Chem. Int. Ed. 43 (2004) 2266.

88

Edited Feb 6

[163] A. K. Boudalis, Y. Sanakis, J. M. Clemente – Juan, B. Donnadieu, V. Nastopoulos, A. Mari, Y. Coppel, J. – P. Tuchagues, S. P. Perlepes, Chem. Eur. J. 14 (2008) 2514.

[164] For example, see: W. O. Koch, J. T. Kaiser, H. – K. Krüger, Chem. Commun. (1997) 2237.

[165] A. E. Malkov, T. B. Mikhailova, G. G. Aleksandrov, E. V. Pakhmutova, I. M. Egorov, A. A. Sidorov, I. G. Fomina, S. E. Nefedov, I. L. Eremenko, I. I. Moiseev, Russ. Chem. Bull., 27 (2001) 2370.

[166] E. K. Brechin, S. G. Harris, S. Parsons, R. E. P. Winpenny, Angew. Chem. Int. Ed. 36 (1997) 1967.

[167] Z. – Q. Jia, X. – J. Sun, L. – L. Hu, J. Tao, R. – B. Huang, L. – S. Zheng, Dalton Trans. (2009) 6364.

[168] C. Benelli, A. J. Blake, E. K. Brechin, S. J. Coles, A. Graham, S. G. Harris, S. Meier, A. Parkin, S. Parsons, A. M. Seddon, R. E. P. Winpenny, Chem. Eur. J. 6 (2000) 883.

[169] C. Cadiou, M. Helliwell, R. E. P. Winpenny, C. R. Chimie 6 (2003) 241.

[170] E. K. Brechin, S. Parsons, R. E. P. Winpenny, J. Chem. Soc., Dalton Trans. (1996) 3745.

[171] A. Graham, S. Meier, S. Parsons, R. E. P. Winpenny, Chem. Commun. (2000) 811.

[172] L. Lisnard, F. Tuna, A. Candini, M. Affronte, R. E. P.Winpenny, E. J. L. McInnes, Angew. Chem. Int. Ed. 47 (2008) 9695.

[173] S. Garretta, P. Santini, G. Amoretti, M. Affronte, A. Candini, A. Ghirri, I. S. Tidmarsch, R. H. Laye, R. Shaw, E. J. L. McInnes, Phys. Rev. Lett. 97 (2006) 207201.

[174] W. Clegg, C. D. Garner, M. H. Al-Samman, Inorg. Chem. 22 (1983) 1534.

[175] O. L. Sydora, P. T. Wolczanski, E. B. Lobkovsky, E. Rumberger, D. N. Hendrickson, Chem. Commun. (2004) 650.

[176] O. L. Sydora, T. P. Henry, P. T. Wolczanski, E. B. Lobkovsky, E. Rumberger, D. N. Hendrickson, Inorg. Chem. 45 (2006) 609.

[177] A. Fumagalli, P. Ulivieri, M. Costa, O. Crispu, R. Della Pergola, F. F. de Biani, F. Laschi, P. Zanello, P. Macchi, A. Sironi, Inorg. Chem. 43 (2004) 2125.

89

Edited Feb 6

[178]   L. – L. Zheng, J. – D. Leng, R. Herchel, Y. Lan, A. K. Powell, M. – L. Tong, Eur. J. Inorg. Chem. (2010) 2229.

[179]   G. J. T. Cooper, G. N. Newton, P. Kogerler, D. – L. Long, L. Engelhardt, M. Luban, L. Cronin, Angew. Chem. Int. Ed. 46 (2007) 1340.

[180]   M. – H. Zeng, M. – X. Yao, H. Liang, W. – X. Zhang, X. – M. Chen, Angew. Chem. Int. Ed. 46 (2007) 1832.

[181]   E. K. Brechin, R. O. Gould, S. G. Harris, S. Parsons, R. E. P. Winpenny, J. Am. Chem. Soc. 118 (1996) 11293.

[182]   T. C. W. Mak, P. J. Li, C. M. Zheng, K. Y. Huang, J. Chem. Soc., Chem. Commun. (1986) 1597.

[183]   M. L. Tong, M. Monfort, J. M. C. Juan, X. M. Chen, X. H. Bu, M. Ohba, S. Kitagawa, Chem. Commun. (2005) 233.

[184]   E. K. Brechin, R. A. Coxall, A. Parkin, S. Parsons, P. A. Tasker, R. E. P. Winpenny, Angew. Chem. Int. Ed. 40 (2001) 2700.

[185]   G. N. Newton, G. J. T. Cooper, P. Kögerler, D. – L. Long, L. Cronin, J. Am. Chem. Soc. 130 (2008) 790.

[186]   B. – W. Li, Y. – L. Zhou, Q. Chen, M. – H. Zeng, Polyhedron 29 (2010) 148.

[187]   J. C. Goodwin, R. Sessoli, D. Gatteschi, W. Wernsdorfer, A. K. Powell, S. L. Heath, J. Chem. Soc., Dalton Trans. (2000) 1835.

[188]   Z. – G. Gu, S. C. Sevov, Inorg. Chem. 48 (2009) 8066.

[189]   R. Shaw, I. S. Tidmarsch, R. H. Laye, B. Breeze, M. Helliwell, E. K. Brechin, S. L. Heath, M. Murrie, S. Ochsenbein, H. U. Güdel, E. J. L. McInnes, Chem. Commun. (2004) 1418.

[190]   A. K. Boudalis, C. P. Raptopoulou, B. Abarca, R. Ballesteros, M. Chadlaoui, J. - P. Tuchagues, A. Terzis, Angew. Chem. Int. Ed. 45 (2006) 432.

[191]   A. N. Georgopoulou, R. Adam, C. P. Raptopoulou, V. Psycharis, R. Ballesteros, B. Abarca, A. K. Boudalis, Dalton Trans. 39 (2010) 5020 and refs. cited therein.

90

Edited Feb 6

[192]   E. K. Brechin, S. G. Harris, A. Harrison, S. Parsons, A. G. Whittaker, R. E. P. Winpenny, Chem. Commun. (1997) 653.

[193]   Y. Bi, X. – T. Wang, W. Liao, X. Wang, X. Wang, H. Zhang, S. Gao, J. Am. Chem. Soc. 131 (2009) 11650.

[194]   P. Alborés, E. Rentschler, Angew. Chem. Int. Ed. 48 (2009) 9366.

[195]   G.D. Ilyushin, V.A. Blatov, Acta Cryst. B65 (2009) 300.

[196]   C. – M. Liu, D. – W. Zhang, X. Hao, D. – B. Zhu, Chem. Eur. J. 17 (2011) 12285.

91